Inverse-Detected Two-Dimensional Nmr Methods: Applications in Natural Products Chemistry

Gary E. Martin, and Ronald C. Crouch

J. Nat. Prod., **1991**, 54 (1), 1-70• DOI: 10.1021/np50073a001
• Publication Date (Web): 01 July 2004

Journal of Natural Products
Vol. 54, No. 1, pp. 1-70, Jan-Feb 1991

INVERSE-DETECTED TWO-DIMENSIONAL NMR METHODS: APPLICATIONS IN NATURAL PRODUCTS CHEMISTRY

GARY E. MARTIN* and RONALD C. CROUCH

Division of Organic Chemistry, Burroughs Wellcome Co., 3030 Cornwallis Road, Research Triangle Park, North Carolina 27709

ABSTRACT.—Applications of inverse-detected 2D nmr methods are reviewed. Sequences presently available for direct (one-bond) heteronuclear correlation via $^1J_{XH}$ (HMQC and others) are discussed individually followed by examples of applications to natural products presented by class. Correlations of heteronuclear pairs other than ^1H-^{13}C and ^1H-^{15}N are briefly considered. Optimization of parameters necessary in the acquisition of inverse-detected heteronuclear chemical shift correlation data are considered, followed by an illustration using the degradation product of 1-bromomaaliol. Methods for performing HMQC-COSY (RELAY) and HMQC-TOCSY experiments are considered with examples. Various ways of utilizing HMQC-TOCSY data are discussed followed by an illustration of the assembly of the protonated portion of the carbon skeleton of the degradation product of 1-bromomaaliol by varying the mixing times in a series of HMQC-TOCSY experiments. Long-range proton-detected heteronuclear chemical shift correlation experiments (HMBC) are presented with extensive examples of the application of these experiments to a diverse assortment of natural products, which are presented by class of compounds. A practical example of the application of the HMBC experiment to the degradation product of 1-bromomaaliol follows. The relatively new HMQC-NOESY experiment is presented followed by a discussion of the relatively few examples of this experiment presently contained in the literature. Finally, examples of proton-detected one-dimensional analogues of 2D nmr experiments are described; these include SELINCOR, selective one-dimensional HMQC-TOCSY, and SIMBA (selective inverse multiple bond analysis).

Two-dimensional nmr methods have profoundly affected the way in which natural product structure elucidation studies are performed. Although 2D nmr techniques have been the subject of several monographs (1–6), it is appropriate to cite some of the milestones leading to the inverse detected 2D nmr methods.

The first 2D *J*-resolved nmr experiments provided access to obscured scalar (*J*) coupling information. Continued developments led to the autocorrelated 2D nmr methods (COSY) providing proton-proton connectivity information that was inaccessible by conventional means. Autocorrelated proton experiments were followed by heteronuclear shift correlation techniques, providing powerful proton-heteronucleus connectivity information.

Pioneering work by Müller (7) examined the possibility of heteronuclear shift correlation via both carbon and proton detection of heteronuclear multiple quantum coherence. Unfortunately, the technical complexities inherent in proton-detected experiments prompted the alternative development of the technically less demanding single-quantum heteronucleus-detected variants (8–11). Normally, fixed-duration delays in the heteronuclear chemical shift correlation pulse sequence are optimized as a function of the one-bond heteronuclear coupling constant, $^1J_{CH}$. A new dimension in structural information was afforded by a pair of experiments developed in the early 1980s: heteronuclear relayed coherence transfer (12–14) and long-range heteronuclear shift correlation (15,16). The former provides direct proton-carbon heteronuclear connectivities augmented by the proton-proton connectivity information relayed between the directly bound proton and, normally, its vicinal neighbor. Long-range correlation experiments offer a means to identify vicinal neighbor protons in some cases and, more effectively and more importantly, three-bond proton-carbon correlations. The latter provides the means to span heteroatoms and quaternary carbons, thus giving the chemist extremely powerful structural information. In addition, long-range heteronuclear shift

correlation experiments also provide the means to link structural fragments together through intervening quaternary carbons. Long-range heteronuclear chemical shift correlation has spawned a considerable number of variants and has been recently reviewed (16).

Essentially concurrent with the development of the long-range heteronuclear correlation experiments, proton-detected heteonuclear shift correlation experiments were examined with renewed vigor. These efforts culminated in inverse-detected direct (HMQC) (17), heteronuclear multiple bond correlation (HMBC) (18), inverse-detected heteronuclear relay (HMQC-TOCSY) (19–21) [the acronym HMQC-TOCSY is suggested in the work of Davis (21) which describes what will probably prove to be the most useful variant of proton-detected heteronuclear relay], and inverse-detected heteronuclear nOe experiments (HMQC-NOESY) (22).

Inverse-detected heteronuclear 2D nmr experiments provide structural information unobtainable only a few years ago. Concerted applications of these techniques facilitate the determination of molecular structures on milligram and submilligram quantities of complex, medium-sized molecules if the experiments are carefully parameterized and the investigator is willing to invest the time to acquire the data. In the case of the direct (one-bond) inverse-detected experiment, heteronuclear correlation data on samples as small as 100 μg can be obtained in reasonable periods of time at 500 MHz. To illustrate the power of these techniques in natural product structure elucidation, we will show their application in the determination of the structure of a 10-mg sample of a degradation product of a brominated marine sesquiterpene.

ONE-BOND HETERONUCLEAR CHEMICAL SHIFT CORRELATION USING PROTON OR "INVERSE" DETECTION—THE PULSE SEQUENCES AVAILABLE.—*The Müller sequences.*—Correlation of heteronuclear spins via proton-detected methods was first proposed, and the possibilities explored, by Müller (7) whose prototypical pulse sequence is shown in Figure 1. Unlike the now more familiar heteronucleus-detected experiment, which can be reasonably explained with vector models and the concept of polarization transfer, inverse-detected heteronuclear chemical shift correlation requires the creation of heteronuclear multiple quantum coherence. Unfortunately, vector models cannot begin to explain the phenomenon of multiple quantum coherence, and we must resort to spin product operator formalisms (23–25) at a minimum or, more rigorously, to full density matrix treatments (26,27). Hence, a detailed description of the inverse-detected heteronuclear chemical shift correlation experiment, hereafter referred to as HMQC (heteronuclear multiple quantum correlation), is beyond the scope of this review.

Modified sequences intended to provide better suppression of unwanted ^{1}H-^{12}C magnetization.—All variants of the HMQC experiment utilize the creation and manipulation of

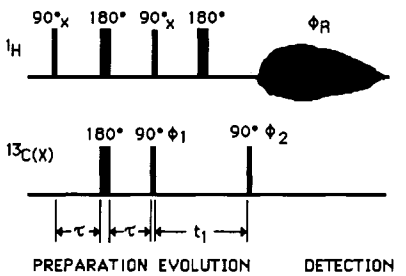

FIGURE 1. Prototypical pulse sequence for heteronuclear chemical shift correlation via multiple quantum coherence (7).

heteronuclear multiple-quantum coherence followed by reconversion to detectable single-quantum proton coherence. One problem inherent in HMQC experiments is suppression of the undesired 99% of the proton signals associated with ^{1}H-^{12}C molecules. The most convenient means of accomplishing this goal is to apply a BIRD pulse (28), which is selective for protons bound directly to ^{12}C, to invert this portion of the proton population, leaving the desired ^{1}H-^{13}C spin pairs as unperturbed z-magnetization. Several approaches to this problem have been reported. Brühwiler and Wagner (29) employed a BIRD pulse followed by homogeneity spoiling pulses as shown in Figure 2. It has subsequently been shown (39) that the 90° pulse following the

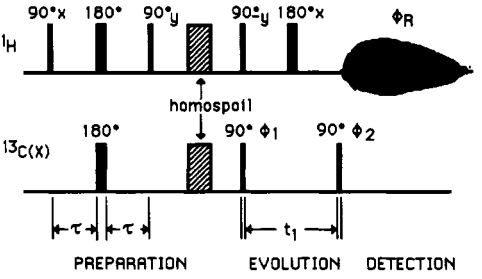

FIGURE 2. Pulse sequence for heteronuclear multiple quantum chemical shift correlation proposed by Brühwiler and Wagner (29). The homogeneity spoiling pulses following the BIRD pulse were intended to provide additional suppression for an unwanted signal arising from ^{1}H-^{12}C spin pairs.

homospoil pulse in the Brühwiler-Wagner sequence could be eliminated, as in the pulse sequence shown in Figure 3. Bax and Subramanian (17) utilized a sequence in which the BIRD pulse was separated from the creation of heteronuclear multiple quantum coherence that derives from earlier work by Bax *et al.* (23). By inserting a delay after the BIRD pulse (Figure 4), the duration of which, ideally, is optimized as a function of the proton T_1 relaxation time, the ^{1}H-^{12}C spins are allowed to relax to a point where they no longer have any z-magnetization component. While it is certainly not optimal, we find that under most circumstances a delay of 0.3–0.4 sec works well for the interval between the BIRD pulse and the following proton pulse for the HMQC experiment. This is, however, not a safe assumption for the HMQC-NOESY experiment described below or for small symmetrical aromatic compounds.

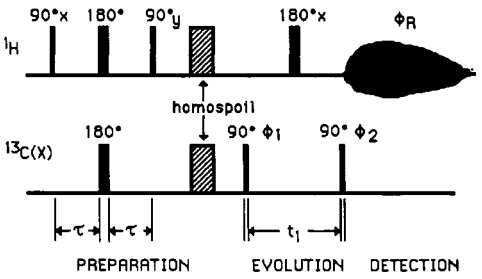

FIGURE 3. Modification of the Brühwiler and Wagner pulse sequence shown in Figure 2 (39).

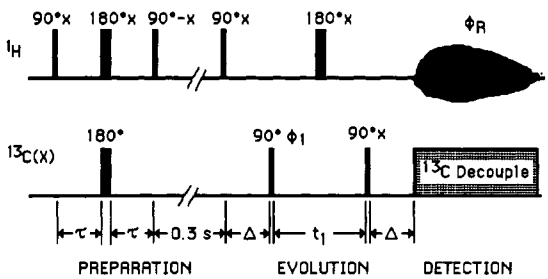

FIGURE 4. Inverse-detected heteronuclear multiple quantum coherence (HMQC) pulse sequence based on the work of Bax and Subramanian (17) and derived from the earlier work of Bax *et al.* (23). Signals from protons bound directly to ^{12}C are first inverted by the BIRD pulse at the beginning of the pulse sequence. This component of magnetization is allowed to relax longitudinally during the null delay, which is frequently set to 0.3 sec as a default parameter. The 90° proton pulse, followed Δ later by the 90° carbon pulse, creates heteronuclear multiple quantum coherence that is allowed to evolve during the evolution period, t_1. The 180° proton pulse midway through the evolution period interchanges zero- and double-quantum coherence terms while simultaneously affording broadband decoupling in F_1. The final 90° carbon pulse converts the evolved multiple quantum coherence into observable single-quantum proton coherence, which is antiphase upon creation. Proton coherence is refocused during the interval Δ at which point the receiver is enabled and broadband heteronuclear decoupling (WALTZ, GARP, etc.) is applied. Phase cycling schemes currently in use with this pulse sequence provide phase-sensitive data.

Once the signal from the ^1H-^{12}C spin pairs has been suppressed, a 90° proton pulse is applied to the unperturbed ^1H-^{13}C spins, followed $\frac{1}{2}(^1J_{CH})$ later by a 90° ^{13}C pulse that creates the desired heteronuclear multiple quantum coherence. This pulse sequence is shown in Figure 4. The original work of Bax and Subramanian (17) applied a ^{13}C pulse coincidently with the first proton pulse, followed $\frac{1}{2}(^1J_{CH})$ later by a second ^{13}C pulse that created the desired multiple quantum coherence. The first carbon pulse in their sequence was, in our experience, not required and was not employed to generate any of the spectra presented in this review. Following the ^{13}C pulse used to create multiple quantum coherence, both zero- and double-quantum coherences are created and allowed to evolve during the ensuing evolution period, t_1 (not to be confused with the spin-lattice relaxation time T_1). A proton 180° pulse midway through the evolution period interchanges zero- and double-quantum terms and refocuses proton chemical shift evolution, leaving the proton spins appropriately "labeled." Heteronuclear multiple quantum coherence is reconverted to observable proton single-quantum coherence by the application of the final ^{13}C pulse in the sequence shown in Figure 4, and the proton spectrum is acquired with ^{13}C broadband (WALTZ) decoupling to collapse heteronuclear couplings and thereby increase sensitivity.

HMQC without a BIRD pulse.—There have been several heteronuclear multiple quantum coherence pulse sequences reported other than the Bax-Subramanian pulse sequence shown in Figure 4. Sklenar and Bax (31) have shown that the central core of the pulse sequence shown in Figure 4 can be applied to large molecules without the preparatory BIRD pulse. In the case of large molecules, the BIRD pulse cannot be em-

ployed, as the negative nOe would attenuate signals from protons attached to the magnetically active heteronuclide. The application of the "shortened" sequence suggested by Sklenar and Bax was demonstrated using hen egg white lysozyme (14,400 Daltons). Methods for determining protein structure based on proton-detected heteronuclear chemical shift correlation methods have also been the focal point of several recent reviews to which the reader interested in applications to large molecules is directed for further information (32–37). While addressing this point, however, it is also worth noting that there have been a number of successful applications of the HMQC sequence minus the BIRD pulse reported for small molecules. Examples are cited below.

Constant evolution time heteronuclear multiple quantum coherence excitation.—Another interesting but seldom utilized pulse sequence was the constant evolution time HMQC experiment devised by Müller *et al.* in 1986 (38) for proton detection of natural abundance ^{15}N spectra. Müller's experiment employs a single 90° proton pulse followed by a fixed time interval, Δ, and later by a 90° ^{13}C or X-nucleus pulse to create heteronuclear multiple quantum coherence as shown in Figure 5. The duration of the evolution period is constant, and a 180° pulse is moved stepwise through the evolution period in a fashion analogous to the COLOC and XCORFE experiments (16). The constant duration evolution period was intended to provide accelerated decay of ^{1}H-^{14}N signals relative to the ^{1}H-^{15}N heteronuclear multiple quantum coherence of interest. This affords better suppression of the undesired magnetization components when the desired heteronuclear multiple quantum coherence is reconverted to observable single-quantum coherence by the final heteronucleus pulse in the sequence. The pulse sequence is shown in Figure 5 without broadband heteronuclear decoupling. Decoupling may be initiated by delaying acquisition for a second fixed time interval, Δ, at which point both decoupling and acquisition are initiated simultaneously.

HMQC sequences employing spin-locking periods.—Radiofrequency inhomogeneity problems inherent to older spectrometers could cause severe problems in attempting to acquire HMQC spectra. One approach to radiofrequency inhomogeneity problems is to use spin-locking periods for filtering by inducing dephasing of unwanted magnetization. This property of spin-locking was exploited by Otting and Wüthrich (39) in the design of a purging scheme for proton-detected heteronuclear correlation spectra. Their

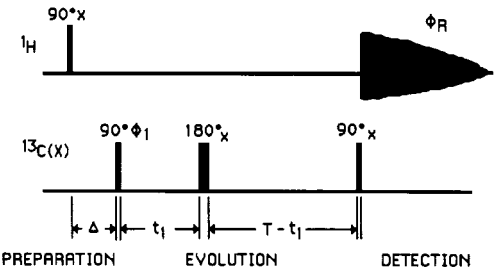

FIGURE 5. Constant evolution time heteronuclear multiple quantum coherence experiment proposed by Müller *et al.* (38). The constant evolution period is designed to promote enhanced decay of ^{1}H-^{14}N coherence relative to the desired ^{1}H-^{15}N heteronuclear multiple quantum coherence, which is finally reconverted to observable single-quantum proton coherence by the final 90° heteronucleus pulse. The sequence is shown without heteronucleus decoupling. If decoupling is desired, broadband heteronuclear decoupling may be initiated by waiting for a second fixed time interval, Δ.

pulse sequence, which is essentially a derivative of the experiment proposed by Bodenhausen and Ruben (30), is presented in Figure 6.

Spitzer *et al.* (40) have also incorporated spin-locking periods in the design of the modified pulse sequence shown in Figure 7. In their experiment, the spin-lock is used to suppress proton precession. Consequently, magnetization is modulated solely by the ^{13}C precession frequency. Homonuclear and heteronuclear scalar couplings are also eliminated, obviating the need for 180° refocusing pulses and the added pulses and delays required in a BIRD pulse. Although it remains to be seen if this experiment will have any long-term utility or significance, the authors were able to demonstrate successfully the application of the experiment in the acquisition of a heteronuclear correlation spectrum for a sample of the alkaloid deoxyvinblastine.

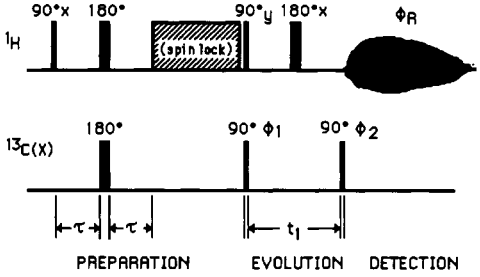

FIGURE 6. Pulse sequence for heteronuclear multiple quantum chemical shift correlation proposed by Otting and Wüthrich (39). The spin-locking interval is employed to help eliminate undesired components of magnetization by inducing their dephasing.

DEPT-HMQC.—Another departure from the Bax-Subramanian HMQC sequence that we will consider is the DEPT-HMQC sequence recently reported by Kessler *et al.* (41) and shown in Figure 8. For complex molecules, DEPT-HMQC offers the opportunity to edit the resulting HMQC spectrum on the basis of carbon multiplicity. Selection for methine, methylene, or methyl resonances is achieved by setting the variable flip angle pulse, β, to 60°, 120°, or 180°, respectively. As in the Bax-Subramanian sequence, suppression of the signals from unwanted ^1H-^{12}C species is achieved by the application of a BIRD pulse at the initiation of the sequence.

Heteronuclear single- and multiple-quantum coherence (HSMQC).—Zuiderweg (42) recently proposed a further modification of the proton-detected heteronuclear chemical shift correlation experiment intended to improve both resolution and sensitivity. This

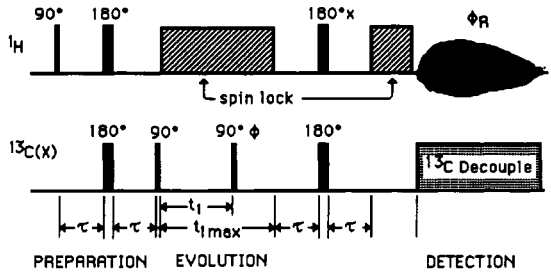

FIGURE 7. Pulse sequence for heteronuclear multiple quantum correlation proposed by Spitzer *et al.* (40).

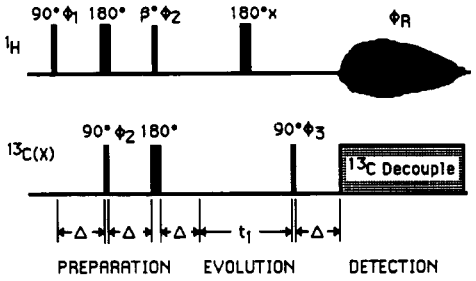

FIGURE 8. Pulse sequence for DEPT-edited heteronuclear multiple quantum chemical shift correlation (HMQC-DEPT) proposed by Kessler *et al.* (41). By varying the flip angle of the pulse, β, the pulse sequence can be used to produce spectra derived from only methine, methylene, or methyl resonances. Choices for the flip angle of the β-pulse are 60°, 120°, and 180° for methine, methylene, and methyl, respectively.

experiment has been christened heteronuclear single- and multiple-quantum coherence (HSMQC). Both single- and multiple-quantum coherence pathways contribute to the observed signal, thereby intermixing the narrow line characteristics of the heteronuclear single-quantum coherence (HSQC) experiment originally described by Bodenhausen and Ruben (30) into the signal obtained from the HMQC experiment. Zuiderweg's pulse sequence is shown in Figure 9.

In the HSMQC experiment, the simultaneous application of proton and carbon 90° pulses at a fixed time, Δ, following the first 90° proton pulse creates terms for both single- and multiple-quantum coherence. In the absence of proton-proton coupling, which can be eliminated by the 180° proton pulse, both single- and multiple-quantum coherences evolve according to single- and pseudo-single-quantum processes. The simultaneous 90° pulses at the end of the evolution period select for observable magnetization from both the single- and multiple-quantum terms. The phase shift employed with the second transient results in an interchange of single- and multiple-quantum dependencies in Ω_1 (F_1). It follows that F_1 chemical shift dependence vanishes upon taking the algebraic difference of the responses in the first and second transients, thereby affording a direct combination of the results that would be obtained from HMQC and HSQC experiments. According to Zuiderweg's work (42), approximately a 50% increase in sensitivity over the HMQC experiment is afforded by the HSMQC experi-

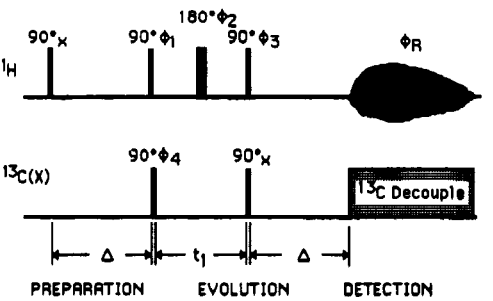

FIGURE 9. HSMQC pulse sequence devised by Zuiderweg (42). The experiment is claimed to provide improved resolution and sensitivity relative to the Bax and Subramanian HMQC sequence by incorporating the narrow resonance characteristics of the HSQC experiment of Bodenhausen and Ruben (30).

ment. The application of the experiment was illustrated using a sample of unlabeled hen eggwhite lysozyme.

APPLICATIONS OF THE HMQC EXPERIMENT.—A computer search of the literature for applications of the HMQC experiment is complicated somewhat by the manner in which this experiment is referenced. Authors have variously referenced their utilization of the technique to the early work of Müller (7), to the early paper by Bax *et al.* dealing with ^{1}H-^{15}N heteronuclear correlation (23), or to the more recent paper by Bax and Subramanian (17). The number of references uncovered on this basis is in excess of 200. Surprisingly, however, there are a relatively small number of applications directed toward small molecule spectral assignment or structure determination. These examples will be discussed here. Access to the literature describing applications of HMQC to large molecules can be gained from several reviews on the topic (32–37). Fortuitously, during the writing of this review, a detailed comparative evaluation of the various methods available for two-dimensional inverse correlation studies of proteins was published by Bax *et al.* (43). The reader interested in the application of the methods described in this review to larger molecules will find the information presented in the comparison just cited of considerable interest.

Applications to the vitamin B_{12} group.—One of the earliest and most intensively studied groups of "small" molecules has been the coenzyme B_{12} group. In the first paper in this area, Summers *et al.* (44) employed an arsenal of 2D nmr experiments that included HMQC and HMBC in completing a total assignment of the ^{1}H- and ^{13}C-nmr spectra of coenzyme B_{12} itself. These techniques were subsequently applied to study the base-off form of coenzyme B_{12} in 1987 (45). Unambiguous assignments of vitamin B_{12} monocarboxylic acids have been reported by Pagano and Marzilli (46). More recently, Pagano *et al.* (47) have again employed these techniques in assigning the ^{1}H and ^{13}C spectra of a coenzyme B_{12} derivative, 5′-deoxyadenosylcobinamide.

Applications to antibiotics.—Structural studies of other families of compounds have also benefitted from applications of the HMQC experiment. The general category of compounds for which the largest number of applications have been reported is the antibiotics. As a group, antibiotics are quite diverse and structurally dissimilar. The first application of the HMQC experiment in this category of compounds was in the assignment of the secondary amide ^{15}N resonances of bleomycin A_2 by Sarkar *et al.* (48). Without recourse to HMQC experiments, ^{15}N-nmr assignments at natural abundance for a molecule like bleomycin would be prohibitively time-consuming. Later in 1986, the elucidation of the structure of the complex macrocyclic antibiotic desertomycin [**1**] was reported by Bax *et al.* (49). The structure was assembled using a combination of di-

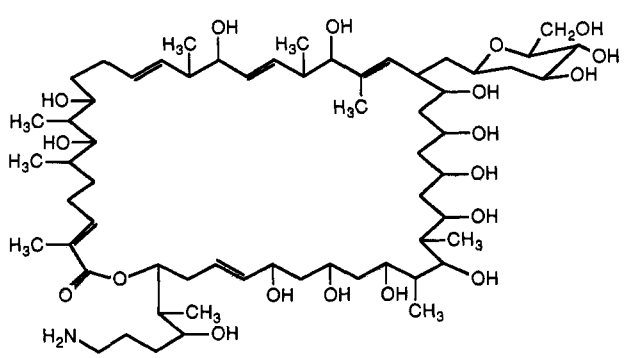

1

rect and long-range heteronuclear correlations in conjunction with other 2D nmr data and resulted in a total assignment of the ^{1}H- and ^{13}C-nmr spectra of the molecule. In a sense, this work is the prototypical structure elucidation paper using HMQC/HMBC in combination. Finally, Bax and coworkers also utilized carbon-coupled HMQC data as a means of obtaining one-bond heteronuclear coupling constants. This approach provides a convenient means of obtaining such information in congested spectra. If satellite spectra are acquired as a single trace, the carbon-coupled HMQC experiment also provides a facile means of obtaining heteronuclear coupling constants. When such data can be extracted from a single proton spectrum, the method affords the means of obtaining heteronuclear coupling constants on samples of material on which even a proton-decoupled carbon spectrum could not be acquired in a reasonable time.

The next application of the HMQC experiment to an antibiotic did not appear until 1987 when Seto *et al.* (50) reported the structure of the polyether antibiotic portmicin [**2**]. This study employed the HMQC experiment in conjunction with both HMBC and proton HOHAHA to assemble the final structure. The work of Seto was followed in 1988 by a paper reporting the structure of the bacterial peptidoglycan synthesis inhibitor liposidomycin B (51). Liposidomycin B [**3**] is a complex nucleoside antibiotic isolated from *Streptomyces griseosporeus*; it inhibits the biosynthesis of the lipid intermediate in peptidoglycan synthesis. Alkaline hydrolysis cleaved an ester and a sulfate ester and was followed by concerted application of the HMQC and HMBC experiments to link the cyclic structural subunits to one another.

During 1989, there were several applications of the HMQC experiment associated with antibiotics. Abuzar and Kohn (52) employed HMQC data in the determination of the structures of reaction products of nucleophilic amino acids with the antibiotic bicyclomycin [**4**]. A group headed by McAlpine at Abbott Laboratories reported the isolation and structures of two groups of antibiotics, the pacidomycins (53) and the coumamidines (54). The former, **5**, were nucleoside antibiotics with anti-*Pseudomonas*

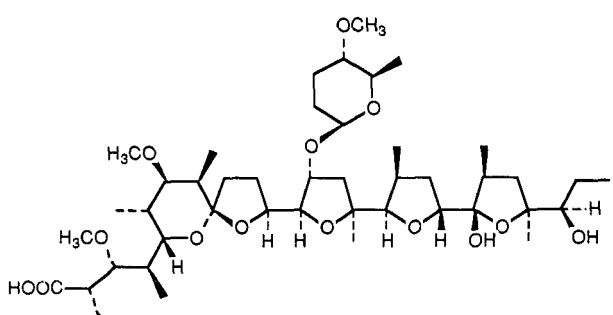

2

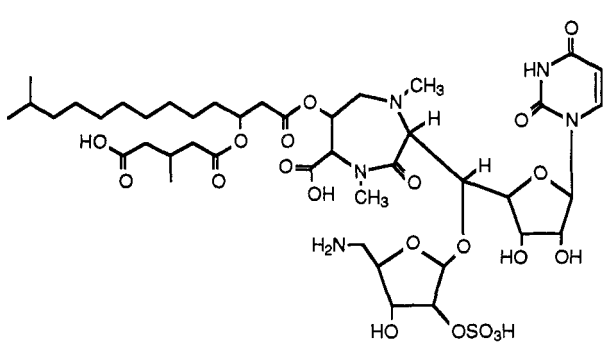

3

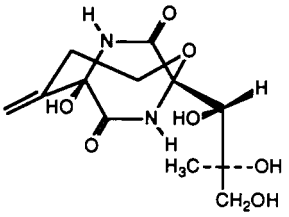

4

aeruginosa activity. The latter, **6**, were carbohydrate phenylpropionic-acid-type antibiotics related to the cinodines (55). One further point that should be made regarding these papers is the reference to the HMQC experiment by McAlpine's group using the acronym HETCOR, which is generally chosen in referring to the heteronucleus-detected variants of the heteronuclear correlation experiment. Hence, care must be exercised to examine the references cited before making a final assessment of which experiment was utilized in a given case.

Applications to alkaloids.—Alkaloids have also been an attractive target for the application of the HMQC experiment. The earliest application to an alkaloid that we are aware of was the study of the biosynthesis of the indolocarbazole alkaloid staurosporine [7] by Meksuriyen and Cordell (56). Limited solubility of staurosporine precluded the use of the HETCOR experiment and necessitated the utilization of the far more sensi-

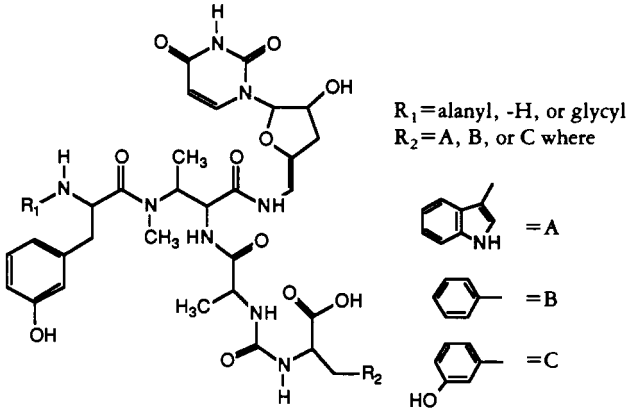

5

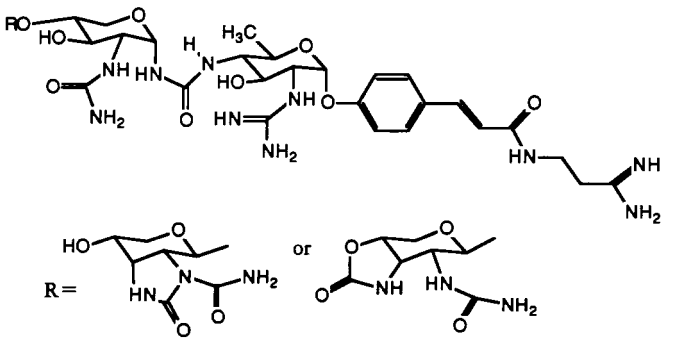

6

tive HMQC experiment. A new indole-derived alkaloid, jadiffine [**8**], was isolated from *Vinca difformis*; the HMQC experiment was employed to establish one-bond proton-carbon shift correlations (57). Later in 1988, Edwards *et al.* (58) reported a study of the pumiliotoxin (R = -H) and allopumilitoxin (R = -OH) [**9**] and related alkaloids from the Panamanian poison frog *Dendrobates speciosus*. Here utilization of the HMQC experiment was necessitated by the limited quantities of sample available, which had to be extracted from the skins of these poisonous frogs.

During 1989, there were two studies reporting the application of the HMQC experiment to alkaloids. DeBruyn *et al.* (59) made use of the HMQC experiment during the assignment of the ^{1}H- and ^{13}C-nmr spectra of the heteroyohimbine alkaloid, reser-

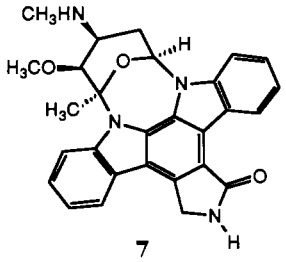

7

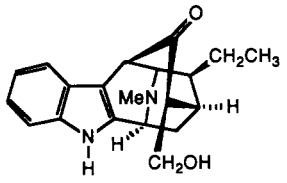

8

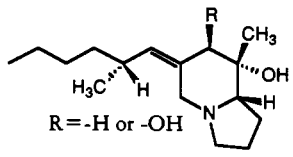

9

piline hydrochloride [**10**]. Carmely *et al.* (60) utilized an HMQC experiment in establishing the structures of a group of four closely related 2-amino imidazole alkaloids from the marine sponge *Leucetta chagosensis* in conjunction with nOe and HMBC data. The structure of one member of this family, naamidin A [**11**], is shown.

Before making the transition to a survey of applications of HMQC experiments to terpenoidal compounds, it is appropriate to consider the application of the HMQC experiment to lassiocarpine, a novel C_{20}-diterpene alkaloid obtained from the root of *Aconitum kojimae* var. *lassiocarpum* (61). The structure of lassiocarpine [**12**] was assembled using a combination of HMQC, HMBC, and NOESY experiments.

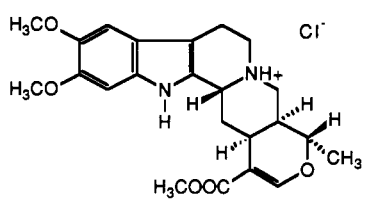

10

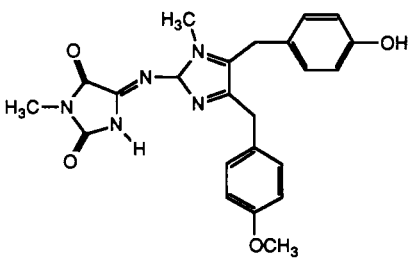

11

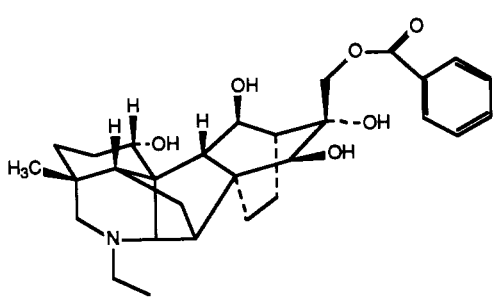

12

Applications to terpenoidal compounds.—Assignment of the nmr spectra of terpenoidal natural products holds promise as another field in which the HMQC experiment can be used to advantage. Kobayashi *et al.* (62) have employed HMQC to assign the protonated carbons and HMBC to establish the structure of metachromin C [**13**], a novel cytotoxic sesquiterpene from an Okinawan marine sponge *Hippospongia metachromia*. Mossa *et al.* (63) have utilized the HMQC experiment to establish the structure of a pair of novel 6,7-seco-6,11-cyclolabdane diterpenes, richardianidins 1 and 2, isolated from the Saudi Arabian medicinal plant *Cluytia richardina*; the structures differ only in the attachment and size of the lactone. Almost paradoxically, in the case of the richardianidin 1 [**14**], the γ-lactone oxygen is attached to the 2 position, while in richardianidin 2, the δ-lactone oxygen is attached to the 1 position.

Berger *et al.* (64) have employed the HMQC experiment to establish the one-bond connectivities of a novel polycyclic triterpenoid, 27-deoxyacetin [**15**]. Taking full advantage of all of the potential information content of an HMQC spectrum, Wright *et al.* (65) have employed the experiment with full heteronuclear carbon coupling to obtain both the one-bond proton-carbon correlations and the heteronuclear coupling constants

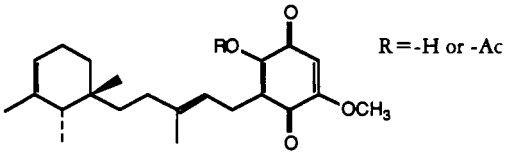

13

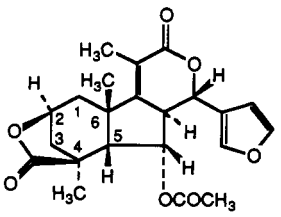

14

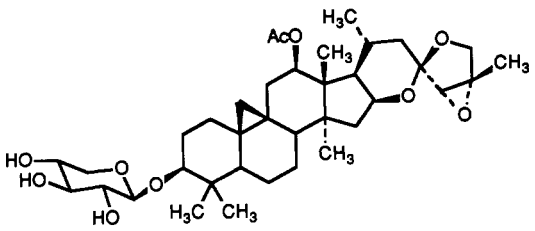

15

of a group of cytotoxic cembranoid diterpenes, bipinnatins a–d [**16**], isolated from the gorgonian coral *Pseudopterogorgia bipinnata*. As noted above and utilized by Wright *et al.*, recording HMQC data with full heteronuclear coupling provides what may be the only means of accessing one-bond heteronuclear coupling constants for some samples. With reasonably well resolved spectra, heteronuclear coupling constants can be had from a one-dimensional satellite spectrum. In contrast, when highly congested spectra are involved, the only means of accessing one-bond coupling constants is through acquisition of the fully coupled HMQC spectrum. Finally, Beale *et al.* (66) have employed the HMQC experiment to establish the one-bond proton-carbon connectivities of a digitoxigenin-based cardenolide **17** of *Digitalis lanata*.

Application to carotenoids.—Englert *et al.* (67) utilized the HMQC and HMBC experiments to assign the ^{1}H- and ^{13}C-nmr spectra of renierapurpurin-20-al [**18**] as part of a study of the configuration of this cross-conjugated caroten-20-al. Noteworthy about this paper is that the work was done on a 1.2-mg sample of the title compound, clearly highlighting the sensitivity of the HMQC experiment.

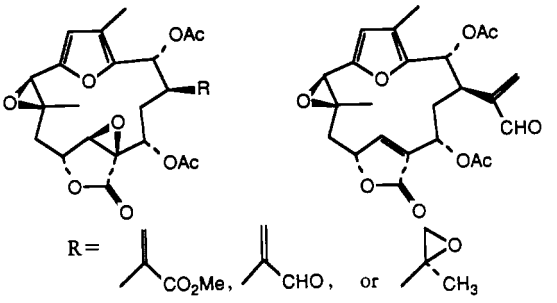

16

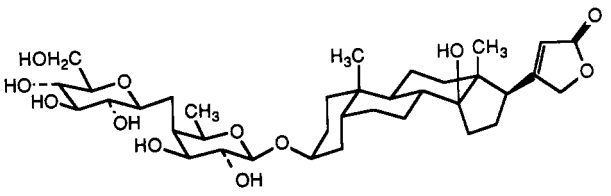

17

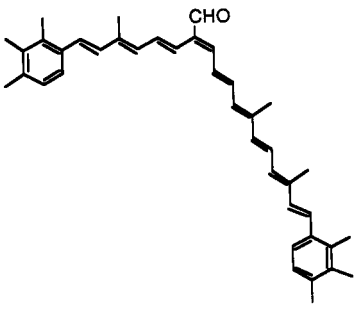

18

Applications to porphyrins.—Another useful paper reports the application of the HMQC experiment to porphyrin and polysaccharide examples. Cavanagh *et al.* (68) have presented these examples in the context of a discussion of the practicalities and advantages of the HMQC and HMBC experiment over conventional heteronucleus-detected experiments. In a more recent effort, Timkovich and Bondoc (69) have also applied the HMQC experiment to a study of d-type porphyrins that were available only in very limited amount: sample sizes ranged from 200 to 600 μg!

Applications to saccharides.—Predating the work of Cavanagh *et al.* (68) by several years and arising from the 1986 work by Bax and Subramanian (17), there have been a number of applications of the HMQC and related inverse-detected experiments in studies of carbohydrates. The first work in the carbohydrate area was actually that of Lerner and Bax (70), which examined the concerted application of HMQC, HMBC, and HMQC-RELAY in the spectral assignment of oligosaccharides. The trisaccharide α-Neu-5Ac(2↦3)-β-Gal(1↦4)-Glc was employed as a model compound for the study. In a more complex application, Byrd *et al.* (71) utilized the HMQC experiment in a study of the *Haemophilus influenzae* type—a capsular polysaccharide. Finally, Kovac and coworkers (72,73) have employed a HMQC experiment to confirm the structure of several synthetically prepared carbohydrates.

Applications to peptides.—Another fertile area for applications of the HMQC experiment is peptide structure elucidation and spectral assignment. Here, we refer to peptides separately and apart from proteins, on which a number of reviews have been written discussing the application of inverse-detected methods. Despite the potential for the application of HMQC in such studies, there are relatively few papers in the literature that report the use of the HMQC experiment. The first of which we are aware was a study by Bermel *et al.* (74) reported in 1987. While the HMQC experiment was employed to establish the one-bond proton-carbon correlations, the main thrust of the paper was in the use of inverse-detected long-range heteronuclear couplings for the unequivocal assignment of the carbonyl resonances of cyclo(Phe-Thr-Trp-Phe-D-Pro-). There have been a number of such applications reported, and these are discussed in detail below. In a related paper, Hofmann *et al.* (75) reported a total assignment of a cyclo(Phe-Pro-Thr-Lys-Trp-Phe-) through the concerted application of HMQC, HMBC, and HMQC-RELAY. Olejniczak *et al.* (76), in a more complex example, have utilized the HMQC experiment to establish direct proton-carbon shift correlations of the 7–23 segment of the 28-amino acid peptide, rat atrial natriuretic factor. Gerothanassis *et al.* (77) have reported a study employing the HMQC experiment to correlate ^{1}H-^{15}N for Leu-enkephalin. In a closely related study, Demarco *et al.* (78) have utilized the HMQC experiment for ^{1}H-^{15}N correlation of Met-enkephalin. Further work in the series of peptide papers by Kessler *et al.* (79) was also reported in 1989; the HMQC experiment was utilized in this case to assign the ^{13}C-nmr chemical shifts of a group of cyclic alanine-containing analogues of thymopoietins. Finally, Goodman and Mierke (80) applied the HMQC experiment in a study of the morphiceptin tetrapeptides (Tyr-Pro-Phe-Pro-NH_2). In studies of peptides of one type or another, we expect that it is simply a matter of time until the HMQC experiment supplants the HETCOR experiment, which has been more traditionally utilized to establish the one-bond proton-carbon chemical shift correlations. HMQC offers superior sensitivity, resolution, and considerable time savings and, with present generation spectrometers, the data is absolutely no more difficult to acquire and process than conventional HETCOR data.

Applications to oligonucleotides.—Applications of the HMQC experiment in studies of oligonucleotides have also begun to appear. The first such application is found in the work of Sklenar *et al.* (81) in the assignment of the ^{1}H and phosphorus spectra of several oligonucleotides. Slightly after the work of Sklenar, a study of duplex d-$(GCATGC)_2$ utilizing HMQC was reported by Leupin *et al.* (82). Similar studies have been reported by a number of groups (83–85) and have led to the combined utilization of HMQC and HMBC, the latter to assign the non-protonated carbon resonances of oligonucleotides (86).

Applications to polynuclear aromatics.—The final chemical category we will consider is the heteroaromatic compounds. The first paper to apply HMQC to this class of compounds was the work of Legendre *et al.* (87), who have assigned the spectra and structures of a series of thieno[3,4-*b*]quinoxolines [**19**] and [**20**]. More recently, Berger and Diehl (88) have utilized the HMQC experiment in the assignment of a series of 2-substituted anthracenes. Finally, Luo *et al.* (89) have employed the HMQC experiment in concert with HMBC and HMQC-TOCSY in assigning the spectra of a pair of naphthobenzothienoquinolines [**21**] and [**22**], one of which had limited solubility, formed in a photocyclization reaction.

CORRELATION OF HETERONUCLEAR PAIRS OTHER THAN ^{1}H-^{13}C AND ^{1}H-^{15}N.—While there have been a number of papers dealing with the detection of low gamma nuclides via proton detection (90–93), most will not be of interest or utility in

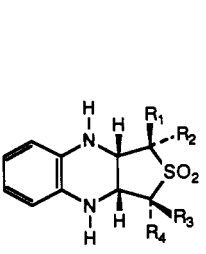

19

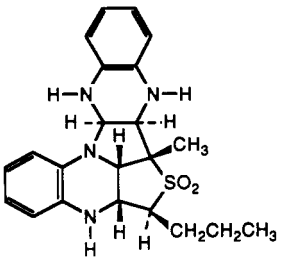

20

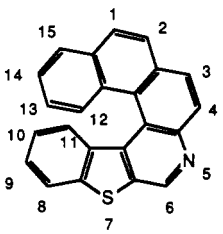

21

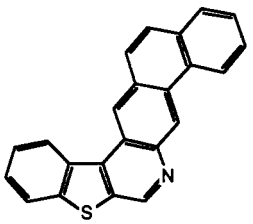

22

natural products structure elucidation. There have been two papers, however, which report the correlation of heteronuclear pairs that may have some application in natural products structure elucidation. The first effort of this type was a method for the correlation of ^{13}C-^{15}N heteronuclear chemical shift pairings by detection of the more abundant ^{13}C nuclide reported by Niemczura *et al.* (94). Unfortunately, despite the advantages of detecting ^{15}N via the more abundant ^{13}C, the method will still probably be restricted to labeled peptides. The other method was reported by Sims *et al.* (95) for the direct and long-range heteronuclear correlation of ^{13}C-^{31}P via the 100% abundant ^{31}P nuclide. Although applications of this method will be limited, and while it requires a triple resonance probe if the observation is to be made with proton decoupling, it is applicable to natural products and can be performed without labeling.

OPTIMIZING PARAMETERS PRIOR TO ACQUIRING SPECTRA.—One of the primary concerns regarding the optimization of the HMQC experiment is the suppression of the ^{1}H-^{12}C magnetization component. Experimentally, several ways to achieve this goal are available and have been discussed by Cavanagh *et al.* (68). The BIRD pulse (28) applied at the beginning of the Bax-Subramanian pulse sequence (17) shown in Figure 4 serves to selectively invert the ^{1}H-^{12}C component of proton magnetization. Superimposed over the function of the BIRD pulse is phase cycling, which is designed to subtract unwanted signals arising from ^{12}C species. In concert, the BIRD pulse and phase cycling routine effectively eliminate contributions from those protons directly bound to ^{12}C, as demonstrated by the proton reference and ^{13}C-satellite spectral segments shown in Figure 11.

Implicit in the acquisition of the ^{13}C-satellite spectrum is the selection of an appropriate delay for the fixed delays found in the HMQC pulse sequence. The fixed delays in the BIRD pulse and the delay used in the creation of heteronuclear multiple quantum coherence are the same and may nominally be optimized as a function of $\frac{1}{2}(^{1}J_{CH})$. For survey conditions with an aralkyl compound, compromise optimization for an average one-bond heteronuclear coupling of 140 Hz works quite well.

Given a reasonable choice for the optimization of the fixed delays, a decision must

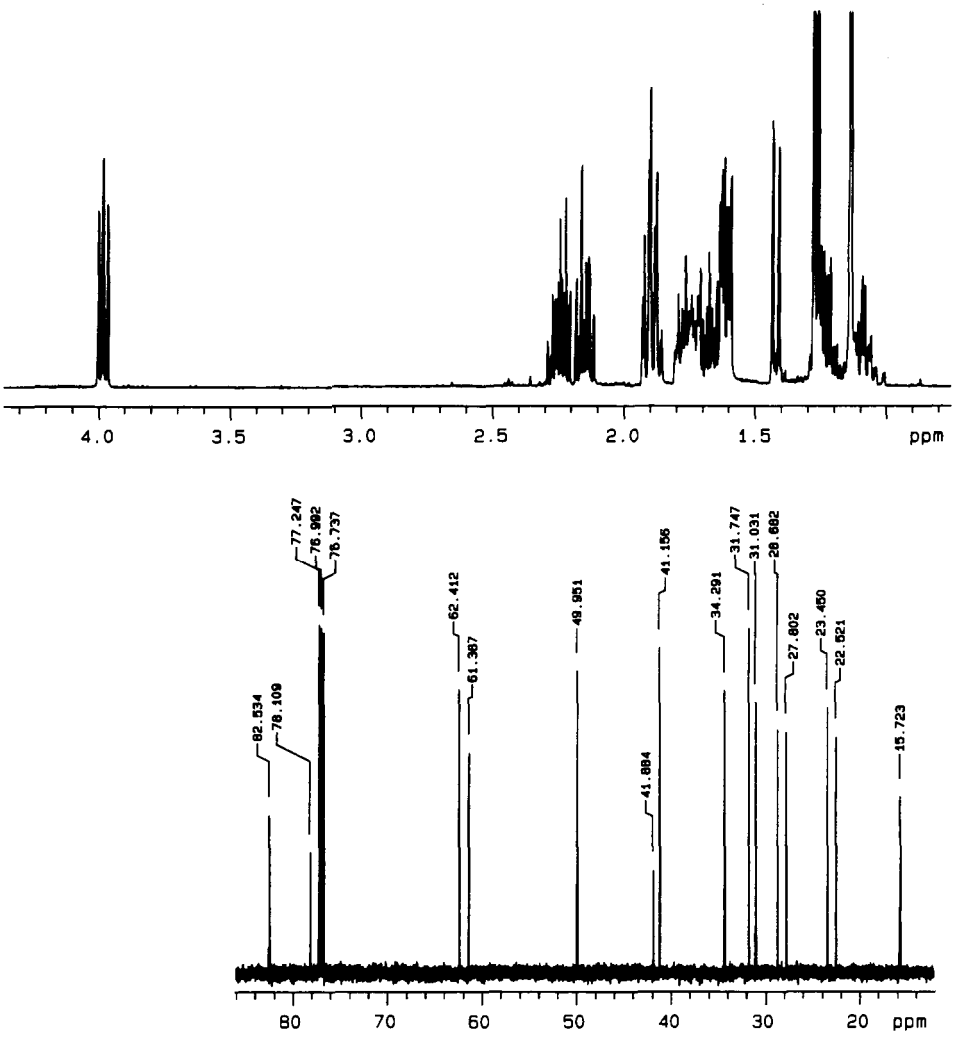

FIGURE 10. ^{1}H- and ^{13}C-nmr reference spectra of the degradation product of 1-bromomaaliol recorded at 500 and 125 MHz, respectively.

next be made regarding the digitization of both frequency domains. Levels of digitization in the proton, or F_2, frequency domain are dictated mainly by heteronuclear decoupling considerations, which typically limit acquisition times to the range of 200 to 300 msec. At an observation frequency of 500 MHz, this restraint still allows digitization with 2K data points. Where a limited carbon spectral window is to be observed, higher digitization can be employed, if necessary, since adequate heteronuclear decoupling can be obtained with lower decoupler duty cycles. Incrementation of the evolution period dictates resolution in the second frequency domain, F_1. Because of the sensitivity of the HMQC experiment, relatively limited numbers of transients may be acquired per evolution time increment, thereby allowing a reasonably generous choice of levels of digitization of the carbon spectral window. For general survey spectra, an initial choice of about 1 to 1.5 ppm digital resolution in the carbon spectrum is generally sufficient.

DETERMINATION OF THE STRUCTURE OF A DEGRADATION PRODUCT OF (1*R*)-BROMO-*ent*-MAALIOL.—To illustrate the application of inverse-detected 2D nmr techniques to natural products structure elucidation, we initially intended to employ a sam-

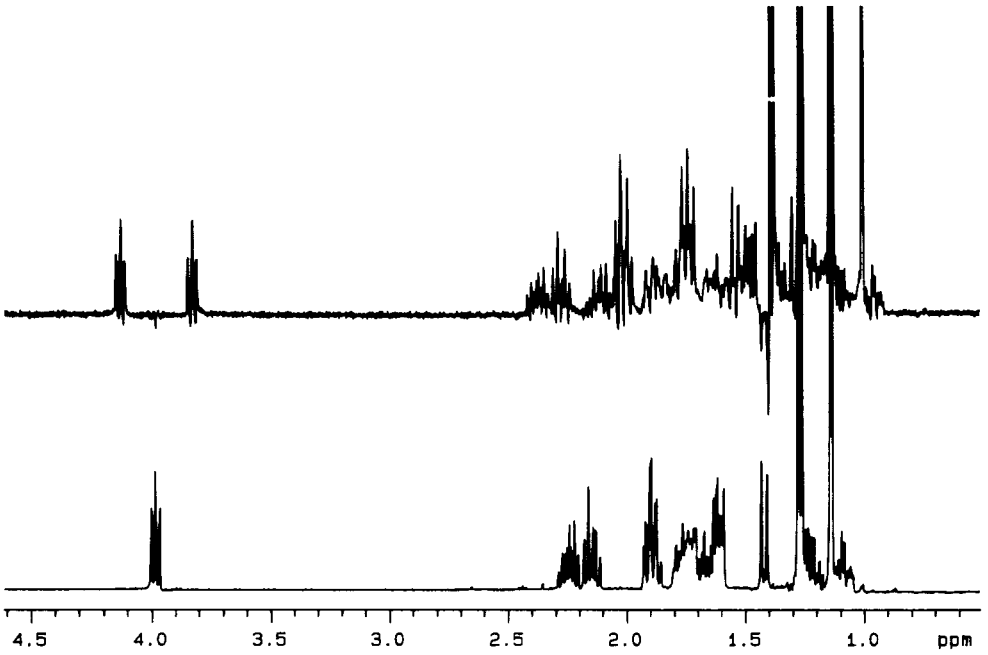

FIGURE 11. Satellite spectrum plotted above ^1H reference spectrum.

ple of a brominated marine sesquiterpene, (1*R*)-bromo-*ent*-maaliol [**23**] (1-bromomaaliol), which was previously characterized in collaboration with Barnekow *et al.* (96). However, when the sample (in $CDCl_3$ in a sealed 5-mm nmr tube that had been stored for 15 months) was examined, we obtained ^1H and ^{13}C reference spectra that were completely different from those recorded previously. The changes noted suggested decomposition or rearrangement of the compound, probably acid-induced, making this a true structure elucidation problem rather than a simple intellectual exercise in demonstrating the application of the inverse-detected 2D nmr experiments.

^1H and ^{13}C reference spectra recorded at 500 and 125 MHz, respectively, are presented in Figure 10. Comparison with the previously reported data (96) showed that the double doublet from the H-1 proton resonating at approximately 3.6 ppm was shifted downfield to 3.985 ppm as an apparent triplet. Another feature immediately apparent is the complete disappearance of the cyclopropyl protons resonating farthest upfield in the spectrum of 1-bromomaaliol along with the unusually upfield shifted H-5 and one of the H-9 resonances. These changes might be attributed to shifts in resonance position and multiplet appearance due to a change in solvent from C_6D_6, in the former study, to $CDCl_3$. However, they are also accompanied by massive changes in the ^{13}C

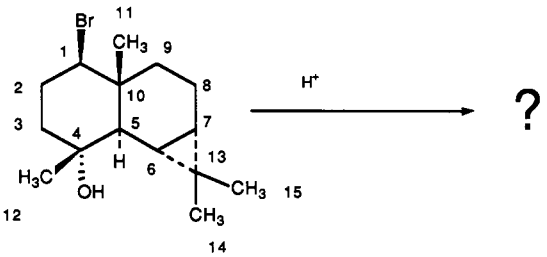

23

spectrum, which supports the contention that the molecule has undergone a degradative rearrangement rather than a simple shift in resonance positions. The first step in determining the structure of the molecule was to acquire a proton-detected heteronuclear multiple quantum coherence spectrum, which is discussed in the following section.

The HMQC spectrum of the degradation product of (*1*-R)-*bromo*-ent-*maaliol*.—Generally, the first step in acquiring an HMQC spectrum is the acquisition of a satellite spectrum to ascertain the number of acquisitions per increment of the evolution period that will be required. The satellite spectrum of 1-bromomaaliol is plotted above a ^1H reference spectrum shown in Figure 11. The HMQC spectrum of the degradation product of **23** is presented in Figure 12 flanked by high resolution ^1H and ^{13}C reference spectra. From these data we note that the HMQC spectrum contains resonances for four methyls, five methylenes, three methines, and, from the ^{13}C reference spectrum, three quaternary carbons. A cursory glance at the structure of **23** shows that the number of methyl and quaternary carbon resonances is unchanged, but the number of methine resonances has decreased by one, with a corresponding increase of one methylene resonance. Initial suspicions, based on changes in the reference spectra, that the molecule underwent degradation or rearranged in some fashion are now more strongly supported.

Utilization of the data contained in the HMQC experiment is parallel to the more familiar heteronuclear correlation or HETCOR spectra and no further explication is necessary. The tracking through the F_1 frequency domain at the chemical shift of the methyl resonances is worth mentioning. This is caused by cycling the experiment somewhat too fast relative to the T_1 relaxation time of the methyl resonances. As a general guideline, it is useful to measure the proton T_1 relaxation times and to cycle the ex-

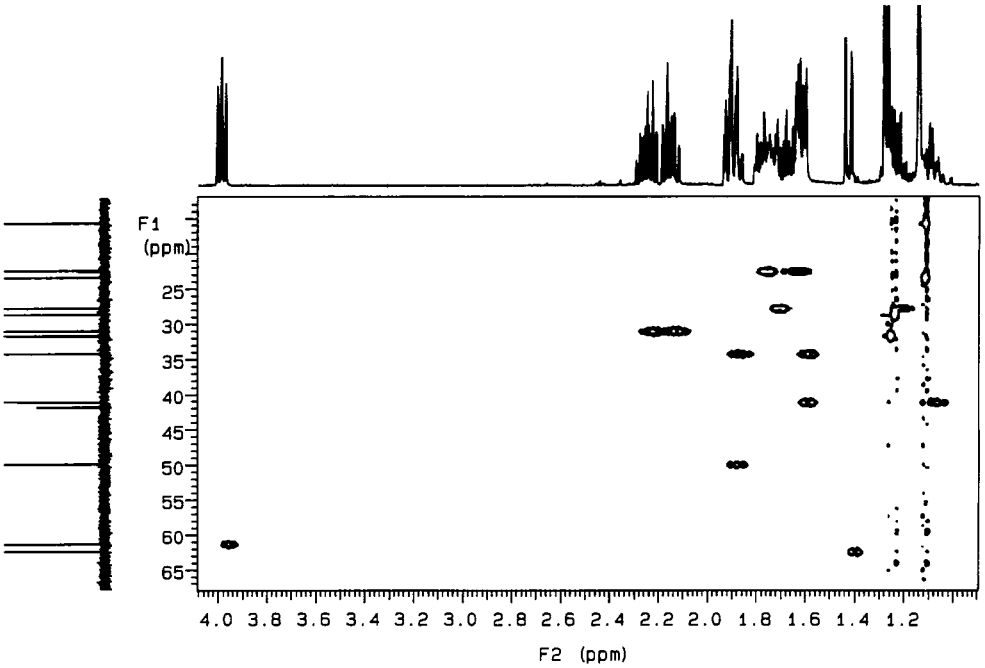

FIGURE 12. HMQC spectrum of the degradation product of 1-bromomaaliol recorded at 500 MHz. The spectrum is flanked by high resolution proton and carbon reference spectra. The HMQC spectrum contains resonances for four methyls, five methylenes, three methines, and, from the ^{13}C reference spectrum, three quaternary carbons. A cursory glance at the structure of **23** shows the number of methyl and quaternary carbon resonances is unchanged, but the number of methine resonances has decreased by one, with a corresponding increase of one methylene resonance.

periment so that the sum of the interpulse delay plus the acquisition time is at least 1.5 times the longest T_1 when feasible.

INVERSE-DETECTED HETERONUCLEAR RELAYED COHERENCE TRANSFER.— Heteronuclear relayed coherence transfer, the pioneering work described in papers by Bolton (12,13), can provide a powerful alternative means of obtaining vicinal proton-proton connectivities, especially when the proton spectrum is highly congested, thus precluding the now familiar COSY experiment. As an example, consider the COSY spectrum presented in Figure 13. Despite the fact that this spectrum was taken with high digital resolution and was zero-filled to 4K × 4K points during processing, there are still protons that are overlapped, e.g., the two resonating at exactly 1.614 ppm (based on a 2D *J*-resolved spectrum), which are bound to different carbons, making it difficult to track connectivities unequivocally through this point in a COSY spectrum. In principle, this problem can be circumvented by resorting to the relayed or RCOSY experiment described originally by Eich *et al.* (97). However, a more powerful alternative is found, in our opinion, in the heteronuclear relay experiments.

Lerner-Bax proton-detected HC-RELAY and HMQC-TOCSY (HMQC-HOHAHA).— Unfortunately, early heteronucleus-detected relayed coherence transfer experiments, whether the original experiment as described by Bolton (12) or Bolton and

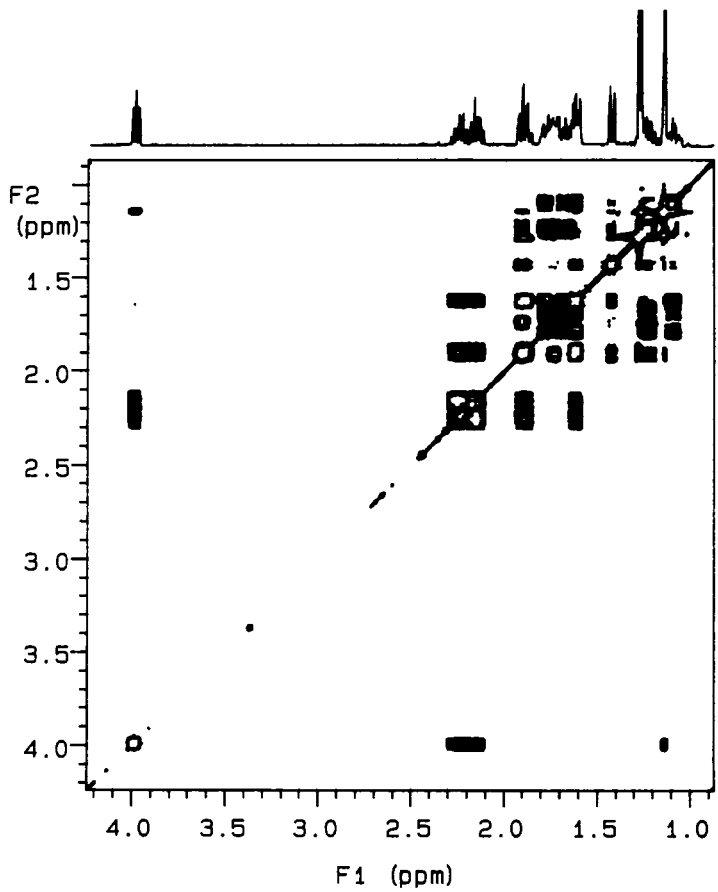

FIGURE 13. COSY spectrum of degradation product of 1-bromomaaliol. The data were recorded as 2K × 1K complex points and were processed with zero filling and symmetrization to give a final data matrix consisting of 4K × 4K points.

Bodenhausen (13) or the somewhat more sensitive variant proposed by Bax (14), suffered from a substantially lower level of sensitivity than did the HETCOR experiments (98). This detraction probably accounts for the relatively limited applications of the heteronucleus-detected experiment in natural products structure elucidation (98–105). The potential solution of the sensitivity problem was first addressed, however, by the report of a proton-detected variant of the heteronuclear relay experiment by Bolton (19). Bolton's report was soon followed by the work of Lerner and Bax (20), which reported a pair of proton-detected heteronuclear relay experiments. The technically less demanding first pulse sequence afforded a single relay in the fashion of its heteronucleus-detected predecessor. This pulse sequence, shown in Figure 14, was a simple modification of the Bax-Subramanian HMQC sequence (17), differing in the addition of a further 90° proton pulse $\frac{1}{2}({}^1J_{CH})$ after the re-creation of proton single-quantum coherence, which transferred coherence at the chemical shift of the directly bound carbon to the vicinal neighbor proton of the directly bound proton. Relayed response intensity with the pulse sequence shown in Figure 14, as with the earlier heteronucleus-detected experiment (98), is strongly dependent on the optimization of delays relative to the homonuclear vicinal scalar coupling constant.

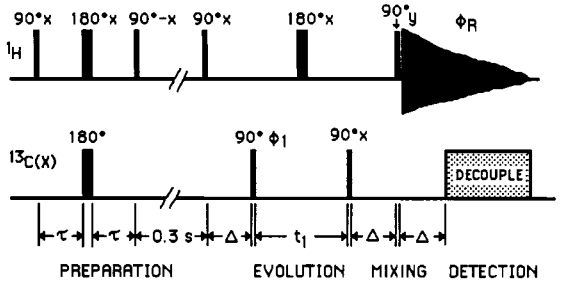

FIGURE 14. Proton-detected heteronuclear relayed coherence transfer pulse sequence proposed by Lerner and Bax. Delaying the initiation of heteronuclear decoupling by the period Δ brings the magnetization for the direct response into an antiphase alignment which is cancelled by the decoupling, leaving a spectrum showing only the relayed responses. For phase integrity of the data, accumulation was initiated at the end of the mixing period (cross-hatched area of FID), but the receiver was not enabled until the point when heteronuclear decoupling was initiated (solid black FID).

Lerner and Bax (20) delayed decoupling and receiver enabling by a fixed interval Δ after the relay period. This procedure eliminated direct responses. As noted in the discussion of the HMQC-TOCSY experiment below, it is sometimes convenient to retain the direct responses. In 1989, a paper reporting this variant of the pulse sequence shown in Figure 14 was reported by Gronenborn *et al.* (108), who used the abbreviation HMQC-COSY to refer to the experiment. To date, there has been a single application of HMQC-COSY reported (107), which unfortunately incorrectly referenced the paper by Gronenborn *et al.* (108) as a 1988 publication.

Fortunately, a second, much more flexible, experimental alternative was proposed in the work of Lerner and Bax (20). This pulse sequence reduced the dependence of the experiment on the optimization of the fixed duration delays relative to the vicinal scalar coupling constant by employing an MLEV-17 isotropic mixing period applied $\Delta = \frac{1}{2}({}^1J_{CH})$ after the re-creation of proton single-quantum coherence as shown in Figure 15A. Coherence is propagated as a function of the duration of the MLEV-17 isotropic

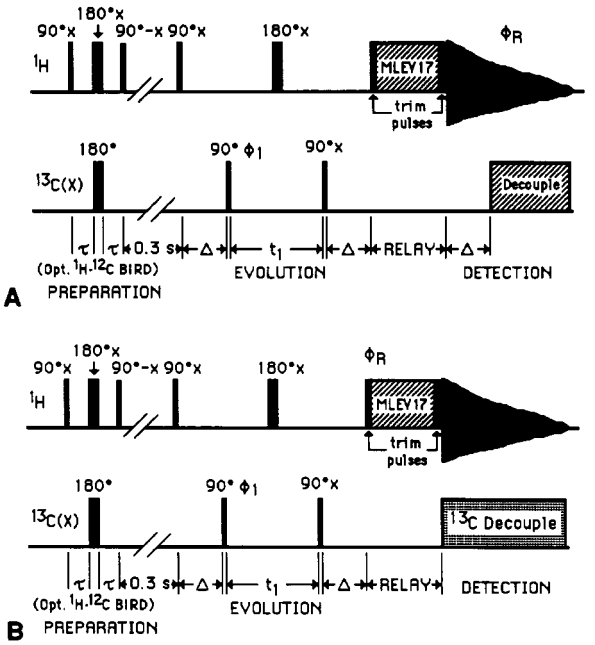

FIGURE 15. Proton-detected HMQC-TOCSY (HMQC-HOHAHA) pulse sequences. (A) Pulse sequence proposed by Lerner and Bax (20). By delaying decoupling for the period Δ, direct responses are eliminated from the spectrum. For phase integrity of the data, accumulation was initiated at the end of the mixing period (shaded area of FID), but the receiver was not enabled until the period Δ had elapsed. Actual data stored in memory are thus indicated by the solid black area of the FID. (B) Modified pulse sequence with decoupling and acquisition initiated simultaneously following the MLEV interval. This version of the pulse sequence affords a spectrum that contains direct responses that the authors have found useful for assignment purposes.

mixing interval, with vicinal responses observed with shorter mixing times. Responses at the chemical shift of contiguous protons that are further removed are observed at longer mixing times. After the work of Davis (21), we have begun referring to the MLEV-based Lerner and Bax experiment as HMQC-TOCSY, although this experiment is also referred to as HMQC-HOHAHA.

The Brühwiler-Wagner HMQC-RELAY experiment.—Soon after the paper describing the HMQC-RELAY and HMQC-TOCSY experiments by Lerner and Bax (20), a paper authored by Brühwiler and Wagner (29) appeared, reporting a slightly different pulse sequence for proton-detected HMQC-RELAY. Their pulse sequence is shown in Figure 16. In principle, if one follows the 90° carbon pulse at the end of the evolution period by the sequence τ_0-180°-τ_0 applied to carbon followed by a 90° pulse applied to proton, we obtain HMQC-RELAY. Unfortunately, all of the undesired components of magnetization that had been coaligned with the z′-axis are returned to the xy plane in this process, thereby creating a major phase-cycling problem if they are to be removed effectively. The sequence shown in Figure 16 is intended to circumvent these problems. The Brühwiler-Wagner HMQC-RELAY sequence (29), as originally published, did not include broadband heteronuclear decoupling. In most applications, it would probably be

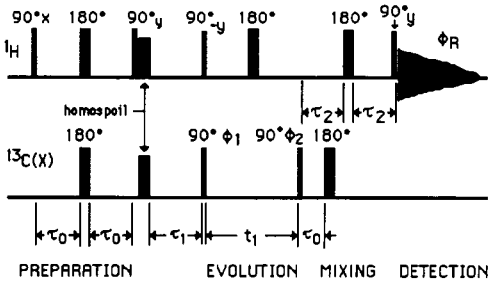

FIGURE 16. The Brühwiler-Wagner (29) pulse sequence for HMQC-RELAY.

preferable to incorporate broadband heteronuclear decoupling. Decoupling could be initiated coincident with the acquisition as shown in Figure 16 or, alternatively, it could be delayed by a fixed interval $\Delta = \frac{1}{2}(^1J_{CH})$ as in the experiments by Bax and Lerner (20) (Figures 14 and 15A), which would provide the means to eliminate direct responses.

The Bolton HMQC-RELAY pulse sequence.—Although presented last here, chronologically the HMQC-RELAY pulse sequence described by Bolton (19) predates those of Lerner and Bax (20) and Brühwiler and Wagner (29). Bolton's sequence is shown in Figure 17. There are no provisions for the elimination of undesired ^{1}H-^{12}C magnetization (e.g., through the use of a BIRD pulse or homogeneity spoiling pulses), thereby necessitating the utilization of a complex 256-step phase cycle. It is probably for this reason that this prototypical proton-detected RELAY experiment has had limited application.

APPLICATIONS OF HMQC-RELAY/TOCSY (HOHAHA).—Although they are relatively modest in number, there are applications of the proton-detected heteronuclear relay experiments found in the literature. Lerner and coworkers (70,73) have applied the HMQC-RELAY/TOCSY pulse sequences in the study of various carbohydrates. Davis (21) has applied the experiment to the problem of assigning the ^{1}H and ^{13}C spectra of the cyclic peptide, bradykinin. Torchia *et al.* (106) have applied the proton-detected HC-RELAY (Figure 14) technique to establish sequential assignments in the α-helical domains of staphylococcal nuclease. More recently, they have used both HMQC-RELAY and HMQC-TOCSY to determine sequential assignments and the solution structure of staphylococcal nuclease (107). Gronenborn *et al.* (108) have utilized HMQC, HMQC-COSY, and HMQC-NOESY for sequential proton resonance assignments in proteins based on ^{1}H-^{15}N multiple quantum coherence. Kessler *et al.* (109)

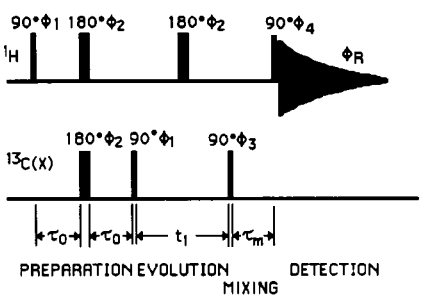

FIGURE 17. The pulse sequence for proton-detected heteronuclear relay proposed by Bolton (19).

have utilized the HMQC-TOCSY experiment to determine the solution structure of [Me-L-Leu7]didemnin B. In this application, although there have been several total spectral assignments of didemnins reported (75,110,111), the change in conformation and structural properties from Me-D-Leu to Me-L-Leu was so dramatic that a total reassignment became necessary. The authors utilized the HMQC-TOCSY experiment to identify spin system components in the congested proton spectra of polynuclear aromatics (89). They also established connectivities between overlapped protons and their vicinal neighbors in a sugar (112) and a polynuclear heteroaromatic (113) through the use of ^{13}C-coupled HMQC-TOCSY spectra. The strategy in the latter two papers was to take advantage of the large one-bond heteronuclear coupling to offset, by $\pm {}^{1}J_{CH}/2$, the components of the direct response, thereby allowing the observation of relayed responses that would otherwise be obscured. This approach to the utilization of HMQC-RELAY/TOCSY data is shown schematically in Figure 33.

INTERPRETING THE INFORMATION CONTAINED IN HMQC-RELAY AND HMQC-TOCSY SPECTRA.—In practice, we have found it useful to modify the Lerner-Bax pulse sequence shown in Figure 15A by eliminating the last fixed delay prior to the initiation of decoupling, which gives the pulse sequence shown in Figure 15B. This modification provides direct responses in the HMQC-TOCSY spectrum that we find convenient to retain for assignment purposes. In contrast, the sequence originally proposed by Lerner and Bax (20) brings the components of magnetization for the direct response into antiphase and then cancels them by initiating decoupling. There are several further options that will be discussed, but first it is important to consider the data generated in the experiment and some of the practical concerns associated with parameters.

Schematically, responses observed in a proton-detected heteronuclear relay experiment of the type shown in Figure 15B can be easily represented as shown in Figure 18

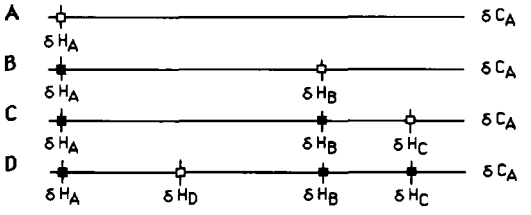

FIGURE 18. Schematic representation of responses observed at the chemical shift of C_A of **24** as a function of increasing durations of the isotropic mixing interval. (A) Response establishing the direct ^{1}H-^{13}C correlation observed using the HMQC experiment. Alternatively, this response would normally be the most intense response of the shortest-mixing-time HMQC-TOCSY spectrum. (B–D) Traces showing responses observed as a function of increasing mixing time durations in the HMQC-TOCSY experiment. For polynuclear aromatic compounds, we have found that durations of the mixing time of 12, 24, and 36 msec afford the response patterns shown in B through D, respectively. All responses have been retained through the entire series of schematically represented spectra above. The direct response will typically begin to decrease in intensity relative to that of its vicinal neighbor as the mixing time increases. With sufficiently long mixing intervals, the direct response would disappear from the trace, accompanied by the diminution of the intensity of the response at the vicinal neighbor, H_B and so on.

for a 1,2-disubstituted aromatic system such as that represented by **24**. Components like **24** provide essentially an ideally behaved model, because all of the proton-proton vicinal couplings are very similar in size. The direct proton-carbon pairings must first be established from an HMQC experiment. Then with the shortest mixing times, typically in the range of 10–15 msec or even less, we observe at the chemical shift of a given carbon, C_A, responses at the proton chemical shift of the directly bound proton, H_A, and at the chemical shift of its vicinal neighbor, H_B. As the mixing times increase into the range of 20–30 msec, the direct C_A/H_A response may decrease in intensity while the C_A/H_B response increases in intensity, accompanied in some cases by the appearance of response at the chemical shift of the vicinal neighbor of H_B which we will label H_C. With further increases in mixing time we may see the disappearance of the direct C_A/H_A response, a decline in the intensity of the C_A/H_B response, an increase in the intensity of the C_A/H_C response, and even the appearance of a C_A/H_D response.

The approach described in Figure 18 is useful and routinely employed with heteronuclear-relayed coherence transfer 2D nmr data. This approach has been used extensively in the work of one of the authors for polynuclear aromatic spectral assignment (114–119). While useful, particularly when the ^{1}H-nmr spectrum is reasonably well dispersed, this approach can become confusing when the ^{1}H spectrum is more heavily overlapped, even in the absence of strong coupling. Such is typically the case with the ^{1}H-nmr spectra of natural products. Hence, an alternative method for digesting the information contained in natural product heteronuclear-relayed coherence transfer spectra is needed and, in fact, readily available. Two-dimensional nmr spectra are nothing more than large data matrices. An operation easily performed on any 2D nmr spectrum is transposition, a process in which the axes are interchanged. We are more accustomed to examining heteronuclear relay data plotted so that the proton chemical shift axis runs horizontally while the carbon chemical shift axis is vertical. This presentation is amenable to analysis in the fashion described above. A somewhat different picture is obtained from the transposed spectrum, whether actually plotted or by simple interpretation in a "transposed" fashion along the orthogonal axis. By examining information content as a function of a proton rather than a carbon chemical shift axis, we will begin with a response at the chemical shift of the directly bound carbon in the HMQC spectrum. At somewhat longer mixing times, new responses appear, but in this orientation they will be at the chemical shift of the vicinal neighbor proton's directly bound carbon. In this fashion, we obtain information equivalent in content to that obtained from the SELINADEQUATE experiment recently proposed by Berger (120), and we begin to assemble the carbon skeleton. Schematically, using **24** as an example, we obtain the information presented in Figure 19 from the same series of HMQC-TOCSY spectra as employed in the previous analysis, assembling the carbon framework as a function of increasing mixing times.

The assemblage of the proton-proton spin connectivity network in natural products can also become more complicated than the linear four-spin system used as an example above. Difficulties arise in that the proton chosen as a starting point may have couplings

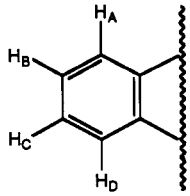

24

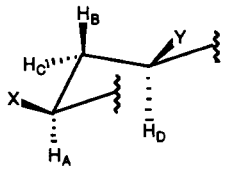

25

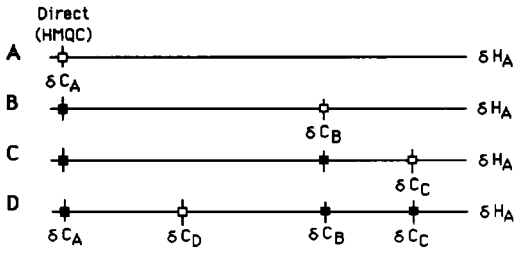

FIGURE 19. Schematic representation of an HMQC-TOCSY spectrum, examining carbon responses at a constant proton chemical shift (transposed presentation). Hypothetical data presented are derived from **24** and are analogous to those presented in Figure 18.

to anisochronous vicinal neighbor protons that are vastly different in size. Consider, for example, the structural fragment represented by **25**. Obviously, this can lead to the appearance of a response to one of the vicinal neighbors much earlier than to the other. Extrapolating, the vicinal neighbor of H_B, H_D in this case, may even appear prior to the response for H_C, the second vicinal neighbor of our starting point, H_A. In this case, care must be taken, but it will generally be apparent that this has happened if the HMQC spectrum is used as a reference point from which to follow the rise of responses as a function of the duration of the spin propagation interval. A schematic representation derived for **25** is presented in Figure 20.

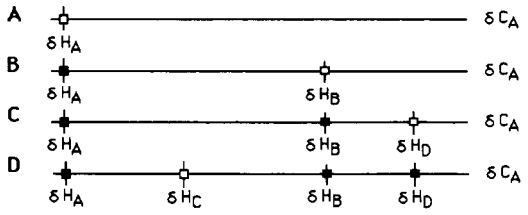

FIGURE 20. Schematic representation of responses that would be expected at the chemical shift of the C_A resonance as a function of increasing mixing time for the hypothetical structural fragment **25**. The first response observed would be for the relay of magnetization from H_A to H_B via the large vicinal coupling. It is quite plausible that the next response to be observed would be due to H_D because the coupling between H_B and H_D is substantially larger than that between H_A and H_C. In such instances, care must be taken to interpret the HMQC-TOCSY data relative to the HMQC spectrum, which would identify anisochronous methylene protons.

APPLICATION OF THE HMQC-TOCSY EXPERIMENT TO THE DEGRADATION PRODUCT OF 1-BROMOMAALIOL.—Figure 21 contains the first of a series of HMQC-TOCSY spectra and was recorded with an isotropic mixing interval of 6 msec, requiring an accumulation time of 2 h 20 min. This spectrum was recorded with ^{13}C WALTZ decoupling during the acquisition period, which limits the duration of the acquisition time as a function of the duty cycle of the amplifier used in the WALTZ decoupling. Practically, with the VXR-500S used to collect this data (and a 100% duty cycle), we were restricted to an evolution time of 150–220 msec before heating of the sample from

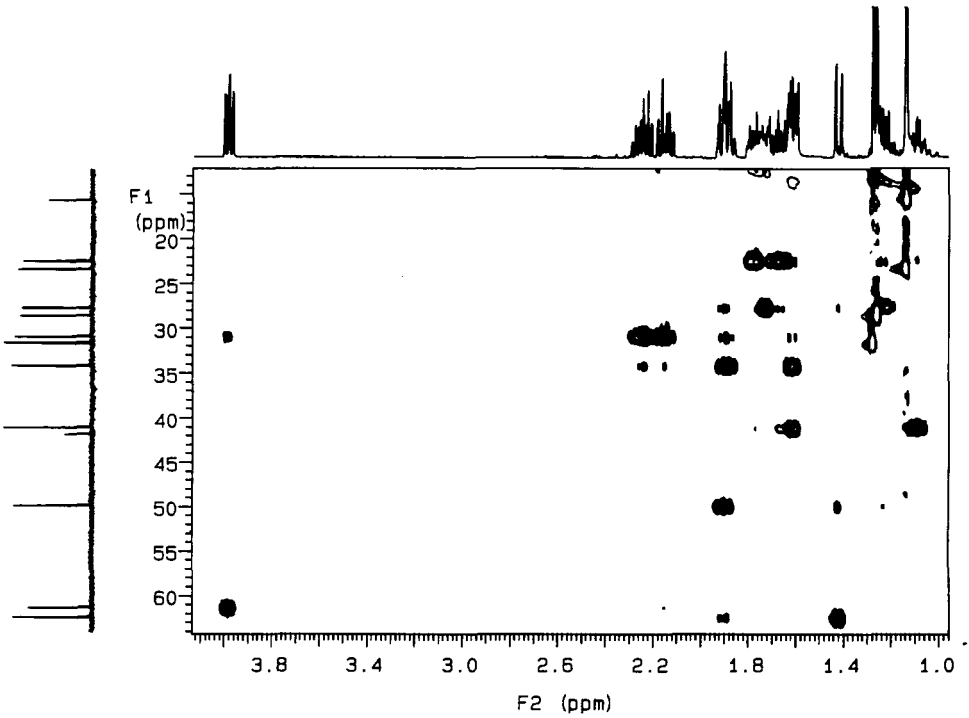

FIGURE 21. HMQC-TOCSY spectrum of the degradation product of 1-bromomaaliol [**23**] recorded using the pulse sequence shown in Figure 15B with a mixing time of 6 msec.

the decoupling became a factor, degrading cancellation of the residual ^{1}H-^{12}C signal. Clearly, there will be instances when longer evolution times are desirable. One solution is to simply forego ^{13}C-decoupling during the acquisition period, thereby allowing acquisition periods as long as one would like. This approach has been applied in these laboratories to both sugars (112) and polynuclear aromatic compounds (113). Data obtained with other mixing times are presented in Figures 22–24.

Other key parameters in the HMQC-TOCSY experiment are the calibration of the pulses used in the MLEV-17 isotropic mixing interval. We find it convenient to calibrate the 90° pulse used for the isotropic mixing phase of the experiment at a somewhat lower power setting relative to pulses used in the prior phases of the experiment. Typically, 90° pulses in the range of 30–40 μsec work quite well in the isotropic mixing interval and can be obtained at power levels about 9 dB below full power pulses. The only other key parameters are the null and recycle intervals. In general, we have found it unnecessary to optimize the null interval following the BIRD pulse in the HMQC-TOCSY pulse sequence (Figure 15B) with any particular care; delays in the range of 0.3–0.4 sec work well. Likewise, we have not found it necessary to pay particular attention to the optimization of the interpulse delay either; good results can be obtained for a wide variety of types of molecules with an interpulse delay on the order of about 1–1.5 sec.

Given this preamble, let us return our attention to the problem of elucidating the structure of the degradation product of 1-bromomaaliol [**23**]. As was noted in the discussion of the HMQC spectrum above, there was a decrease of one in the number of methine resonances, with a concurrent increase of one methylene resonance. Clearly, the next task is to begin assembling the one-dimensional nmr data into usable structural fragments.

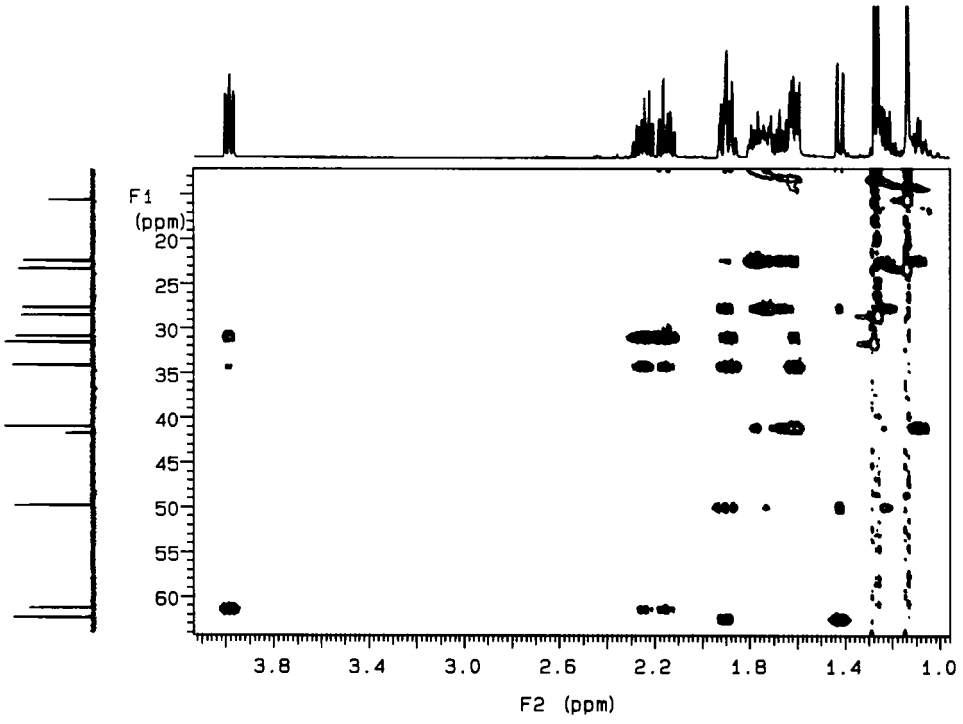

FIGURE 22. HMQC-TOCSY spectrum of the degradation product of 1-bromomaaliol [23] recorded using the pulse sequence shown in Figure 15B with a mixing time of 14 msec.

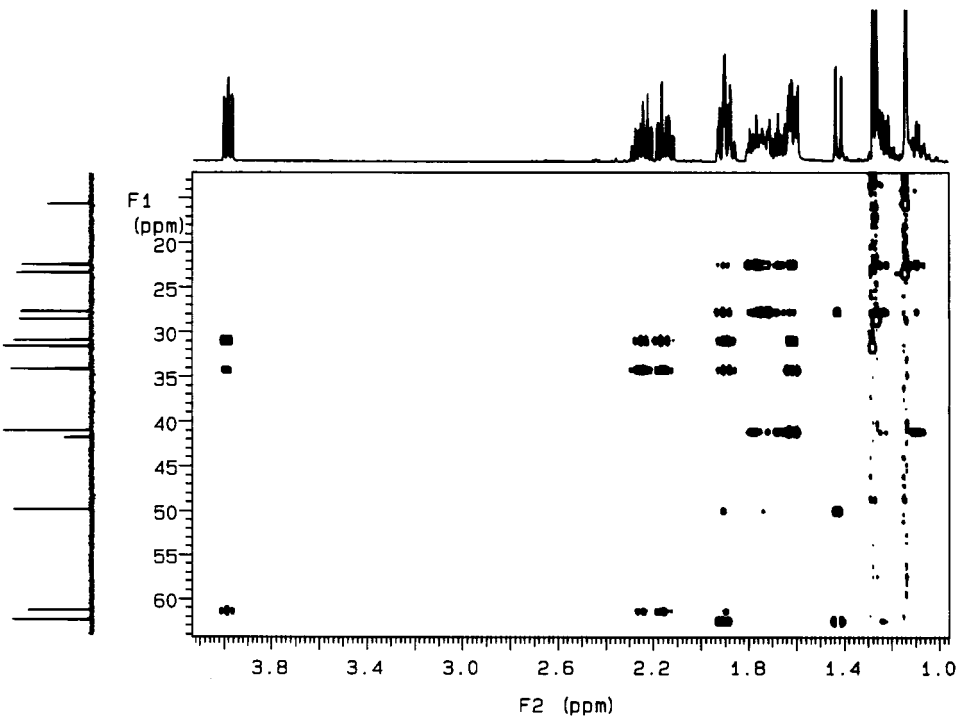

FIGURE 23. HMQC-TOCSY spectrum of the degradation product of 1-bromomaaliol [23] recorded using the pulse sequence shown in Figure 15B with a mixing time of 24 msec.

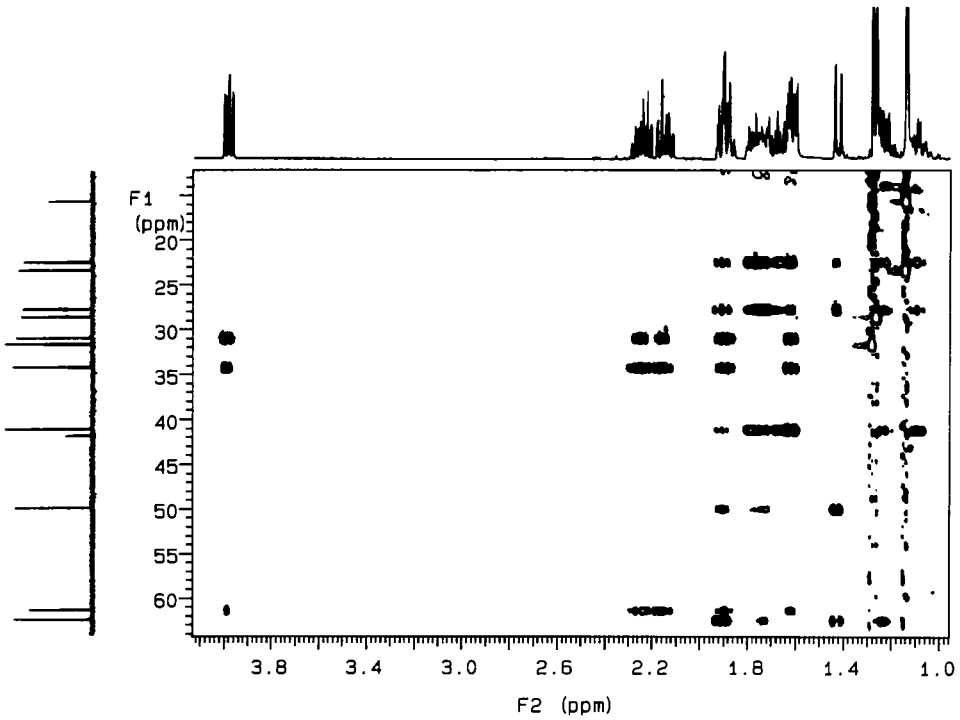

FIGURE 24. HMQC-TOCSY spectrum of the degradation product of 1-bromomaaliol [**23**] recorded using the pulse sequence shown in Figure 15B with a mixing time of 32 msec.

Starting from the methine proton resonating farthest downfield at 3.986 ppm (direct carbon 61.38 ppm, HMQC) (Table 1) we observed from the COSY spectrum (Figure 13) that this proton was coupled to two further protons, constituting an AB pair that was centered at 2.250/2.145 ppm. At the carbon chemical shift (61.38 ppm, HMQC) of the direct response for the proton resonating at 3.986 ppm, a weak response relayed to the upfield proton of the anisochronous pair resonating at 2.145 ppm is observed with a mixing time of 6 msec. At a mixing time of 14 msec (Figure 22), strong responses are observed to both of the strongly coupled protons but no farther. At this point, if no data for longer mixing times were available, we could simply examine responses along the chemical shift axis of the AB pair, 31.04 ppm from the HMQC spectrum. For the moment, rather than pursuing further assignments along other chemical shift axes, let us instead look at the effect of the duration of the isotropic mixing interval. As we proceed from Figure 22 to Figure 23, the latter with a mixing time of 24 msec, we note that there is a weakening of the direct response and the vestige of a response beginning to appear at 1.902 ppm. Finally, with the 32 msec HMQC-TOCSY spectrum, which is shown in Figure 24, we observe propagation from the 2.250/2.149 ppm anisochronous methylene pair to a further pair of anisochronous methylene resonances at 1.902 and 1.614 ppm. From the HMQC spectrum (Figure 12) the directly bound carbon for this pair of protons resonates at 34.30 ppm.

Following along the axes defined by the carbon chemical shifts of 31.03 and 34.30 ppm, we note that no further connectivities may be established, suggesting that the second methylene carbon resonating at 34.30 ppm must be bound to either a quaternary carbon or a heteroatom, the former far more likely on the basis of chemical shift. These operations lead us to the partial structure represented by **26**. While considering the other chemical shift axes, note that the connectivity network established above

TABLE 1. Comparison of the ^1H- and ^{13}C nmr Chemical Shifts of (1*R*)-Bromo-*ent*-maaliol [**23**] and Its Degradation Product, 1-Bromomaalioxide [**30**].

Position	Compound					
	23 (C_6D_6, 300 MHz)			**30** ($CDCl_3$, 500 MHz)		
	Chemical Shift		mult.	Chemical Shift		mult.
	^1H (ppm)	^{13}C (ppm)		^1H (ppm)	^{13}C (ppm)	
1	3.55	67.5	d	3.986	61.38	d
2	2.50, 1.90	31.5	t	2.250, 2.149	31.04	t
3	1.28, 1.05	42.8	t	1.902, 1.614	34.30	t
4	—	71.2	s	—	78.11	s
5	0.44	47.7	d	1.422	62.43	d
6	0.53	23.0	d	1.888	49.96	d
7	0.45	21.0	d	1.732, 1.231	27.80	t
8	1.73, 1.43	16.8	t	1.781, 1.662	22.52	t
9	1.82, 0.45	39.5	t	1.614, 1.090	41.17	t
10	—	40.1	s	—	41.89	s
11	1.30	16.2	q	1.134	15.72	q
12	0.85	30.1	q	1.277	31.75	q
13	—	18.8	s	—	82.53	s
14	0.95	29.5	q	1.142	23.44	q
15	0.75	16.7	q	1.261	28.68	q

could be derived from the trace at 31.04 ppm in the 6-msec experiment (Figure 21). Likewise, using the axis of the second methylene carbon at 34.30 ppm, we first identify the anisochronous methylene protons resonating at 2.250/2.149 ppm in the 6-msec spectrum followed by the inclusion of the proton resonating at 3.986 ppm in the 14-msec experiment (Figure 23).

Clearly, the structural fragment just assembled is highly reminiscent of the C-1–C-3 fragment of 1-bromomaaliol [**23**]. The methine carbon is shifted upfield relative to **23**, as is the methylene carbon resonating at 34.30 ppm. These changes could possibly be interpreted as either an intramolecular S_N2 reaction with displacement of bromide to form a bicyclo[2.2.1] system in place of ring A of **23** or a significant change in the conformation of this ring for some other reason. The former is not unprecedented and would give **27**, assuming the stereochemistry of the A/B ring juncture of **23**. This structure is, however, difficult to rationalize in terms of the chemical shift of the methine carbon, which would normally be expected to shift downfield rather than upfield in converting **23** to **27**.

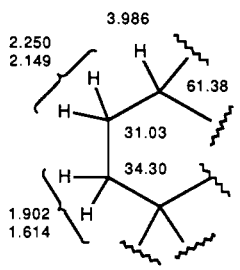

26

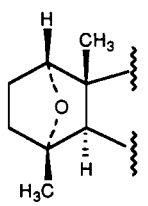

27

Before either of the conjectural possibilities just presented can be pursued, it is necessary to assemble more structural information. A second useful starting point to pursue the structure of the degradation product of **23** is afforded us by the methine proton/carbon pair resonating at 1.422/62.43 ppm. Rather than interpreting the data in Figures 21–24 in the fashion just described, it is illuminating to use the alternative approach to the interpretation of HMQC-TOCSY data described above. Examining the 6-msec HMQC-TOCSY spectrum shown in Figure 21 in the vertical direction along the proton chemical shift axis of 1.422 ppm (this is equivalent to a horizontal slice taken from the transposed data matrix of Figure 21), a moderate intensity response is observed at 49.96 ppm in F_1 with a still weaker response at 27.80 ppm in F_1 arising from a methine and a methylene carbon, respectively (HMQC, Figure 12).

The cyclopropyl protons of **23** were not observed, presumably a consequence of the opening of the cyclopropyl ring. When considered in conjunction with the loss of a methine and the gain of a methylene resonance, we have, at this point, accounted for all of the methine resonances of the structure with the contiguous methine resonances at 62.43 and 49.96 ppm just identified.

The intensity of the 49.96 and 27.80 ppm responses along the 1.422 ppm chemical shift axis increases in the 14-msec spectrum (Figure 22), while that of the direct response begins to wane. No new information is observed in the 24-msec spectrum (Figure 23), but we do observe a response to another methylene carbon resonating at 22.52 ppm in the 32-msec spectrum (Figure 24). At this point, examining the responses horizontally along the 22.52 ppm axis in the 32-msec HMQC-TOCSY spectrum, we note a response to the proton resonating at 1.090 ppm that is part of yet a further anisochronous methylene pair, its counterpart resonating at 1.614 ppm in a heavily congested region of the spectrum.

Through the series of connectivities just delineated, we have accounted for all of the methine and methylene resonances and can assemble the five-carbon structural fragment represented by **28**. At this point, we must account for the two downfield quaternary carbon resonances and the methyl resonances. It is also appropriate at this point to consider the mass spectral data.

As suggested above, it is useful to consider the transposed data. This approach illustrates the propagation of magnetization in a useful manner in that it effectively delineates the carbon skeleton as we go. Focusing our attention on the methine proton resonating at 1.422 ppm, a series of contour regions was plotted from the series of HMQC-TOCSY spectra that we have been considering. Thus, as a function of increasing mixing time, as presented in Figure 25, we may construct the carbon backbone one carbon at a time.

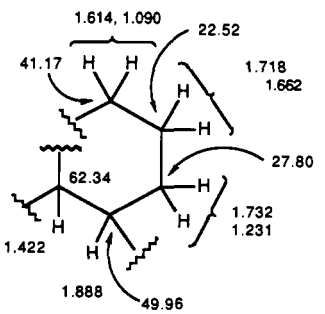

28

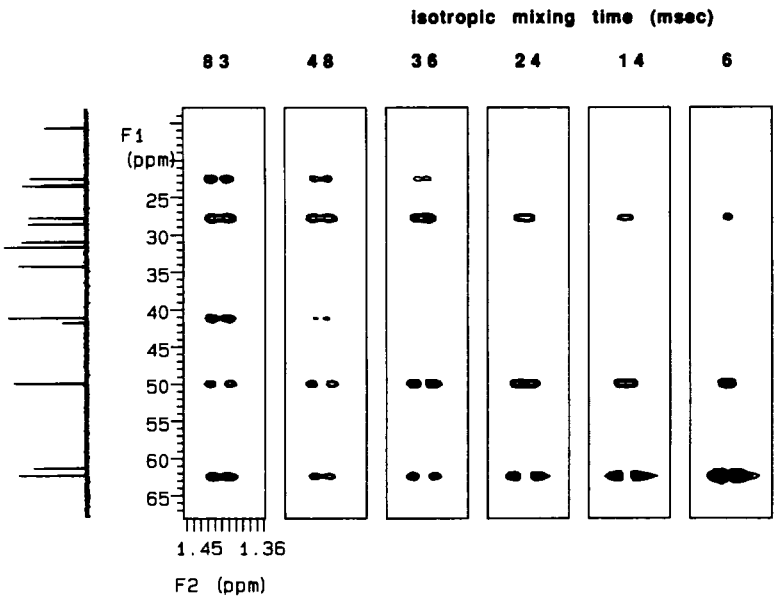

FIGURE 25. Segments from a series of HMQC-TOCSY spectra of the degradation product of 1-bromomaaliol [**23**] recorded using the pulse sequence shown in Figure 15B with mixing times ranging from 6 to 83 msec. Only the region of the spectrum corresponding to the methine proton resonating at 1.422 ppm (HMQC, 62.34 ppm) is shown. Propagation of magnetization along the contiguous protons allows the assemblage of the carbon skeleton **28**, the protons simultaneously assigned.

ASSEMBLING OTHER FRAGMENTS OF STRUCTURAL INFORMATION.—No parent ion was observed with eims or cims, although there were a pair of ions observed at $m/z = 285/287$ with intensities consistent with a bromine isotope pattern. On this basis, bromine was apparently retained in the degradation product. While **23** gave an ion corresponding to the loss of water $[M - H_2O]^+$ ($m/z = 282/284$), the counterpart in the case of the degradation product was clearly not observed, suggesting that the hydroxyl group might be tied up as an ether. This leaves open the possibility of an intramolecular S_N2 reaction to give a species such as **27** involving the connectivities from structural fragment **26**. Concurrent with the intramolecular S_N2 reaction, however, we must have reincorporated HBr into the structure of the degradation product. Structure **29** may be postulated to account for the intramolecular nucleophilic displacement and incorporation of the HBr. Another alternative structure may be proposed and is represented by **30**, which would also entail the opening of the cyclopropyl ring but incorporates reaction of the 4-hydroxyl group to give a highly substituted tetrahydrofuran system. The latter proposed structure retains the bromine and stereochemistry at the 1-position of **23**, and we must, therefore, invoke conformational changes to account for the observed changes in the chemical shift of the H-1 and C-1 resonances. The corresponding sesquiterpene analogue **31** of maaliol was reported in the 1964 work of Narayanan *et al.* (121).

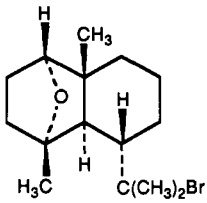

29

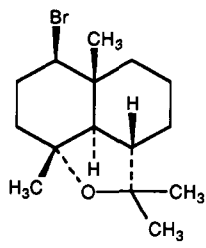

30

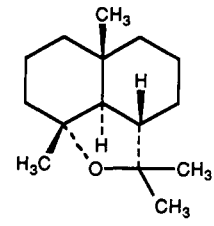

31

LONG-RANGE PROTON-DETECTED HETERONUCLEAR CHEMICAL SHIFT CORRELATION (HMBC).—Carbon-detected heteronuclear chemical shift correlation spectra have been an area of intensive investigation since about 1984 and have been the subject of a recent review by Martin and Zektzer (16). Relative to the direct heteronuclear correlation experiment, the long-range variants suffer from reduced sensitivity and problems with one-bond modulations that can cause losses of long-range responses to a given carbon as a function of the modulations of signal intensity for that carbon caused by its directly attached proton (16, 122–129). While modified long-range heteronuclear correlation experiments have been devised to circumvent this, the issue of low sensitivity has not been solved for heteronucleus-detected long-range correlation experiments. A solution has been provided, however, by the proton-detected heteronuclear multiple bond correlation (HMBC) experiment described in 1986 by Bax and Summers (18). The pulse sequence is shown in Figure 26 and differs from the heteronuclear multiple quantum experiments that have been considered thus far in this review. Most readily

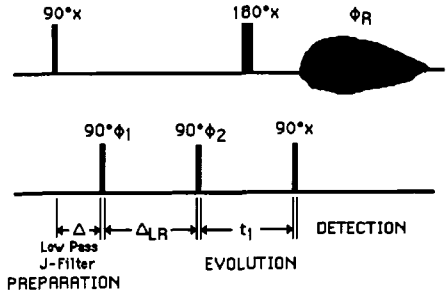

FIGURE 26. Heteronuclear multiple bond correlation (HMBC) pulse sequence proposed by Bax and Summers (18). The first 90° proton pulse creates transverse proton magnetization in the xy plane. The low pass *J*-filter is optimized as a function of the one-bond coupling to bring the components of proton magnetization, driven by $^1J_{CH}$, antiphase at the end of the interval, Δ. The 90° carbon pulse applied at this point creates one-bond multiple quantum coherence. By cycling the phase of the first 90° carbon pulse as 02022020 . . . , the undesired one-bond component of magnetization is ultimately added and then subtracted (filtered) from the FID. After a further period of time, Δ_{LR}, a second 90° carbon pulse is applied to create multiple quantum coherence from the desired long-range proton-carbon couplings. This magnetization is manipulated as in the HMQC experiment, reconverted to observable proton single quantum coherence, and recorded.

notable is the absence of the BIRD pulse at the beginning of the experiment. Because we will be dealing with two markedly different components of heteronuclear multiple quantum coherence in this experiment, it is possible to treat the coherences differently. Following the first 90° proton pulse after a fixed delay, $\Delta = \frac{1}{2}({}^1J_{CH})$, the first 90° carbon pulse creates heteronuclear multiple quantum coherence for the one-bond components of magnetization. These undesired components of magnetization are eliminated by a process known as low-pass *J*-filtering (130), which was first implemented in carbon-detected heteronuclear relayed coherence transfer experiments. By inverting the phase on successive transients, giving a 02022020 . . . phase cycle for the first 90° carbon pulse, we generate components of multiple quantum coherence that cancel one another after even numbers of transients. While the process just described is occurring in any given transient, the magnetization components that eventually lead to long-range multiple quantum coherence continue to evolve, driven by the much smaller long-range heteronuclear coupling constant. At a suitable point, typically 50–110 msec after the first proton 90° pulse, a second carbon 90° pulse is applied, converting now the long-range components of magnetization into heteronuclear multiple quantum coherence. Evolution of the long-range heteronuclear multiple quantum coherences continues through the evolution period with a 180° pulse applied midway, interchanging zero- and double-quantum terms in a manner analogous to the HMQC experiment described above (24). At the end of the evolution period, heteronuclear multiple quantum coherence is reconverted to observable proton single-quantum coherence, which is then detected without decoupling (18).

Partially phase-sensitive HMBC.—Phase modulation of the detected proton signal by homonuclear scalar coupling initially caused problems precluding the acquisition of phase-sensitive spectra. Bax and Marion (131) have addressed this problem. Their method affords data that are phase-sensitive in one dimension and require mixed-mode processing. A hypercomplex transform of the data was performed, resulting in data that are absorptive with respect to ^{13}C, after which an absolute value calculation is performed in the proton dimension. According to this work, their approach offers a $\sqrt{2}$ improvement in sensitivity plus significantly better ^{13}C resolution.

Phase-sensitive HMBC.—Williamson *et al.* (132) carried the work of Bax and Marion (131) a step further by assuming that a modest amount of phase modulation due to scalar coupling would be negligible, thereby allowing two-dimensional phase-sensitive presentation. Their pulse sequence is shown in Figure 27. This sequence differs from

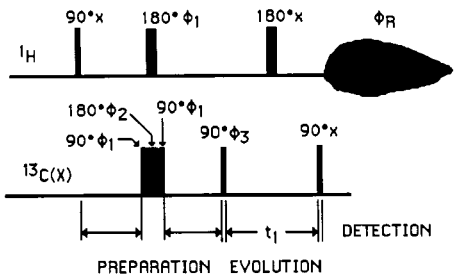

FIGURE 27. Phase-sensitive proton-detected long-range shift correlation pulse sequence proposed by Williamson *et al.* (132) to provide absorptive data in both frequency domains. The sequence has been demonstrated to work for distamycin A [**32**], which exhibits only modest (2 Hz) scalar coupling.

the more familiar HMBC sequence in the elimination of the low-pass *J*-filter, placement of a 180° proton and composite 180° ($90°_x$-$180°_y$-$90°_x$) carbon refocusing pulses midway through the interval, which corresponds to Δ_{LR} of the HMBC experiment, and storage of alternate scans in separate memory locations to allow hypercomplex transformation of the data.

In the example reported (132) in which homonuclear couplings were about 2 Hz, the method shown in Figure 27 allowed the observation of crucial $^4J_{CH}$ couplings from the H-5 aromatic protons to the carbonyl, linking one pyrrole to the preceding pyrrole ring in the DNA-binding drug distamycin A [**32**]; these couplings were necessary for a complete assignment. For example, H-5C was four-bond-coupled to the amide carbonyl between pyrrole rings B and C. In similar fashion, H-5B was coupled to the amide carbonyl between rings A and B. The corresponding coupling from H-5A to the carbonyl of the amidine-containing side-chain was not observed. The authors contend that without the improvement in sensitivity offered by fully phase-sensitive data the observation of these H-5-carbonyl connectivities would not be possible. It remains to be seen if this experiment will have wider utility, as this is presently the only application.

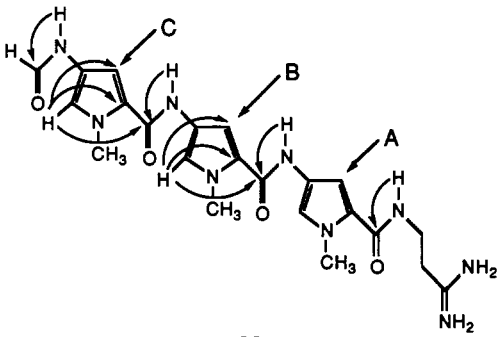

32

Parameterization of HMBC experiments.—Parameterization of the HMBC experiment is a more critical concern than with the HMQC-TOCSY experiment. Fixed delays are normally optimized as a function of $\Delta = \frac{1}{2}(^1J_{CH})$ and $\Delta_{LR} = \frac{1}{2}(^nJ_{CH})$ where n= 2, 3. If heteronuclear coupling constants are unknown, which is usually the case, optimization of Δ based on an assumed average one-bond coupling constant of 140 Hz works quite well. Typically, we have found it useful to optimize the Δ_{LR} delay for values in the range of 10 Hz (50 msec) to about 6 Hz (83 msec) for survey spectra, although values within the range of 20–110 msec also work quite well when the application warrants. Optimizations of about 10 Hz work quite well with highly rigid systems as encountered with some alkaloids, e.g., strychnine and aromatics, while the latter (6 Hz) works well with terpenes, peptides and other less rigid molecules.

The interpulse delay, if high quality data are to be obtained, should generally be set to a minimum of 1.5 × the longest proton T_1. If this approach is to be used, we find it useful to actually determine the proton T_1 relaxation times from an inversion-recovery experiment, which normally takes less than 5 min. If there are numerous or tightly clustered methyl singlets in the proton spectrum, it may be preferable to consider employing "steady-state pulses" of the form homospoil–90°–homospoil at the beginning of every interpulse delay to begin each transient with exactly the same magnetization.

As an alternative to setting the interpulse delay on the basis of T_1 relaxation time, an experimental method for selecting the interpulse delay and the number of transients based on the HMQC experiment has worked well in our hands. First, you can acquire an

"HMQC" spectrum without using either the BIRD pulse or ^{13}C decoupling during the acquisition period. By running a series of these experiments in which the interpulse delay is systematically varied, the optimal delay can be selected on the basis of the spectrum affording the best suppression of the ^{1}H-^{12}C signal. This approach also assumes accurately calibrated pulses. Second, after choosing the best interpulse delay, a single-increment HMBC spectrum can be acquired with an appropriate long-range optimization (e.g., 10 Hz), which is periodically inspected during accumulation for the long-range responses. In this fashion, when adequate signal-to-noise for the long-range responses is obtained you will have an estimate of the number of transients needed per increment of the HMBC experiment.

Finally, as with all of the inverse-detected 2D nmr experiments, it is advisable to run the experiment without spinning the sample but with temperature regulation.

APPLICATIONS OF HMBC.—There have been numerous applications of the HMBC experiment in the four years since the inception of the technique. Quite probably, the number of applications of HMBC have been much higher than corresponding HMQC applications because there is a perceived need for broadband heteronuclear decoupling during acquisition with HMQC, a feature still not available on many spectrometers. Levels of sophistication in the applications of the HMBC experiment have varied dramatically. In some instances, a selective one-dimensional experiment would have been more appropriate. In other cases, the applications have been truly elegant. The topic of HMBC has been very briefly reviewed by Seto (133) with some applications described. A much more comprehensive presentation of applications, subgrouped by broad class of compounds, follows the order of presentation, insofar as possible, that was established during our discussion of HMQC applications.

Applications to Vitamin B_{12}.—The first applications of the HMBC experiment were simultaneously reported with HMQC applications in the work of Summers *et al.* (44) with vitamin B_{12} analogues. HMBC was extensively employed in establishing unequivocal assignments of the ^{1}H and ^{13}C spectra of coenzyme B_{12} (44), particularly in the corrin ring. The more recent study of the solution behavior of the base-off form of coenzyme B_{12} reported by Bax *et al.* (45) made similar extensive use of the HMBC technique to assign the numerous resonances of the corrin macrocycle that have similar chemical shifts. Connectivities observed in this study are shown by **33**.

More recently, Pagano and Marzilli (46) have used the HMBC experiment to assign carbonyl resonances to differentiate isomers of vitamin B_{12} monocarboxylic acid. Pagano *et al.* (47) have also employed the HMBC experiment in a study of 5′-deoxy-

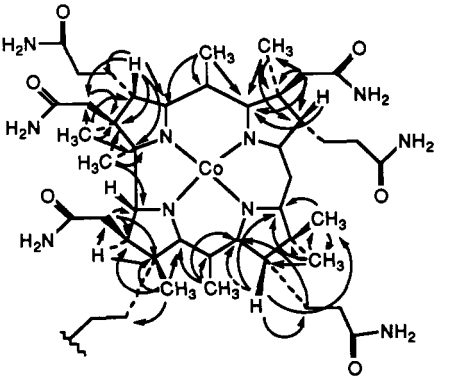

33

adenosylcobinamide, the experiment used again in this case to aid in the unequivocal assignment of the ^{1}H- and ^{13}C-nmr spectra of the molecule.

Applications to antibiotics.—Applications of HMBC in structural studies of antibiotics are more numerous than for any other class of compounds. Doubtless this is a function of the extreme diversity encountered when isolating antibiotics that required rigorous structure confirmation. Early applications were sparse: only one in 1986 and one in 1987. Applications appearing in 1988 increased dramatically in number with still more during 1989.

The first application of HMBC to an antibiotic was that of Bax *et al.* (49) to the complex macrocyclic antibiotic desertomycin [**1**]. Here, the exceedingly complex macrocyclic ring of desertomycin was assembled using the numerous long-range connectivities observed in the HMBC spectrum of a 16-mg sample (*m/z* 1193) in the antibiotic in DMSO-d_6 optimized for a long-range coupling of 7.7 Hz ($\Delta_{LR} = 65$ msec). As in the example of portmicin [**34**] described in more detail below, two- and three-bond con-

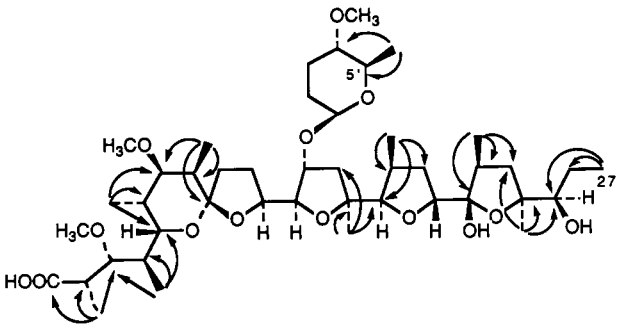

34

nectivities from the methyl carbons were of great utility in assembling large contiguous pieces of the molecular structure.

During 1987, the sole application of HMBC to an antibiotic was the structural study of portmicin [**2**] reported by Seto *et al.* (50). Seto makes a useful and noteworthy point in this application. While differentiating $^{2}J_{CH}$ from $^{3}J_{CH}$ coupling pathways is usually extremely difficult, the process is much more facile when methyl groups are involved. A COSY spectrum would identify protons neighboring the methyl group. Their attached carbon(s) can be identified from a HETCOR or HMQC spectrum. Quaternary carbons require the HMBC experiment if heteroatoms and other factors affect their chemical shifts along with the attached methyl groups. Thus, connectivities between the methyl and the carbon to which it is bound are easily identified and differentiated from the three-bond connectivities to the flanking carbons. This behavior is typical of the methyls of portmicin [**34**] and, as shown, establishes much of the connectivity network necessary for the elucidation of the structure of this polyether antibiotic.

The application of the HMBC experiment was also of pivotal importance in establishing the structure of lipsidomycin B, a bacterial peptidoglycan synthesis inhibitor (51). Following alkaline hydrolysis to give anhydrodeacyllipsidomycin [**35**], long-range connectivities from an HMBC spectrum were used to establish linkages between the four cyclic subcomponents. Unfortunately, no details regarding the optimization of the HMBC experiment were given in the communication reporting this work.

To provide a firm basis for studies of the biomimetic chemical reactivity (52,134) of bicyclomycin [**4**], the ^{1}H- and ^{13}C-nmr spectra were rigorously assigned using a combination of carbon-detected (124) and HMBC data (135). Long-range connectivities

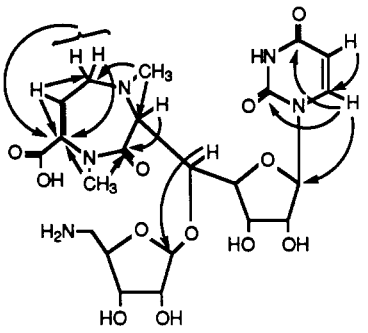

35

observed in the HMBC spectrum, which was optimized for 10 Hz (50 msec), are shown by **36** and were largely comparable to those observed in the carbon-detected experiment, albeit with considerably higher sensitivity per unit time.

A number of applications of the HMBC experiment appearing during 1988 were associated with the description of new antibiotic structures. The first of these was the description of urdamycins C and D, new angucycline antibiotics produced by *Streptomyces fradiae*, reported by Rohr *et al.* (136). Key long-range connectivities employed in elucidating the structure of urdamycin C are shown by **37**. Connectivities for urdamycin D, which had a pendant 3-indolyl substituent rather than the phenyl attached to the δ-lactone of urdamycin C, were quite similar.

A new nucleoside antibiotic, capuramycin [**38**], one of the molecules used as an example in the review by Seto (133), was described during 1988 by Seto *et al.* (137). Again, long-range connectivities from an HMBC spectrum were employed to link and orient the various cyclic components of the structure to one another. H-1′ of the sugar was linked to the vinyl and C-6 carbonyl of the pyrimidine, establishing the nucleoside core of the molecule. The methoxyl was located at the 3′ position of the sugar via a three-bond correlation. The carboxamido group was placed at 5′ through a two-bond coupling from H-5′. A second carboxamido group was placed on the 6″ position of the dihydropyran using connectivities from H-2″, H-4″, and H-5″. Finally, the attachment of the carboxamido group to the ϵ-lactam was established at the δ position by long-range couplings of the δ proton to both the carboxamido and lactam carbonyls, the latter coupled to the lactam NH proton. Seto *et al.* (137) remarked that a long-range connectivity was not observed between H-1′ and C-4′ or in the opposite direction from

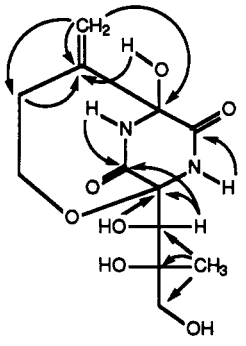

36

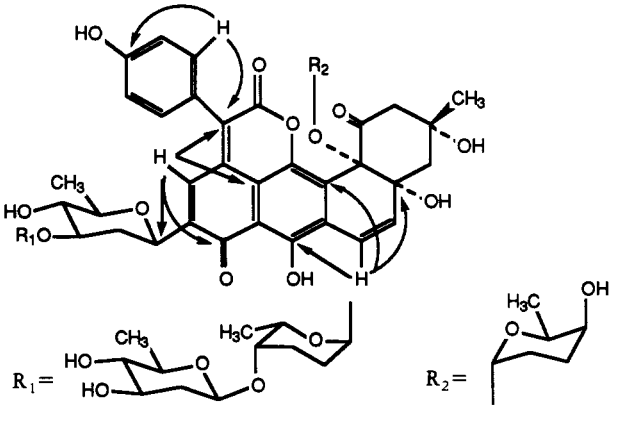

37

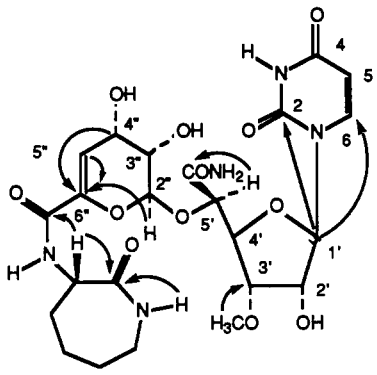

38

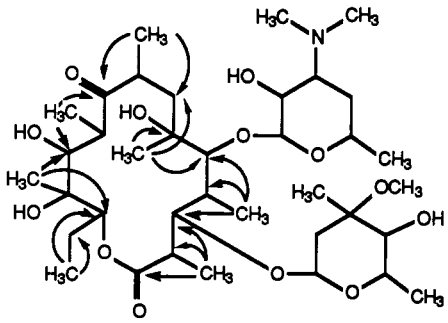

39

H-4′ to C-1′ in this study. This result is consistent with the experience of the authors in dealing with numerous ribose-containing nucleosides.

In a fashion similar to that employed with desertomycin [**1**] and portmicin [**34**], methyl connectivities have also been exploited in a model study with the polypropionate antibiotic erythromycin A [**39**] (138).

HMBC data were extensively employed to assemble and locate substituents on the dioxobenzo[*a*]napthacene aglycone nucleus, benanomicinone, of benanomycins A and B [**40**] reported by Gomi *et al.* (139).

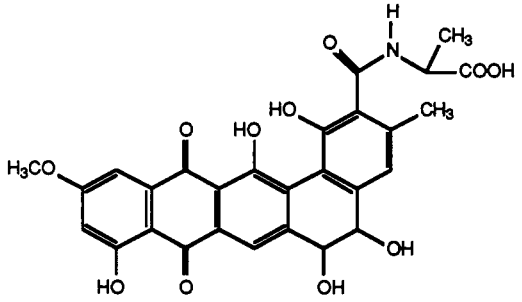

40

Later in 1988, a novel polyene antibiotic of the manumycin group, colabomycin A [**41**], was isolated from *Streptomyces griseofulvis* by Grote *et al.* (140). An interesting point concerns the long-range responses observed for the two polyene chains of colabomycin A. In the case of the side chain containing C-7 to C-14, which is all trans, each carbon except for those terminating the chain, C-7 and C-14, exhibits a response to the proton three bonds distant in either direction. In contrast, the other polyene chain (C-2′ to C-9′) is all trans except for the $\Delta^{6',7'}$ bond which is cis. Now, in addition to the terminating vinyls, C-2′ and C-9′, there is one additional vinyl carbon, C-6′, which exhibits only one long-range coupling. It is still possible to differentiate C-6′ from either C-2′ or C-9′ by observing the long-range coupling behavior for H-6′, which is long-range coupled to two carbons, C-4′ and C-8′. In contrast, both H-2′ and H-9′ have only one, three-bond, long-range coupling possibility to a vinyl carbon, C-4′ and C-7′, respectively. Hence, based on long-range connectivity patterns, it is possible to precisely locate the cis double bond in the side chain, provided that all of the carbons and protons can be resolved in the experiment.

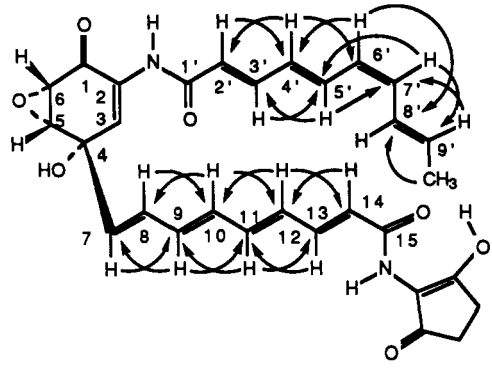

41

The first of a number of applications of the HMBC experiment in the elucidation of antibiotic structures was reported by Hochlowski *et al.* (141) late in 1988. The first report in this group described the elucidation of the structure of a complex of elfamycin-type antibiotics that were named phenelfamycins, for which the general structure **42** is shown (141). From the discussion of the connectivities in the polyene chains of colabomycin A just presented, it is easy to see how the polyene chains of the phenelfamycin nucleus could be assembled and then linked to other structural features on the basis of the non-vinyl connectivities exhibited for the terminal vinylic protons of each chain.

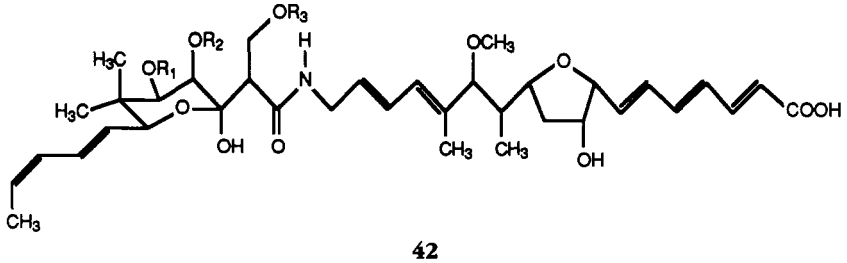

42

Next, in early 1989, Chen *et al.* (53) reported the isolation and structure elucidation of the pacidamycins, for which long-range couplings are shown by **43**.

Numerous long-range connectivities were observed for pacidamycin 1. Nevertheless, the authors report assembling the structural fragments by ms-ms. In retrospect,

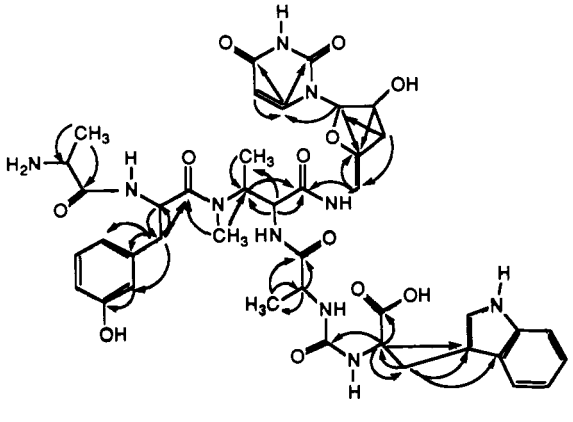

43

however, it probably would have been possible almost totally to assemble the structure from the HMBC data. It is also noteworthy that Chen *et al.* (53) referred to the long-range experiments performed by the acronym LR-HETCOR and that they referenced the first paper of Summers *et al.* (44) for the long-range correlation experiment. This contrasts with the much more commonly used acronym HMBC and reference to the paper by Bax and Summers (18).

Soon after studying the pacidamycins, Chen *et al.* (54) reported the isolation of the coumamidines [**6**], a group of broad-spectrum antibiotics of the cinodine type. Here again, Chen *et al.* used the acronym LR-HETCOR to describe proton-detected, long-range correlation data. Clearly, when following the literature, until some of the acronyms become as standardized in usage as COSY, it will be necessary to check the experimental description and the techniques referenced.

Fushimi *et al.* (142) reported the isolation and structure elucidation of the phospholactomycins [**44**] in mid-1989. The structural components were linked in this study to the quaternary carbon, C-8, using principally two-bond connectivity information from an HMBC spectrum.

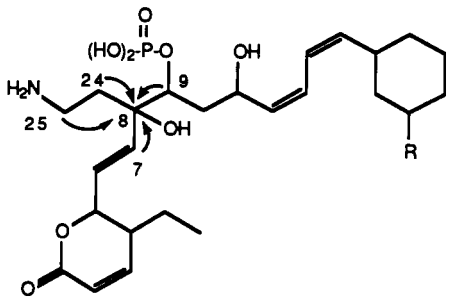

44

Imai *et al.* (143) also reported the structure of lavanducyanin [**45**], an antitumor substance produced from a *Streptomyces* sp., soon after the description of the phospholactomycins. The side chain was assembled from the HMBC data for lavanducyanin and linked to one-half of the phenazine nucleus. The balance of the phenazine nucleus was independently assembled from the HMBC data.

Later in 1989, Shindo *et al.* (144) reported the isolation and structure elucidation of the thiazostatins [**46**], which made more practical usage of HMBC data in assembling the thiazoline and thiazolidine rings.

The most recent application of the HMBC experiment to an antibiotic that we are aware of was the elegant structure elucidation of complestatin [**47**], an inhibitor of pro-

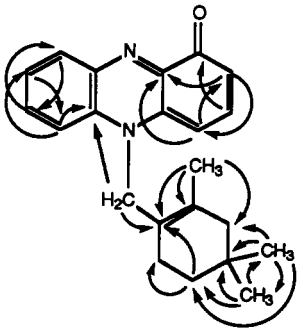

45

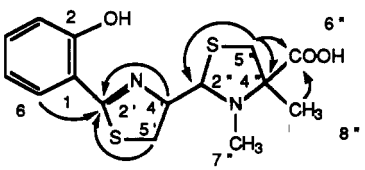

46

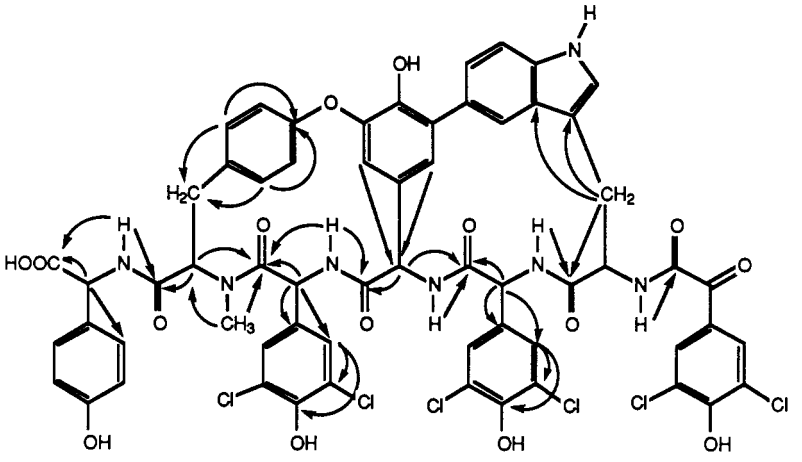

47

tease activity, reported by Seto *et al.* (145). Seven partial structures, six amino acids and one fragment with a ketone functionality, were first assembled and then linked together using the HMBC data. The sequence was derived by long-range couplings between the α-methine and/or amide protons and the carbonyl carbon of the adjacent amino acid fragment.

Clearly, the future for applications of the HMBC experiment in the elucidation of antibiotic structures is bright. To date, there have been a number of elegant applications of the technique to highly complex molecules. There also exists the need for a selective, one-dimensional, long-range experiment when only limited data are required. In principle, this experiment already exists in the form of the SELINCOR experiment, which was described by Berger (146), although long-range applications of the technique have not been reported. Selective one-dimensional analogues of the proton-detected experiments are considered briefly below.

Applications to Alkaloids.—The first application of the HMBC experiment to an alkaloid structural problem we are aware of was reported by Kobayashi *et al.* (147) in the elucidation of the structures of cystodytins A, B, and C isolated from an Okinawan tunicate, *Cystodytes dellachiajei*. The carbon skeleton of these novel alkaloids was assembled stepwise from the HMBC spectrum, as shown for cystodytin A [**48**]. Individual rings were assembled by successive three-bond connectivities (e.g., H-1 to C-3, H-2 to C-4, H-3 to C-4a, H-4 to C-11a, H-2 to C-11a, etc.). Structural segments were then linked to one another by further connectivities, such as that between H-4 and C-4b linking the benzene and pyridine rings.

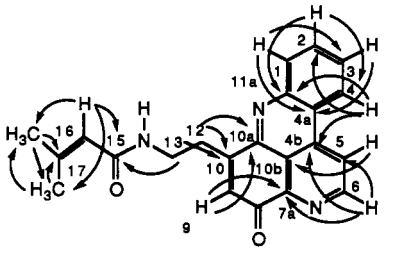

48

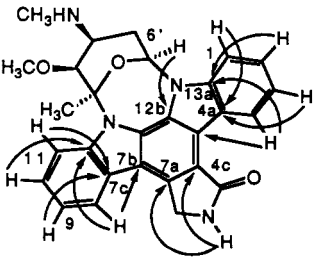

49

Slightly later in 1988, Meksuriyen and Cordell (56) employed the HMBC experiment in the assignment of the ^{1}H- and ^{13}C-nmr spectra of staurosporine [**7**]. Long-range connectivities critical to the assignment of the quaternary carbon resonances of the indolocarbazine portion of the molecule are shown by **49**.

Here again, there were multiple correlations to each quaternary carbon, thus providing the means of unequivocally assigning the quaternary carbons and the proton four-spin systems. For example, H-11 was long-range-coupled to C-7c and to H-9, thereby removing an ambiguity in the assignment of H-9 and H-10; the former was coupled to C-7c, the latter to C-11a.

In late 1988, Cheng *et al.* (148) reported another application of the HMBC experiment in the elucidation of the novel sulfur-containing alkaloids, prianosins B, C, and D, which were isolated from a marine sponge, *Prianos melanos*. A related compound, prianosin A, lacking the linkage between the nitrogen and the cyclohexenone moiety, was isolated in 1987 (149), its structure confirmed by an X-ray crystal structure. Given prianosin A to provide initial insight into the possible structure of the molecule, the carbon skeleton of prianosin D acetate [**50**] was assembled from HMBC data, the extensive long-range couplings of the spiro-center, C-6, providing an excellent starting point.

During 1989, there was a marked increase in the number of applications of the HMBC experiment in alkaloid structure elucidation; we are aware of the appearance of six papers. The first of these was the brief report of the structure of the C_{20}-diterpene alkaloid lassiocarpine [**12**] by Takayama *et al.* (61). Here, the HMBC data were employed primarily to position the various functional groups on the carbon skeleton.

Copp *et al.* (150) utilized the HMBC experiment in the elucidation of an alkaloid **51** containing a 1,2,3-trithiane moiety, isolated from a New Zealand ascidian and its alkaline degradation product.

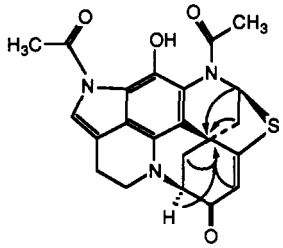

50

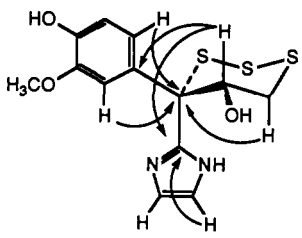

51

Gunawardana *et al.* (151) utilized the HMBC experiment in conjunction with the COLOC experiment in the elucidation of the structures of a series of alkaloids with a pyrido[4,3,2-*mn*]acridine skeleton from deep water sponges of the family Pachastrellidae. The structure of one of these alkaloids, cyclodercitin [**52**], is shown.

A new pentacyclic shermilamine alkaloid, also based on the pyrido[4,3,2-*mn*]acridine nucleus, was reported later in 1989 by Carroll *et al.* (152). Shermilamine B [**53**] was isolated from extracts from a tunicate of the Trididemnum family. Here again, the HMBC experiment was extensively utilized in the assembly of the structure and the complete assignment of the spectra.

Later in 1989, Kobayashi *et al.* (153) again utilized the HMBC experiment in elucidating the structure of a group of alkylpyridine alkaloids, the theonelladins. The utilization of the HMBC experiment in this example was limited to the relatively trivial positioning of the olefinic and aliphatic side chains on the pyridine nucleus. The structure of theonelladin A [**54**] is shown.

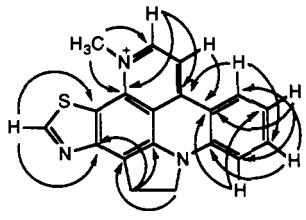

52

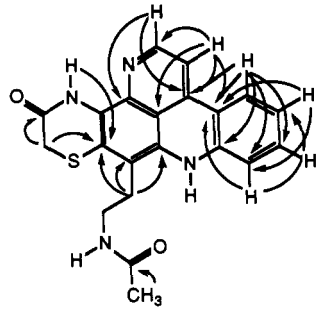

53

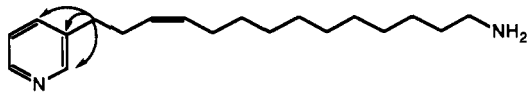

54

Fusetani *et al.* (154), in late 1989, reported on the structure of a pair of macrocyclic alkaloids from a sponge of the genus *Haliclona*. A number of partial structures were assembled through the use of HMBC, in conjunction with other spectral data, to deduce the structure of haliclamine B [**55**] and the closely related haliclamine A, which differs only in lacking the *E*-disubstituted double bond in the lower connecting alkyl chain. The breakpoints in the structural fragments deduced from the HMBC data are shown by wavy lines on the structure. Unfortunately, specific details of the long-range couplings observed were not reported in this communication.

Probably the last application of an HMBC experiment to an alkaloid to appear during 1989 is found in the work of Kashman *et al.* (155), who reported the structure of ptilomycalin A [**56**], a novel polycyclic guanidine alkaloid isolated from the Caribbean

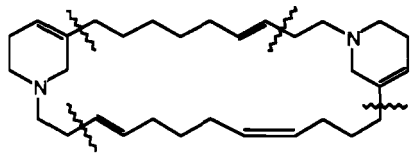

55

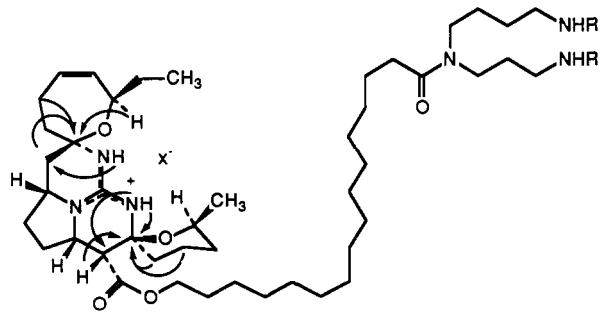

56

sponge *Ptilocaulis spiculifer*. Only partial details of the structure elucidation were communicated. The structure was assembled using both COLOC and HMBC experiments. Key long-range connectivities observed in the HMBC spectrum of the molecule are shown.

The most recent application of the HMBC experiment to an alkaloid problem, that we are aware of, was our own study (156) of the known alkaloid holstiine [**57**]. Here, the HMBC experiment was used in conjunction with HOHAHA and NOESY spectra to totally assign the ^{1}H and ^{13}C spectra of the molecule. This study also confirmed the correct structure was that originally proposed by Bisset *et al.* (158), rather than the previously suggested structure of Bosly (157).

Applications to terpenes.—One application of the HMBC experiment to a terpene has already been discussed above in the form of the diterpene alkaloid lassiocarpine in the previous section. HMBC data were utilized in the study of only two other terpenes during 1988. The first example was in the elucidation of the structure of a spirostanol glycoside **58** reported by Pant *et al.* (159), in which extensive use of the HMBC data was made in determining the structures of the glycoside moieties.

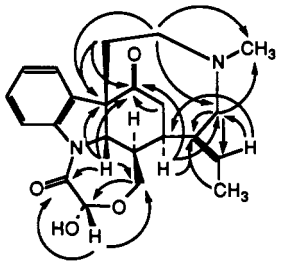

57

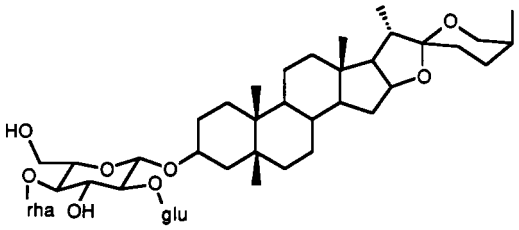

58

Later in 1988, Sharma and Alam (160) reported the structures of schlerophytins A and B, novel tetracyclic, cytotoxic diterpenes from the coral *Schlerophytum capitalis*. The structure of schlerophytin A [**59**] is shown. This communication was followed in 1989 by a full paper describing the structures of four additional schlerophytins; the structure of one member of the series was confirmed by X-ray crystallography (161).

The only remaining 1988 paper describing the application of HMBC to terpenes was again work by Seto *et al.* (162) in which the structures of four lycopodium triterpenes were reported. Extensive use was made of connectivities from the six methyl groups as shown for lyoclavanol A [**60**]. Once again, both two- and three-bond connectivities were observed, although in this case the connectivities were largely complementary and easily differentiated.

Early in 1989, the structures of a series of bitter triterpenoids isolated from the fungus *Ganoderma applanatum* were elucidated (163). Partial structures determined from spectral data were linked via quaternary and carbonyl carbon resonances using long-

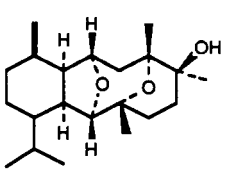

59

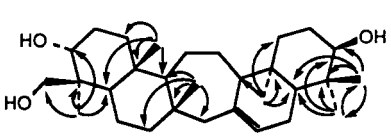

60

range connectivities form HMBC spectra. The structure of one member of the series, ganoderenic acid G [**61**], is shown.

HMBC data were also employed by Kobayashi *et al.* (62) to establish the structure of a cytotoxic sesquiterpene, metachromin C [**62**], from an Okinawan marine sponge, *Hippospongia metachromia*. Although the optimization of the delays for long-range transfer in the HMBC experiment was not specified, the connectivities shown below highlight one of the problems frequently encountered with terpenoidal structures—fairly numerous two-bond ($^2J_{CH}$) connectivity responses. Hence, care must be exercised in interpreting HMBC data for terpenes to ensure that two-bond correlations are not mistaken for three-bond responses, which are more common. When sufficient material is available, the means of differentiating two-bond from three-bond correlations is provided by the XCORFE pulse sequence devised by Reynolds *et al.* (127).

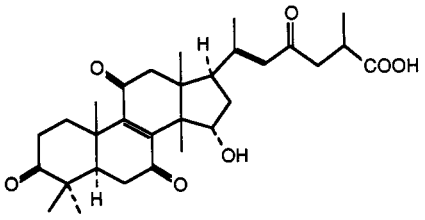

61

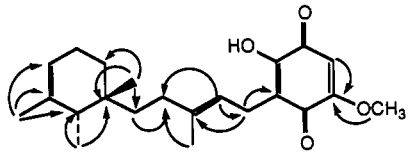

62

Later in 1989, structures of a series of three brominated marine sesquiterpenes were determined using HMBC in conjunction with zero-quantum proton (ZQCOSY) and other 2D nmr experiments (96). One of the compounds reported in this study, 1-bromomaaliol [**23**], is the precursor of the compound being used to illustrate the application of techniques in this review, and these compounds will not be discussed further here.

A novel saponin, ginsenoside L_a [**63**], was isolated from the leaves of *Panax ginseng* (164). A series of structural fragments was assembled from COSY and conventional HETCOR data, which were then linked by extensive usage of HMBC data, again, heavily relying on long-range connectivities from the methyl groups.

The most recent application of HMBC to a terpenoidal problem was the late 1989 report of Fusetani *et al.* (165), describing the structures of astrogorgadiol [**64**] and astrogorgin [**65**] from a gorgonian coral, *Astrogorgia* sp. The former structure, a secosterol, was elucidated by first deducing the structures of two fragments that could then be linked through the ethylene bridge by means of connectivities observed in the HMBC spectrum. The latter structure, **65**, was closely related to the known diterpene orphirin, which was also isolated from the EtOH extract. The HMBC data were used to

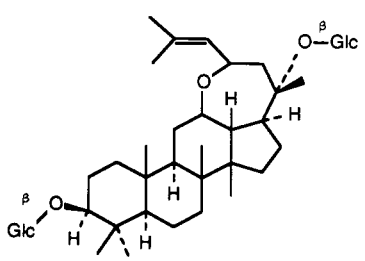

63

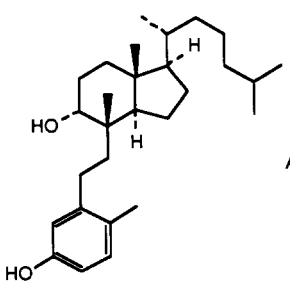

64

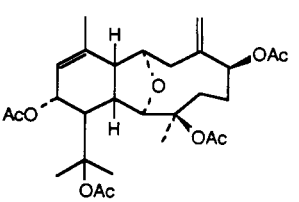

65

position the exomethylene group and the acetoxyl groups in the case of astrogorgin [**65**].

Applications to carotenoids.—At present, only a single application of HMBC data to the structure of a carotenoid has appeared. It was reported by Englert *et al.* (67) and was discussed in the context of applications of HMQC above. As with some of the polyene antibiotics, numerous long-range connectivities were observed, enabling the authors to make assignments in the extended polyene network. Once again, the authors noted the utility of responses associated with the methyl groups.

Applications to porphyrins.—As in the preceding section, there is also only a single representative example of the application of HMBC data in the assignment of a porphyrin (68). The numerous studies of the vitamin B_{12} analogues present similar problems in the assignment of the corrin ring and could be used as a reference for the assignment of other porphyrin systems (44–47). The reader interested in this class of compounds is referred to the discussion of applications to vitamin B_{12}, above.

Applications to saccharides and polysaccharides.—There has been a paucity of applications of HMBC experiments to saccharides and polysaccharides. Byrd *et al.* (71) have utilized the HMBC experiment in a study of the capsular polysaccharide of *Haemophilus influenzae*. This is the single application to a large polysaccharide of which we are aware. There have, however, been a number of applications to glycosides (see Applications to Terpenes, above) to which the interested reader could turn for additional insight. One such example that will be presented here is lavandulifolioside [**66**], a phenylpropanoid glycoside from *Stachys lavandulifolia* (166) which does not fall conveniently into any other classification category.

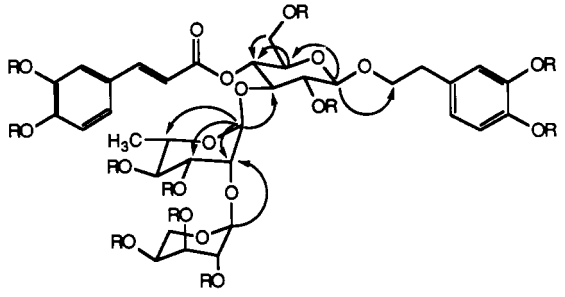

66

Connectivities from an HMBC experiment, optimized for 5 Hz, involving the sugar portions of the molecule, are shown. In each case, correlations across the sugar ethereal oxygen are observed. In addition, other connectivities that link one sugar to the next in the sequence make it possible to conveniently sequence the sugars in a glycoside.

Applications to peptides.—Applications of the HMBC experiment to peptides are subdivisible into two categories: resonance assignments of peptides of known structure, particularly carbonyl resonances, and true structure elucidation problems, since a number of interesting and biologically active peptides are now being isolated from natural sources.

In the former area, the first paper to apply inverse-detected HMBC to the problem of assigning carbonyl resonances was that of Bermel *et al.* (74). Using the older sequence of Bax *et al.* (23) optimized for long-range transfer, Bermel and coworkers addressed the assignment of the carbonyl resonances of cyclo(-Phe-Thr-Ala-Trp-Phe-D-Pro-). Not only was it possible to assign unequivocally the carbonyl resonances, they were also able

to confirm the sequence of the peptide. As an example, consider D-Pro and Ala. Direct assignment of the carbonyl resonance was possible via the three-bond coupling to the β-proton resonances. Correlations to the NH resonances of Phe_A and Trp then establish the connectivities D-Pro-Phe_A and Ala-Trp. By extending this procedure, the complete sequence of the peptide was assembled.

A more novel approach to the problem of assigning carbonyl resonances of peptides with the necessary high digital resolution in F_1 was described by Davis (167). Using a modified version of the HMQC experiment in which "soft" pulses were applied to the α protons, Davis illustrated the assignment of the carbonyl resonances of the cyclic nonapeptide bradykinin.

There have also been a number of more routine applications of the HMBC experiment in the assignment of the spectra of various synthetically prepared, or known, peptides. The first of these applications was reported by Kessler *et al.* (168) in a study of six analogues of cyclo(-D-Pro-Phe-Thr-Lys(*Z*)-Trp-Phe-). Later that year, Kessler *et al.* (169) reported a total assignment of the ^1H- and ^{13}C-nmr spectra of the cyclic depsipeptide didemnin A (169). The following year, Hofmann *et al.* (75) took advantage of the dispersion in F_1 afforded by the ^{13}C chemical shift to assign the overlapped spectra of cyclo(-Phe-Pro-Thr-Lys(*Z*)-Trp-Phe-). Most recently, Kessler *et al.* (170) utilized "semisoft" excitation by Gaussian pulses after the fashion of Davis (167) to complete a total assignment of the ^1H- and ^{13}C-nmr spectra of an [Me-L-Leu_7]-didemnin B analogue.

One final note pertains to the abbreviation used to refer to the long-range experiment. Despite what seems to be rather widespread acceptance and usage of the HMBC abbreviation to describe the long-range proton-detected heteronuclear correlation experiment, Kessler, in several of his papers, has unfortunately elected to coin the terminology "inverse-COLOC." The generation of a new acronym to refer to the HMBC experiment will almost inevitably lead to increased difficulty in future literature searches in this area, and it would probably be better if it were not used.

Probably the first application of the HMBC experiment in the elucidation of a novel peptide structure from a natural source was the reported elucidation of the structure of cyanoviridin RR [**67**] by Kusumi *et al.* (171). Cyanoviridin RR is a cyclic peptide toxin isolated from the blue-green alga *Microcystis viridis* and has been implicated as the toxin in blooms of this cyanobacterium in drinking water reservoirs in Japan.

Efforts to sequence cyanoviridin RR using standard ROESY-based methods left ambiguities because of weak intensities for some cross peaks. A conventional COLOC experiment at 500 MHz was unsuccessful, because the compound had limited solubil-

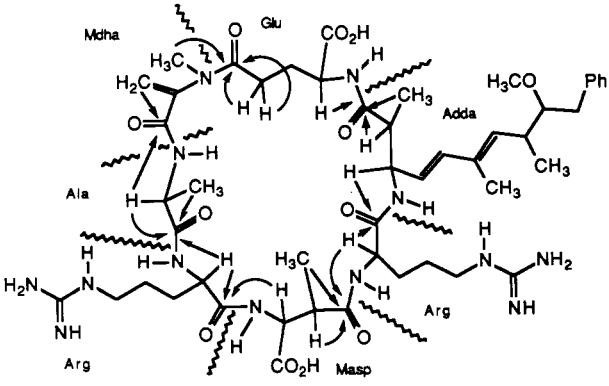

ity and also slowly decomposed in the acidic MeCN/TFA solvent system being used. In contrast, the HMBC spectrum allowed the unequivocal sequencing of the peptide **67**, based on the long-range connectivities shown.

The next application of the HMBC experiment in the sequencing of a peptide was a report on the isolation and structures of dolostatins 11 and 12 [**68**] from the sea hare *Dolabella auricularia* by Pettit *et al.* (172). Unfortunately, three of the ten carbonyl resonances in the structure were unresolvable in the HMBC experiment, thereby precluding a total determination of the sequence. Three structural fragments were determined using the HMBC data (limits indicated by wavy lines), which allowed the final elucidation of the structures based on observed nOe's.

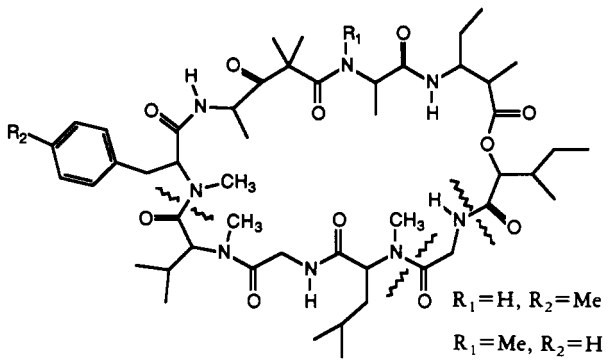

68

In mid-1989, Williams *et al.* (173) reported the isolation and structure elucidation of the cyclic peptide ulithiacyclamide B [**69**]. A combination of HETCOR and HMBC experiments confirmed the presence of three inferred structural subunits and facilitated their subsequent assembly into the final structure of the molecule. Connectivities observed in the HMBC spectrum, which completely sequenced the molecule, are shown on the structure. The work of Williams *et al.* (173) also demonstrated that the assignment of several of the carbon resonances of ulithiacyclamide A (174,175) were incorrect.

In the late summer, Gunasekera and Gunasekera (176) reported the isolation and structure of the brominated tyrosine metabolite dihydroxyaerothionin and the known compound aerophobin 1 [**70**] from the deep-water sponge *Verongula rigida*. HMBC data were used to confirm that the latter compound was identical to aerophobin.

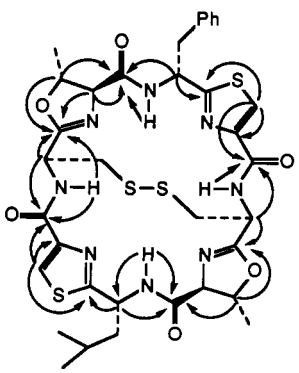

69

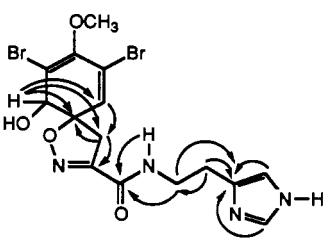

70

In a study of peptides from the ascidian *Lissoclinum patella*, Schmitz *et al.* (177) reported the structures of a number of cyclic peptides. In the case of one, lissoclinamide 6 [**71**], only 2.5 mg of material was isolated, necessitating the use of HMBC rather than INAPT, which was applied to the other peptides in the series isolated in greater quantity.

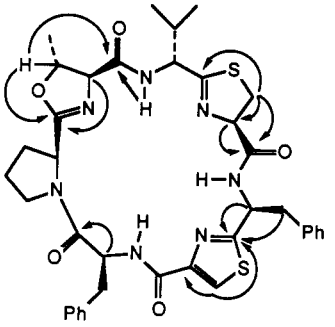

71

Late in 1989, Pettit and coworkers first reported the structure of the cyclic depsipeptide dolastatin 13 [**72**], from the sea hare *Dolabella auricularia* (178), followed by a paper reporting the structure of the linear depsipeptide dolastatin 15 [**73**] (179). In the former, combined utilization of a series of homonuclear double- and triple-relayed coherence transfer experiments and HMBC provided the means to assemble the structure of the molecule. The single gap left across the ester linkage by the HMBC data was closed on the basis of an nOe.

The latter compound, dolastatin 15 [**73**] (179), was interesting in several respects. The peptide was sequenced using a combination of mass spectrometry, nOe's, and

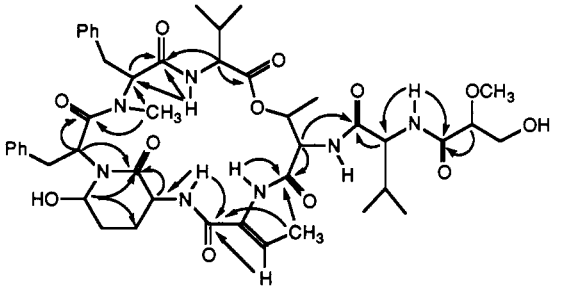

72

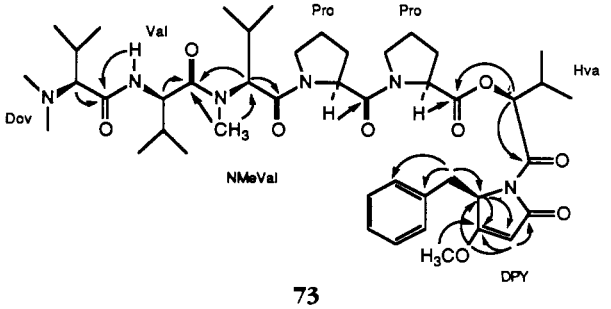

73

HMBC. The HMBC data were particularly important in assembling the structure of the previously unreported biosynthetic product of phenylalanine, which was labeled dolapyrrolidone (DPY).

The final applications of the HMBC that will be considered in this section are applications to proteins. Thus far, there have been relatively few applications of the HMBC experiment in this area, although the prospects for change are rapidly increasing with the availability of techniques to produce highly labeled proteins in quantity. The first example in this area is found in the work of Bax *et al.* (180). They applied the HMBC experiment, modified to eliminate the low-pass *J*-filter, in a study of staphylococcal nuclease (S Nase), which had in one sample all Leu, Ile, and His residues labeled with $^{15}N\alpha$ and in the other all Thr residues labeled with ^{13}C in the carbonyl. Long-range ^{15}N-^{1}H HMBC spectra were also utilized as an adjunct technique in the assignment of sequential proton resonances of the DNA-binding protein Ner that was reported by Clore *et al.* (181). Davis (182) applied the HMBC experiment, again without the low-pass *J*-filter, in the assignment of the quaternary aromatic carbon resonances of lysozyme. Gronenborn *et al.* (183) used HMBC in a study of the secondary structure of the DNA-binding protein Ner from Phage Mu. Wang *et al.* (184) employed the HMBC experiment in their continuing study of staphylococcal nuclease. Finally, Forman-Kay *et al.* (185) applied the HMBC experiment in their study of the solution conformation of human thioredoxin.

Applications to polyether compounds.—To date, there is a single application of the HMBC experiment to a polyether compound. Prospects are good for further applications because there is a growing interest in polyether marine toxins which are frequently isolated only in minute quantity. The existing example, reported by Blunt *et al.* (186), used the HMBC experiment to confirm the assignments of the spectra of thyrsiferyl acetate [**74**], which were initially made using the XCORFE experiment.

Applications to polynuclear aromatics.—The first application of the HMBC experiment to a polynuclear aromatic that we are aware of is that of Zektzer *et al.* (187) to benzo[*b*]triphenyleno[1,2-*d*]thiophene [**75**]. Several interesting comparisons are made in this work. COSY and ZQCOSY were compared for their ability to elucidate long-range proton-proton coupling pathways. More importantly, data obtained using the HMBC experiment were compared to those obtained from a conventional carbon-detected long-range heteronuclear correlation experiment modified to decouple one-bond modulations of response intensity. Long-range coupling pathways used to assign the quaternary carbon resonances are shown on the structure.

Later in 1988, Fischer *et al.* (188) utilized the HMBC experiment in the course of determining the stereochemistry of a polysubstituted [2.2]*para*-cyclophane **76**.

In early 1989, Johnston *et al.* (189) employed the HMBC experiment to totally assign the carbon spectrum of phenanthro[9,10-*b*]thiophene [**77**]. Because of the long proton T_1 relaxation times of the molecule, it was necessary to dope the sample with

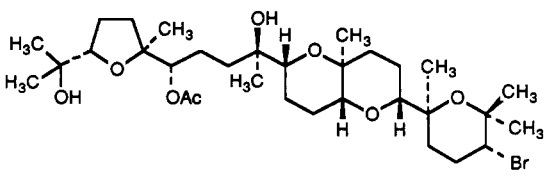

74

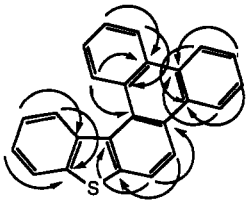

75

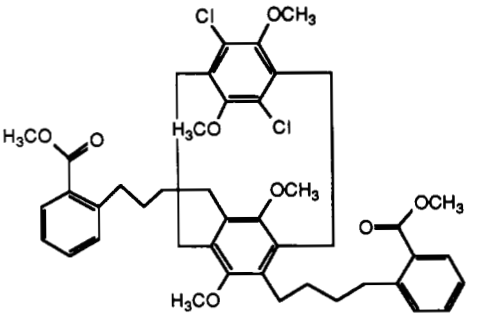

76

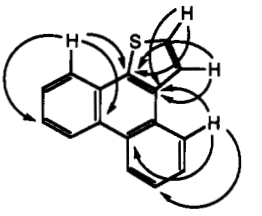

77

$Cr(AcAc)_3$ to acquire the HMBC data within a reasonable period of time, albeit at the expense of line shape in the ^1H spectrum.

Tezuka *et al.* (190) utilized HMBC data to determine the structure of a dimeric dihydrophenanthrene **78**, isolated from extracts of the roots of *Spiranthes sinensis*. The HMBC data provided the basis for unequivocally locating each of the substituent groups in the dimeric dihydrophenanthrene nucleus. More importantly, the HMBC data also provided the means of unequivocally linking the two dihydrophenanthrene subunits together, which was a critical concern as the 3 position of one of the dihydrophenanthrene subunits is linked asymmetrically to the 6 position of the other.

Finally, Luo *et al.* (89) have utilized HMBC data in conjunction with HMQC and HMQC-TOCSY spectra to complete a total assignment of the ^1H- and ^{13}C-nmr spectra of a pair of isomeric benzothienonaphthoquinolines, **21** and **22** (89). The total assignment of the nmr spectra of the former was necessary since it was employed as a model compound for an HMQC-NOESY experiment discussed below.

Applications to macrocyclic lactones.—An area in which HMBC spectra have had a significant impact is the elucidation of the structures of macrocyclic lactones. Some examples of this have already been considered, e.g., erythromycin [**39**], which is considered above.

The first application of the HMBC experiment in the elucidation of the structure of a macrocyclic lactone was amphidinolide C [**79**], a novel, 25-membered macrocyclic compound with potent antineoplastic activity that was reported by Kobayashi *et al.* (191). Using COSY, RCOSY, and conventional HETCOR, it was possible to assemble

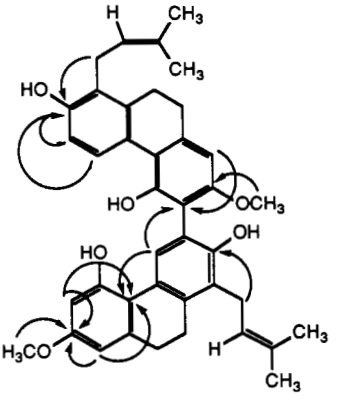

78

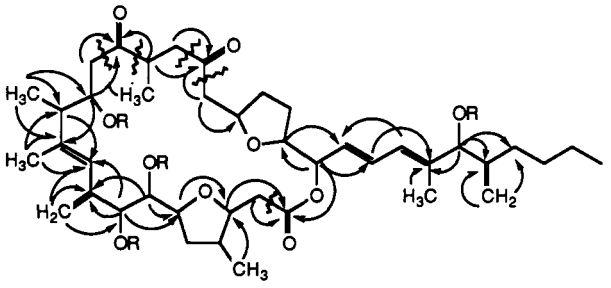

79

three structural fragments dividing the molecule at the two ketone carbonyls and the ester carbonyl of the 25-membered lactone. HMBC not only confirmed the structural segments, it also linked the three segments across the carbonyls, thereby completing the elucidation of the structure.

A related example, patellazole B [**80**], was isolated from the marine tunicate *Lissoclinum patella* and reported by Corley *et al.* (192). The cyclic peptides ulithiacyclamide B (173) and lissoclinamide 6 (177) were also isolated from this species (see above). Structurally, however, patellazole B was a more complex problem than amphidinolide C. Ten fragments were generated which had to be assembled to complete the elucidation of the structure. Break points between the individual structural fragments are designated by short, wavy lines and connectivities that linked fragments together are shown.

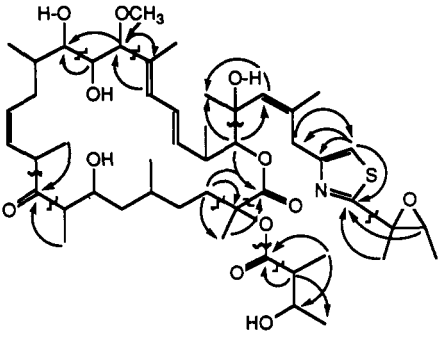

80

In late 1988, Kobayashi *et al.* (193) reported the structure of another pair of macrocyclic lactones, iejimalides A and B, which were isolated from the Okinawan tunicate *Eudistoma rigida*. These macrolides differed from amphidinolide C in that they contained a 24- rather than a 25-membered macrocyclic ring. A total of five structural fragments were assembled from conventional 2D nmr data; the fragments were then linked together on the basis of two- and three-bond connectivities observed in the HMBC spectrum. Unfortunately, there were relatively few additional details given about the connectivities observed in the HMBC spectra of these compounds. The structure of iejimalide B [**81**] is shown with the connectivities from the HMBC spectrum used to link the previously assembled structural fragments.

In late 1989, Kobayashi *et al.* (194) reported yet another cytotoxic macrolide, amphidinolide D [**82**], also isolated from a marine dinoflagellate of the genus

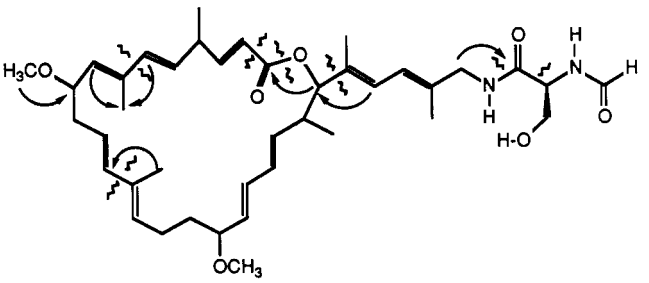

81

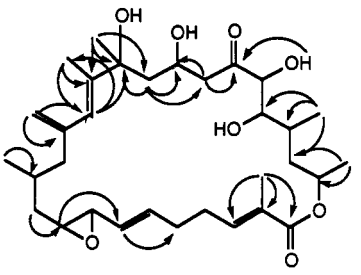

82

Amphidinium. More information was provided in this study about the numerous long-range connectivities observed in the HMBC spectrum of the molecule. The structure of amphinolide B was also revised in this work and shown to be closely related to amphinolide D.

Applications of HMBC in biosynthetic studies.—There have been several applications of the HMBC experiment that focused on biosynthetic studies but do not fit conveniently into any of the chemical categories discussed above. One such application dealt with a study of the biosynthesis of the primary carbon dioxide acceptor of methanogenic bacteria known as methanofuran (195). The other application was a study of deoxygenation in the biosynthesis of polyketides (196).

APPLICATION OF HMBC TO THE DEGRADATION PRODUCT OF 1-BROMOMAALIOL.—Having surveyed applications of the HMBC experiment, we now refocus our attention on the utilization of the experiment to complete the skeletal structure of the degradation product we are considering within the context of this review. We began with a spectrum recorded with a 71.4-msec optimization of Δ_{LR}, which corresponds to a 7 Hz coupling. The spectrum, plotted to show all of the responses, is presented in Figure 28. This spectrum contains considerable F_1 tracking from the methyl resonances despite the fact that the interpulse delay was 2.1 sec, giving an overall duration of 2.5 sec/transient. Methyl relaxation times ranged upwards from 0.9 sec, and a conscious decision was made to allow F_1 tracking to occur, because the two protons near the methyl resonances were sufficiently offset to be observed in any case. Responses to the methyl resonances themselves can also be observed by simply adjusting the threshold accordingly so that only the long-range responses of interest are observed, as shown in Figure 29. While most of the necessary long-range coupling information was obtained from the 71.4-msec optimized experiment, spectra were ultimately recorded at 50, 71.4, 83, 110, 143, and 180 msec to illustrate the range of responses that can be observed in a rigorously assigned set of spectra. Typical acquisition times ranged from 12 to 19 h.

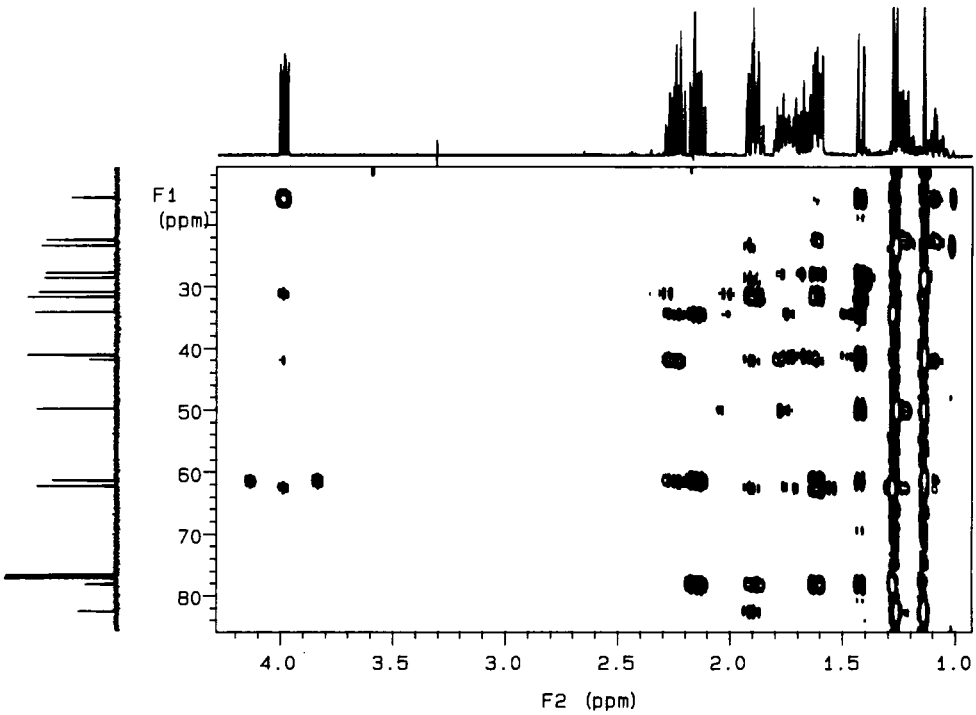

FIGURE 28. HMBC spectrum of the degradation product of 1-bromomaaliol plotted to show all responses, which tends to accentuate trailing in the F_1 frequency domain.

Beginning from the two protons resonating at 3.986 and 1.422 ppm, which we have utilized to assemble structural fragments **26** and **28**, we were able to link these structural components as follows. Beginning from the proton resonating at 3.986 ppm in the 71.4-msec HMBC spectrum presented in Figure 28, we note first a long-range

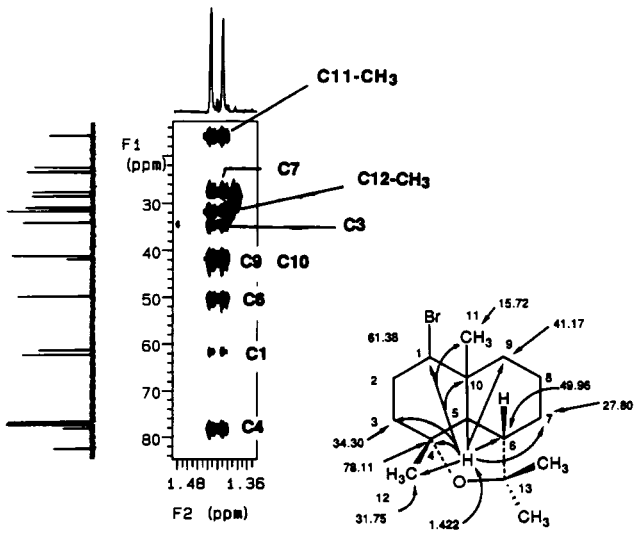

FIGURE 29. HMBC spectrum of the degradation product of 1-bromomaaliol plotted with a somewhat higher threshold to show all responses from the proton resonating at 1.422 ppm in a more clearly resolved fashion.

connectivity from this proton to the methyl carbon resonating at 15.72 (1.134 ppm HMQC, Figure 12). While information from the proton resonating at 3.986 ppm is admittedly limited, the same cannot be said for the methine proton resonating at 1.422 ppm. From Figure 28 we note that there is some tracking through F_1 when the threshold is set low enough to see some of the responses for the more extensively coupled proton resonances. In contrast, when the threshold is raised slightly, as shown in Figure 29, we note that the 1.422-ppm methine resonance is extensively long-range coupled. Indeed, responses are observed to the following carbon resonances, the chemical shifts of their directly attached protons following each parenthetically: 15.72 (1.134), 27.80 (1.732, 1.231), 31.75 (Me, 1.277), 34.30 (1.902, 1.614), 41.17 (1.614, 1.090), 41.89 (quaternary), 49.96 (1.888), 61.38 (weak, 3.986), 78.11 (quaternary).

From the structural fragment represented by **28**, we can begin to make some attributions from these long-range connectivities. First, we know from the HMQC-TOCSY data that the methylene carbon resonating at 34.30 ppm is the terminal carbon to which connectivity could be extended in **26** and that there is presumably a quaternary carbon attached to this carbon. Linking the 34.30 ppm carbon long-range to the 1.422 ppm proton bridges this quaternary carbon resonance, thereby linking structural fragments **26** and **28** via a quaternary carbon. Because we observe connectivities to two quaternary carbon resonances (41.89 and 78.11 ppm), one of these must clearly be the intervening quaternary carbon. Moreover, since **23** originally bore methyl and hydroxyl groups at the 4 position, it is logical to assume, at least initially, that the intervening carbon is that resonating at 78.11 ppm.

Next, the methine carbon resonating at 49.96 ppm bears the vicinal neighbor of the proton resonating at 1.422 ppm (based on the HMQC-TOCSY data). The carbon resonating at 27.80 ppm is the neighbor one step farther removed. Because the carbon resonating at the terminus of **28** at 41.17 ppm is also coupled to the proton resonating at 1.422 ppm, the structure of the degradation product must retain a six-membered ring as in **23**, which is logical. This series of operations assembles a larger structural fragment, **83**, on which the connectivities just identified are shown by arrows going from the proton to the carbon to which long-range coupling was observed. The bridgehead carbon at the 10 position is assigned as the 41.89-ppm quaternary carbon resonance. Given the structure of **83** as a working premise, we must next look for correlations to confirm this carbon skeleton and to complete the structural problem.

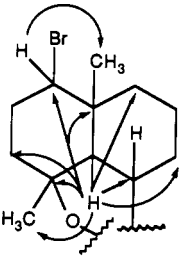

83

At this point, we must attempt to confirm the assignment of the 4-methyl resonance as that resonating at 31.75 ppm. Referring to Figure 30, which was plotted to show only responses from the methyl resonances, we note a pair of responses from methyl signals to other methyls. The methyl singlet resonating at 1.261 ppm in the ^1H spectrum correlates with the methyl carbon resonating at 23.44 ppm. Conversely, one

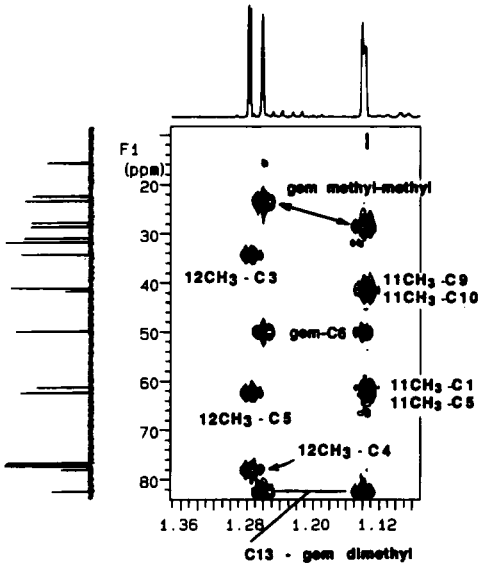

FIGURE 30. HMBC spectrum of the degradation product of 1-bromomaaliol plotted with a somewhat higher threshold to show only responses from the methyl groups of the molecule in a clear fashion. It should be noted that a methyl-methyl connectivity is observed in this spectrum that can only arise in the case of a *gem*-dimethyl arrangement of a structural fragment.

of the upfield methyl singlets (these differ only slightly, resonating at 1.134 and 1.142 ppm) is also correlated to the methyl carbon resonating at 28.68 ppm. The only structural moiety that can have a methyl proton resonance correlated long-range to a methyl carbon resonance is a *gem*-dimethyl, a structural feature present in **23** in the form of the dimethyl cyclopropyl group. Both of the methyls in question also correlate to the quaternary carbon resonating at 82.53 ppm. The downfield methyl proton resonance at 1.261 ppm also correlates with the methine carbon resonating at 49.96 ppm, which would correspond to the 6 position, assuming that the proposed structure, **83**, is correct. While we have substantial structural information at this point, there are a few additional connectivities that would be useful, specifically those from the other two methyls attached at the 4 and 10 positions.

We have tentatively assigned the 4-methyl resonance as the carbon resonating at 31.75 ppm, which is associated with the 1.277-ppm proton singlet in the HMQC spectrum (Figure 12). It is useful that the resonance at 1.277 ppm exhibits correlations to the carbons resonating at 34.30, 62.43, and 78.11 ppm. These correlations clearly establish this resonance as the 4-Me, since the carbons to which correlations were observed are C-3, C-5, and C-4, respectively. Finally, correlations are observed for the remaining 10-Me resonance to the carbons resonating at 41.17, 41.89, 61.38, and 62.34 ppm. These responses are consistent with those expected for the 10-methyl, corresponding to correlations to C-9, the C-10 quaternary, C-1, and C-5, respectively.

The long-range correlations observed nearly complete the structure of the degradation product. The only feature remaining is the oxygen. Clearly, on the basis of carbon chemical shifts, the quaternary carbons resonating at 78.11 and 82.53 ppm must bear oxygen. Given the connectivities already established, these carbons have been located as C-4 and the carbon derived from the dimethyl cyclopropyl group of **23**, which has been irrefutably linked to the C-6 methine. As there was only one oxygen atom in **23** to

begin with, we can now logically form a highly substituted furan by invoking an ether linkage between C-4 and the *gem*-dimethyl carbon. Connectivities observed for the methyls are presented as structure **84** and, except for stereochemistry, which remains to be established, structure **84** is identical to **30**. A comparison of the ^{1}H and ^{13}C chemical shifts of (1*R*)-bromo-*ent*-maaliol [**23**] and the degradation product **30** is presented in Table 1.

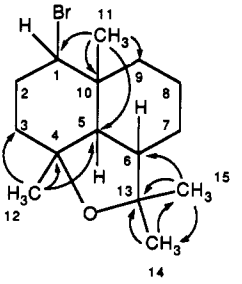

84

Before dealing with the remaining issue of the stereochemistry of **30**, it is useful to consider the responses observed in the HMBC spectra of **30** as a function of the optimization of the experiment for various long-range couplings. To this end, a series of values were acquired in which the optimization of the Δ_{LR} interval was varied using values of 50, 71.4, 83, 110, 143, and 183 msec, which correspond to couplings in Hz of 10, 7, 6, 4.5, 3.5, and 2.8 Hz, respectively. These data are summarized in Table 2. With this compound the best overall data were obtained from the 83-msec optimization. Rather than gaining access to progressively smaller coupling pathways as delay time increased, the responses resulting from large couplings tended to disappear as the optimization was increased, favoring the retention of responses due to smaller and smaller couplings.

TABLE 2. Long-range Coupling Responses Observed for Compound **30** with an Optimization Time (Δ_{LR}) of 83 msec.[a]

Proton (ppm)	Assignment	Correlation (carbon)
3.986	1	11,2,9,5
2.250	2a	3,10,1
2.145	2b	3,1,4
1.902	3a	2,4,12,5, 13 (weak)
1.614	3b	4,1,5,12
1.422	5	11,7,2,3,6,1,4,9,10
1.888	6	4,13
1.732	7a	8,5,9
1.231	7b	8,6,5,13
1.781	8a	7,9,6
1.662	8b	7,9
1.614	9a	8,7,10,11
1.090	9b	11,8,10,5
1.134	11	10,1,5
1.277	12	3,5,4
1.142	14	7,6,13,15
1.261	15	14,6,13

[a]Responses are noted for the carbons to which protons showing responses were long-range coupled.

ASSIGNMENT OF STEREOCHEMISTRY BY HMQC-NOESY.—Conventionally, stereochemical orientation of the substituents of **30** can be assigned on the basis of proton-proton nOe's. This well-established method was employed to map the substituent stereochemical orientation of 1-bromomaalioxide [**30**]. The issue of stereochemistry, however, also provides a springboard for the introduction of the HMQC-NOESY experiment (22,23).

HMQC-NOESY is essentially a variant of the isotope-directed nOe experiment, which has recently been reviewed by Griffey and Redfield (197). The variant utilized in these laboratories was first reported by Sohn and Opella (22) in an application to ^{15}N-labeled proteins. To our knowledge, the only reported application of this experiment to a small molecule (<500 Daltons) at natural abundance is the work of Luo *et al.* (89) and Crouch *et al.* (112). The pulse sequence for the experiment is shown in Figure 31 and, quite simply, has a proton NOESY segment "tacked on" the back of an HMQC experiment. As utilized in these laboratories, the experiment affords phase-sensitive data in which the nOe responses are antiphase to the direct responses. At natural abundance, the experiment places extremely severe demands on the spectrometer for sensitivity because the desired nOe responses have intensities that are only a few percent of the much more intense direct responses. Nevertheless, the experiment can provide vital nOe information when it cannot be obtained by conventional methods because of the overlap of the protons of interest—provided, of course, that the carbons in question are resolved.

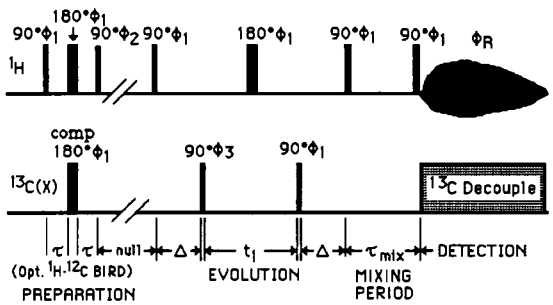

FIGURE 31. Pulse sequence for HMQC-NOESY used in the authors' laboratory. The pulse sequence is essentially the HMQC sequence of Bax and Subramanian (17) which was shown in Figure 4. Following the reconversion of heteronuclear multiple quantum coherence into observable single-quantum coherence, a fixed delay is allowed to elapse to bring the antiphase proton magnetization into phase. At this point, the pair of proton 90° pulses separated by the mixing period establishes proton-proton nOe's. The signal which is finally detected is sorted in the second frequency domain by carbon chemical shift and shows those protons to which the directly attached proton has an nOe.

Optimization of HMQC-NOESY experiments.—Before discussing the results obtained with the HMQC-NOESY experiment, it is essential that several points be made about the optimization of the experiment, which is critical if it is to have any chance of being employed successfully at natural abundance. First, the proton T_1 relaxation times must be measured. Second, the duration of the interval between the BIRD pulse and the start of the HMQC portion of the experiment must be very carefully optimized for the sample in hand. We generally find it convenient to optimize the null interval by setting the

interpulse delay to about twice what it will be set to for the actual experiment. This time, determined as a function of the proton T_1 relaxation times, is typically about $3 \times T_1$. Next we array the duration of the null interval and perform a series of HMQC experiments in which a single increment (the first) of the evolution time is acquired without ^{13}C decoupling. The optimal setting for the null interval will then be the duration that gives the best satellite spectrum. The mixing period for the nOe portion of the experiment following the HMQC sequence is typically optimized as a function of $0.75-1.25 \times T_1$. As noted above, sensitivity demands for the HMQC-NOESY experiment are high, and we typically find it necessary to employ a minimum of twice the number of acquisitions required for "good" HMBC data. Given the length of time/transient because of the duration of the mixing period, null interval, and interpulse delay, it may be necessary to use relatively coarse digital resolution in F_1 to keep total experiment times reasonable. Even with these concessions, the duration of the HMQC-NOESY will normally be two to three times that required for "good" HMBC data. Thus, it will normally be far more expedient to utilize the much more sensitive conventional NOESY experiment. However, when nOe's are required for protons that are not scalar coupled but overlapped, the HMQC-NOESY experiment becomes a necessary evil!

Applications of HMQC-NOESY to small molecules.—As noted above, there are virtually no applications of the HMQC-NOESY experiment to be found in the current literature other than two prototypical studies of the authors (112,198). The first study utilized the polynuclear aromatic helicene [**22**] as a model compound to evaluate the HMQC-NOESY experiment as a potential method to orient spin systems of aromatic systems relative to one another when their proton spectra are too congested for the successful use of conventional methods. This study also probed the ability of the HMQC-NOESY experiment to provide proton-proton internuclear distances.

It was demonstrated that the observed nOe in an HMQC-NOESY experiment is quite sensitive to the care taken in optimizing the experiment. For example, when parameters that would yield a perfectly satisfactory HMQC spectrum were employed with a mixing time of 600 msec, the observed nOe between H-2 and H-3 was <4%. When the experiment was more carefully optimized and the mixing time set to 1400 msec on the basis of measured proton T_1 relaxation times, the nOe between H-2 and H-3 increased to a more realistic 19.0%. Interestingly, an nOe between H-11 and H-12 was also observed in this study (5.4%), which afforded an opportunity to evaluate the ability of the HMQC-NOESY experiment to provide interproton distance information. Thus, based on molecular dynamics simulation, the H-11 to H-12 distance was estimated at 3.249 Å. Using the H-2 to H-3 distance, which is readily calculated as a basis for computation, the computed distance between H-11 and H-12 from the HMQC-NOESY experiment was 3.37 Å, whch agrees reasonably well with the distance from the molecular dynamics simulation. Hence, when necessary, the HMQC-NOESY experiment can probably be used to estimate interproton distances, although for reasons of sensitivity this would probably be the method of last choice.

The only other application of HMQC-NOESY to a small molecule was a report of the assignment of the stereochemistry of a carbocyclic analogue **85** of adenosine by the authors (198). Because of an accidental overlap of the H-1′ and H-2′ protons, the stereochemical assignments can only be made by using a HMQC-NOESY spectrum (Figure 32). Thus, by virtue of the fact that C-1′ will resonate upfield of C-2′, the orientation of H-1′ as α can be assigned through the nOe observed between H-1′ and H-6′α at the chemical shift of C-1′. In similar fashion, the orientation of H-2′ can be established as β based on the observed nOe between H-2′ and H-6′β and H-2′ and H-3′β; both of these responses are observed along the axis defined by the chemical shift of C-2′ in the HMQC-NOESY spectrum.

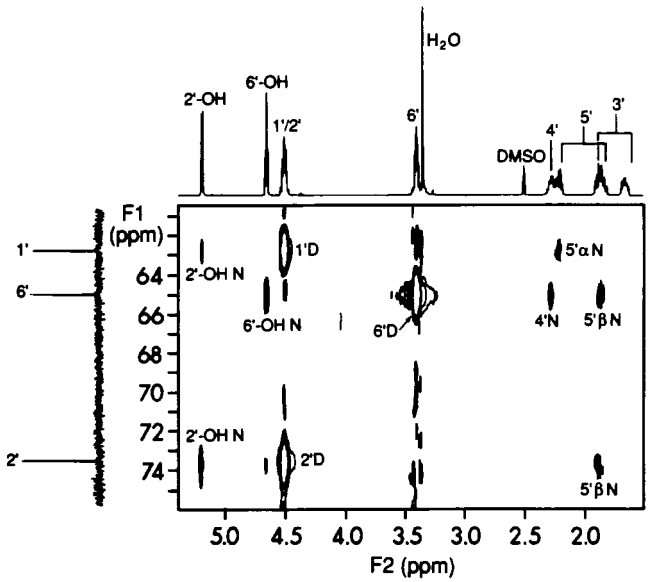

FIGURE 32. HMQC-NOESY spectrum of a simple carbocyclic nucleoside **85**. The overlap of the H-1′ and H-2′ protons precluded confirmation of the stereochemistry by conventional methods. However, by sorting proton-proton nOe's as a function of the carbon chemical shifts in the second frequency domain, it is possible to differentiate nOe's between H-1′ and H-2′ and the other protons in the molecule. Responses are labeled D = direct response and N = nOe response.

It is also possible to use the HMQC-NOESY experiment to establish an nOe between protons in different parts of the molecule that have (accidentally) similar chemical shifts with no coupling between them. This can be done by simply recording the HMQC-NOESY experiment without applying heteronuclear decoupling during the acquisition period. This approach was demonstrated in the work of the authors (198) with the HMQC-TOCSY experiment. As shown schematically in Figure 33, the direct response in the decoupled spectrum would obscure the NOESY or TOCSY response sought. However, when the data are acquired without decoupling, the components of the direct response are offset by $\pm {}^{1}J_{CH}/2$, leaving the NOESY or TOCSY response observed at the chemical shift of the direct carbon in question. Although not reported, the carbon-coupled HMQC-NOESY experiment of **85** (Figure 34) affords several NOESY responses that are unobservable in the decoupled HMQC-NOESY experiment. There is no conventional 1D analogue to the HMQC-NOESY experiment that reliably permits the observation of this class of nOe's.

Applications of HMQC-NOESY to large molecules.—Applications of the HMQC-NOESY experiment to large molecules are becoming reasonably common with the increasing availability of heavily labeled peptides and proteins through molecular biological techniques. Indeed, the initial work of Sohn and Opella (22), which provided the basis for the HMQC-NOESY experiment used in the authors' laboratory, was based on a ^{15}N-enriched protein. Gronenborn *et al.* (108) discussed the HMQC-NOESY experiment in the context of an integrated experimental approach to the assignment of proton resonances of proteins. Marion *et al.* (199) described the HMQC-NOESY experiment in the context of the expansion from 2D to 3D nmr experiments. Gronenborn and Clore

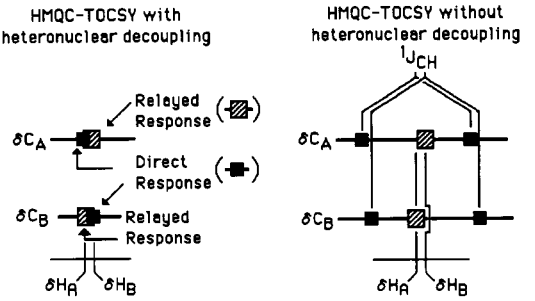

FIGURE 33. Schematic representation of responses observed in HMQC-TOCSY/NOESY spectra between protons with overlapping proton chemical shifts. In the normal pulse sequence (left), which applied carbon decoupling during acquisition, the direct and relay, or nOe, response would be overlapped with the latter obscured. By acquiring the data without carbon decoupling (right) the direct response will be separated by the chemical shift of the direct proton by $\pm {}^1J_{CH}/2$ leaving the relayed, or nOe, response easily observed.

(32) touched on the HMQC-NOESY experiment briefly in their review of 2D and 3D nmr methods for determining protein structure. Finally, Gooley *et al.* (200) employed the HMQC-NOESY experiment in the assignment of the ^{1}H- and ^{15}N-nmr spectra of ferrocytochrome c2 from *Rhodobacter capsulatus*.

ONE-DIMENSIONAL ANALOGUES OF PROTON-DETECTED 2D NMR EXPERIMENTS.—Two-dimensional nmr experiments, in many cases, yield a tremendous amount of information per unit time. Often, only a part of the information obtained from 2D nmr experiments is required. In such cases, selective 1D analogues of the 2D experiment would be highly desirable. At present, there have been two such pulse sequences reported. The first was the SELINCOR sequence reported by Berger (146), and the second was a selective HMQC-TOCSY sequence reported by Crouch *et al.* (201).

SELINCOR.—The first selective 1D analogue of a proton-detected 2D nmr experiment was reported by Berger (146) in 1989. Berger utilized the pulse sequence of Bax and Subramanian (17), which was shown in Figure 4 and in which the final carbon 90° pulse was replaced by a frequency-selective Gaussian pulse. Although Berger's sequence was reported without broadband heteronuclear decoupling during the acquisition period, we have found it convenient to use the modified version of the sequence

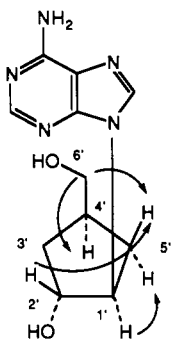

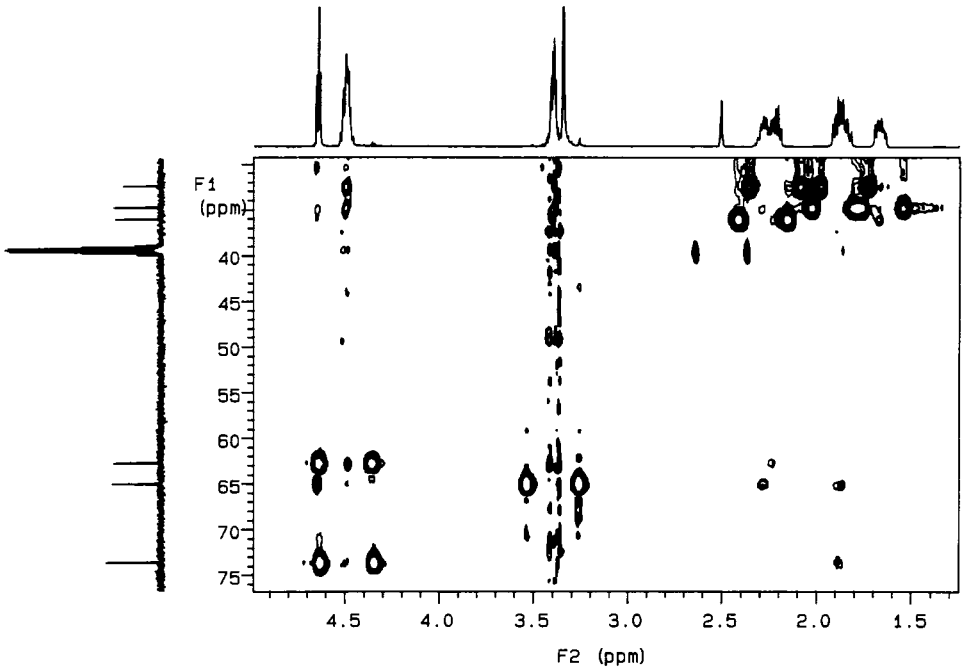

FIGURE 34. Carbon-coupled HMQC-NOESY spectrum of **85** showing nOe responses that are normally obscured by the direct responses in the carbon-decoupled HMQC-NOESY spectrum and conventional NOESY spectra.

shown in Figure 35, which provides heteronuclear decoupling. Heteronuclear decoupling can be applied provided that the frequency utilized for the selective Gaussian pulse is the same as that used for the other pulses applied in the sequence.

Unfortunately, the utility of the SELINCOR experiment is largely limited to those cases in which the chemical shift of the attached carbon is already known. There have been no applications of Berger's pulse sequence reported. One potential application of the SELINCOR sequence that may yet be exploited involves the selective establishment of long-range correlations between a given carbon and those protons to which it is long-

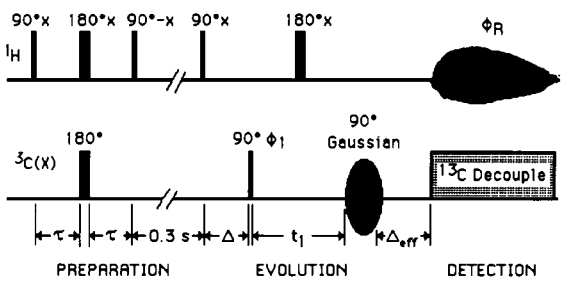

FIGURE 35. SELINCOR pulse sequence of Berger (146) as modified by the authors to provide heteronuclear decoupling during acquisition. By applying the hard and selective carbon pulses at the same frequency followed by an effective refocusing delay, broadband heteronuclear decoupling may be applied during acquisition, affording, ultimately, the spectrum of solely the proton to which the carbon subjected to the Gaussian pulse is directly bound.

range coupled. There are problems inherent to such applications that we are currently attempting to side-step but that have, thus far, not been surmounted.

Selective one-dimensional HMQC-TOCSY.—Another selective 1D analogue of a proton-detected 2D nmr experiment is the selective HMQC-TOCSY experiment recently described by the authors (201). This application is quite similar to the SELINCOR sequence in terms of positioning of the selective pulse, except that the authors elected to employ a square rather than a Gaussian pulse. Following the application of the selective pulse, a fixed delay, $\Delta_2$eff, is employed, after which the MLEV isotropic mixing sequence is applied as in the normal HMQC-TOCSY sequence (Figure 36).

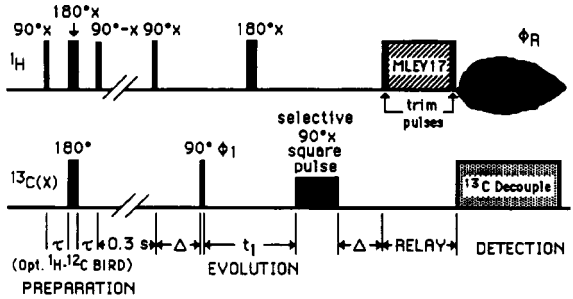

FIGURE 36. Selective HMQC-TOCSY pulse sequence to acquire TOCSY subspectra associated with a single proton-carbon pairing as originally reported by the authors (201). This experiment could be used when TOCSYs using a series of mixing times are needed for only a single proton-carbon pairing.

As with the SELINCOR sequence, there have not yet been any applications of the selective HMQC-TOCSY sequence other than the authors' initial report of the experiment. It was demonstrated using the carbocyclic adenosine analogue **86**, also used to illustrate the application of the HMQC-NOESY experiment to small molecules, above.

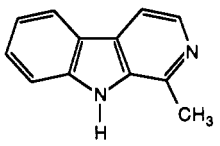

86

SIMBA: Selective Inverse Multiple Bond Analysis.—A final, selective 1D analogue of the 2D HMBC experiment has recently been described, for which the authors have proposed the acronym SIMBA—selective inverse multiple bond analysis (202). The pulse sequence is shown in Figure 37 and differs from the conventional HMBC experiment (Figure 26) in that the final carbon pulse is replaced by either a selective square or shaped pulse. Practically, the SIMBA experiment places considerable demands on the R_f capabilities of the spectrometer on which it is performed. Specifically, the experiment requires a power level switch of at least 50 dB in an interval of only a few microseconds. More stringently, the power switch must occur with retention of phase coherence.

Practically, the SIMBA experiment has several uses. First, it provides an alternative to a full 2D HMBC experiment when connectivities to only one or two carbons are required. Second, the experiment also provides an unequivocal and highly sensitive method for measuring long-range heteronuclear coupling constants, because the pro-

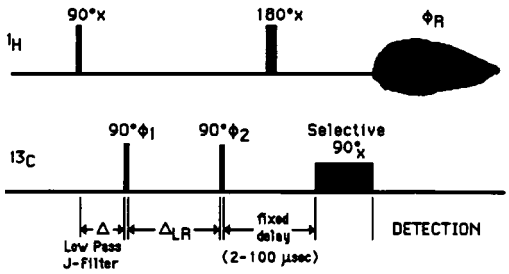

FIGURE 37. Pulse sequence for selective inverse multiple bond analysis (SIMBA). The experiment is derived from the HMBC pulse sequence (18) and functions in an analogous fashion. The first 90° ^{13}C pulse serves as a low-pass J-filter; the second 90° ^{13}C pulse creates heteronuclear multiple quantum coherence, which is refocused by the ^1H 180° pulse and reconverted, selectively, by the final ^{13}C 90° pulse into observable magnetization. Phases can be cycled exactly as reported by Bax and Summers (18).

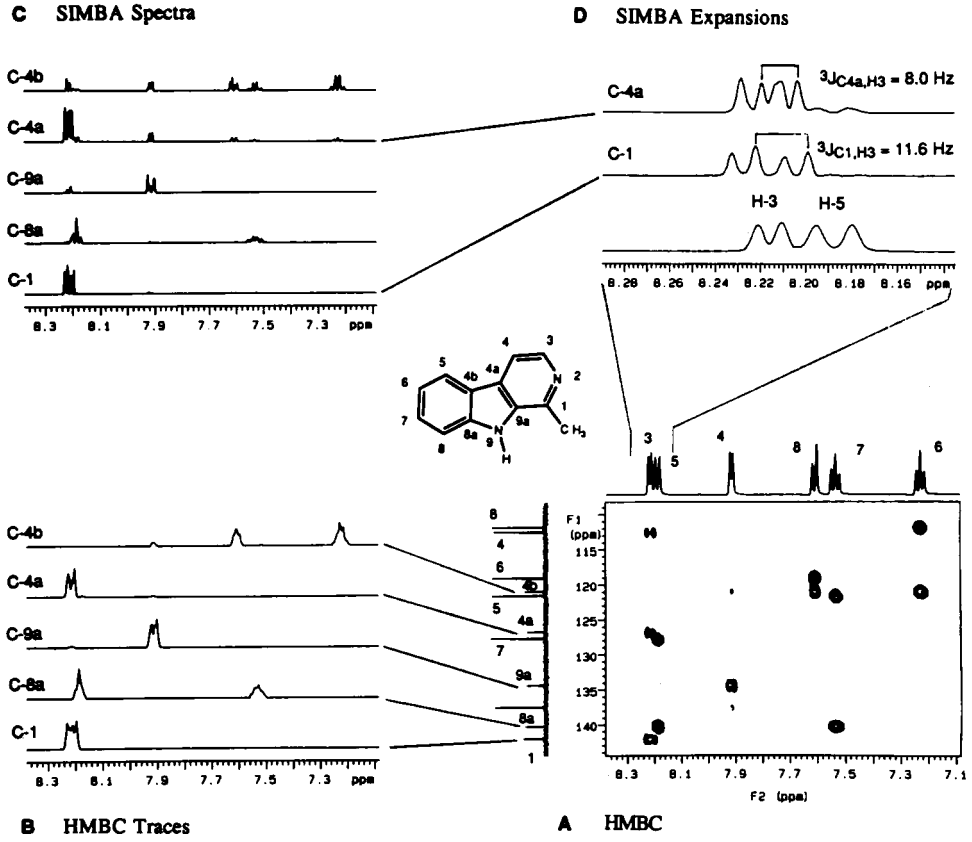

FIGURE 38. Comparisons of the 2D HMBC spectrum and the SIMBA spectra that result from the selective excitation of each quaternary carbon in harmane. The concentration was 0.09 M in DMSO-d_6 solution. (A) The HMBC contour plot. The HMBC data was acquired with acquisition times of 0.314 sec in F_2 and 9 msec in F_1, 64 transients for each of 96 files. (B) Traces for all quaternary carbons which are extracted from the full HMBC dataset. (C) The SIMBA spectra which parallel the HMBC traces shown in B. Each SIMBA spectrum was acquired in 3.2 min (64 transients) with an acquisition time of 1.3 sec. (D) The expansions from the H-3, H-5 region for the SIMBA spectra relative to the ^1H reference spectrum. $^3J_{C1,H3}$ (11.6 Hz) and $^3J_{C4a,H3}$ (8.0 Hz) are highlighted.

ton's multiplets (Figure 38) exhibit the long-range heteronuclear coupling for the particular proton-carbon coupling pathway excited in the experiment.

The results obtained with the SIMBA experiment relative to the more familar HMBC experiment are shown in Figure 38 for the simple alkaloid norharmane [**86**]. Figure 38A presents the HMBC spectrum which was recorded in 4 h. The slices extracted from the HMBC experiment at the chemical shift of the quaternary carbons are presented as the stacked spectra shown in Figure 38B. The individual SIMBA traces are shown in Figure 38C. Acquisition of each SIMBA trace required only 3.2 min. It should also be noted that the SIMBA traces have considerably higher digital resolution than would normally be practical in an HMBC experiment. Suppression of non-excited protons is generally excellent. Responses in the SIMBA spectra which do not appear in the corresponding HMBC traces uniformly arise from partial excitation of carbons in close proximity to those of interest. Expansions of the regions of interest from the SIMBA spectra of C-4a and C-1 are shown in Figure 38D with the heteronuclear coupling constant information provided by the experiment, which is not normally observable in the proton multiplet in question, highlighted by the splitting diagram.

The authors are of the opinion that the future for applications of 1D analogues of 2D nmr experiments is quite bright. They can provide vital structural information with minimal investment in time when compared to the acquisition of a full 2D nmr experiment. An example where SIMBA could have been beneficially employed is the 1989 report of Fushimi *et al.* (203) describing the simple amino acid herbicidal antibiotic homoalanosine, in which the position of the carboxyl group was assigned from HMBC data. Here, a selective 1D analogue of the HMBC experiment could have been used to advantage. Doubtless, numerous other opportunities for the application of selective 1D analogues of 2D nmr experiments will continue to be encountered.

ACKNOWLEDGMENTS

The authors thank Drs. J.H. Cardellina II and D.E. Barnekow for providing the sample of 1-bromo-*ent*-maaliol which degraded in our refrigerator, Drs. L.C.E. Taylor and S.Y. Chang for obtaining the mass spectra of 1-bromo-*ent*-maalioxide, and especially Ms. M. Day for extensive assistance with the literature search and Mr. A. Jones for proofreading and correcting this manuscript.

NOTE ADDED IN PROOF.—One of the referees of this review has made an excellent comment regarding the selection of inverse-detected experiments that we initially overlooked and feel obliged to include here. Although multiple quantum-based experiments such as HMQC will work quite well for small- to intermediate-sized molecules, including most natural products, this may not be the case for macromolecules. When $T_2(^1H) < T_2(X$ where X = ^{13}C or $^{15}N)$ a single quantum coherence sequence which involves heteronucleus magnetization during the evolution period may actually be superior. This point is discussed in the work of T.J. Norwood, J. Boyd, J.E. Heritage, N. Soffe, and I.D. Campbell, *J. Magn. Reson.*, **87**, 488 (1990). A step in this general direction is also reflected by the work of Zuiderweg (42) on the heteronuclear single- and multiple-quantum coherence experiment. We refer readers interested in larger molecules to these papers or to the other reviews concerned with macromolecules which are cited in this review as references 32–37.

LITERATURE CITED

1. A. Bax, "Two-Dimensional Nuclear Magnetic Resonance in Liquids," Delft University Press, Delft, The Netherlands, 1982.
2. R.R. Ernst, G. Bodenhausen, and A. Wokaun, "Principles of Nuclear Magnetic Resonance in One and Two Dimensions," Clarendon Press, Oxford, U.K., 1987.
3. A.E. Derome, "Modern NMR Techniques for Chemistry Research," Pergamon Press, New York, 1987.
4. G.E. Martin and A.S. Zektzer, "Two-Dimensional NMR Methods for Establishing Molecular Connectivity: A Chemist's Guide to Experiment Selection, Performance and Interpretation," VCH, New York, 1988.
5. J.K.M. Sanders and B.K. Hunter, "Modern NMR Spectroscopy: A Guide for Chemists," Oxford University Press, Oxford, U.K., 1987.

6. W.S. Brey, Ed., "Pulse Methods in 1D and 2D Liquid-phase NMR," Academic Press, San Diego, 1988.
7. L. Müller, *J. Am. Chem. Soc.*, **101**, 4481 (1979).
8. A.A. Maudsley and R.R. Ernst, *Chem. Phys. Lett.*, **50**, 368 (1977).
9. A.A. Maudsley, L. Müller, and R.R. Ernst, *J. Magn. Reson.*, **28**, 463 (1977).
10. R. Freeman and G.A. Morris, *J. Chem. Soc., Chem. Commun.*, 684 (1978).
11. A. Bax and G.A. Morris, *J. Magn. Reson.*, **42**, 501 (1981).
12. P.H. Bolton, *J. Magn. Reson.*, **48**, 336 (1982).
13. P.H. Bolton and G. Bodenhausen, *Chem. Phys. Lett.*, **89**, 139 (1982).
14. A. Bax, *J. Magn. Reson.*, **53**, 149 (1983).
15. K. Hallenga and G. Van Binst, *Bull. Magn. Reson.*, **2**, 343 (1980).
16. G.E. Martin and A.S. Zektzer, *Magn. Reson. Chem.*, **27**, 633 (1988).
17. A. Bax and S. Subramanian, *J. Magn. Reson.*, **67**, 565 (1986).
18. A. Bax and M.F. Summers, *J. Am. Chem. Soc.*, **108**, 2093 (1986).
19. P.H. Bolton, *J. Magn. Reson.*, **62**, 145 (1985).
20. L. Lerner and A. Bax, *J. Magn. Reson.*, **69**, 375 (1986).
21. D.G. Davis, *J. Magn. Reson.*, **84**, 417 (1989).
22. K. Sohn and S.J. Opella, *J. Magn. Reson.*, **82**, 193 (1989).
23. A. Bax, R.H. Griffey, and B.L. Hawkins, *J. Magn. Reson.*, **55**, 301 (1983).
24. O.W. Sørensen, G.W. Eich, M.H. Levitt, G. Bodenhausen, and R.R. Ernst, *Prog. Nucl. Magn. Reson. Spectrosc.*, **16**, 163 (1983).
25. H. Kessler, M. Gehrke, and C. Griesinger, *Angew. Chem., Int. Ed. Engl.*, **27**, 447 (1988).
26. A. Bax, *J. Magn. Reson.*, **52**, 76 (1983).
27. M. Munowitz and A. Pines, *Adv. Chem. Phys.*, **66**, 1 (1987).
28. J.R. Garbow, D.P. Weitekamp, and A. Pines, *Chem. Phys. Lett.*, **93**, 504 (1982).
29. D. Brühwiler and G. Wagner, *J. Magn. Reson.*, **69**, 546 (1986).
30. G. Bodenhausen and D. Ruben, *Chem. Phys. Lett.*, **69**, 185 (1980).
31. V. Sklenar and A. Bax, *J. Magn. Reson.*, **71**, 379 (1987).
32. A.M. Gronenborn and G.M. Clore, *Anal. Chem.*, **62**, 2 (1990).
33. A. Bax, *Ann. Rev. Biochem.*, **58**, 223 (1989).
34. G.M. Clore and A.M. Gronenborn, *Crit. Rev. Biochem. Mol. Biol.*, **24**, 479 (1989).
35. G. Wagner, *Methods Enzymol.*, **176**, 93 (1989).
36. J.L. Markley, *Methods Enzymol.*, **176**, 12 (1989).
37. M.R. Jefson, *Annu. Rep. Med. Chem.*, **23**, 275 (1988).
38. L. Mueller, R.A. Schiksnis, and S.J. Opella, *J. Magn. Reson.*, **66**, 379 (1986).
39. G. Otting and K. Wüthrich, *J. Magn. Reson.*, **76**, 569 (1988).
40. T. Spitzer, M.E. Kuehne, W. Bornmann, and C. Anklin, *J. Magn. Reson.*, **84**, 654 (1989).
41. H. Kessler, P. Schmieder, and M. Kurz, *J. Magn. Reson.*, **85**, 400 (1989).
42. E.R.P. Zuiderweg, *J. Magn. Reson.*, **86**, 346 (1990).
43. A. Bax, M. Ikura, L.E. Kay, D.A. Torchia, and R. Tschudin, *J. Magn. Reson.*, **86**, 304 (1990).
44. M.F. Summers, L.G. Marzilli, and A. Bax, *J. Am. Chem. Soc.*, **108**, 4285 (1986).
45. A. Bax, L.G. Marzilli, and M.F. Summers, *J. Am. Chem. Soc.*, **109**, 566 (1987).
46. T.G. Pagano and L.G. Marzilli, *Biochemistry*, **28**, 7213 (1989).
47. T.G. Pagano, P.G. Yohannes, B.P. Hay, J.R. Scott, R.G. Finke, and L.G. Marzilli, *J. Am. Chem. Soc.*, **111**, 1484 (1989).
48. S.K. Sarkar, J.D. Glickson, and A. Bax, *J. Am. Chem. Soc.*, **108**, 6814 (1986).
49. A. Bax, A. Asalos, Z. Dinya, and K. Sudo, *J. Am. Chem. Soc.*, **108**, 8056 (1986).
50. H. Seto, K. Furihata, K. Saeki, N. Otake, Y. Kusakabe, C. Xu, and J. Clardy, *Tetrahedron Lett.*, 3357 (1987).
51. M. Ubukata, K. Isono, K. Kimura, C.C. Nelson, and J.A. McCloskey, *J. Am. Chem. Soc.*, **110**, 4416 (1988).
52. S. Abuzar and H. Kohn, *J. Org. Chem.*, **54**, 4000 (1989).
53. R.H. Chen, A.M. Buko, D.N. Whittern, and J.B. McAlpine, *J. Antibiot.*, **42**, 512 (1989).
54. R.H. Chen, D.N. Whittern, A.M. Buko, and J.B. McAlpine, *J. Antibiot.*, **42**, 533 (1989).
55. J.H. Martin, M.P. Kunstmann, F. Barbatschi, M. Hertz, G.A. Ellestad, M. Dann, G.S. Redin, A.D. Dornbush, and N.A. Kuck, *J. Antibiot.*, **31**, 398 (1978).
56. D. Meksuriyen and G.A. Cordell, *J. Nat. Prod.*, **51**, 884 (1988).
57. J. Garnier, J. Mahuteau, M. Plat, and C. Merienne, *Phytochemistry*, **28**, 308 (1988).
58. M.W. Edwards, J.W. Daly, and C.W. Myers, *J. Nat. Prod.*, **51**, 1188 (1988).
59. A. DeBruyn, W. Zhang, and M. Budesinsky, *Magn. Reson. Chem.*, **27**, 935 (1989).
60. S. Carmely, M. Ilan, and Y. Kashman, *Tetrahedron*, **45**, 2193 (1989).

61. H. Takayama, J.-J. Sun, N. Aimi, S. Sakai, S.-T. Lu, and I.-S. Chen, *Tetrahedron Lett.*, 3441 (1989).
62. J. Kobayashi, T. Murayama, Y. Ohizumi, T. Ohta, S. Nozoe, and T. Sasaki, *J. Nat. Prod.*, **52**, 1173 (1989).
63. J.S. Mossa, J.M. Cassady, J.F. Kozlowski, T.M. Zennia, M.D. Antoun, M.G. Pellachia, A.T. McKenzie, and S.R. Byrn, *Tetrahedron Lett.*, 3627 (1988).
64. S. Berger, P. Junior, and L. Kopanski, *Planta Med.*, **27**, 579 (1988).
65. A.E. Wright, N.S. Burres, and G.K. Schulte, *Tetrahedron Lett.*, 3491 (1989).
66. J.M. Beale, H.G. Floss, T. Lehmann, and M. Luckner, *Phytochemistry*, **27**, 3143 (1988).
67. G. Englert, E. Glinz, and S. Liaaen-Jensen, *Magn. Reson. Chem.*, **26**, 55 (1988).
68. J. Cavanagh, C.A. Hunder, D.N.M. Jones, J. Keeler, and J.K.M. Sanders, *Magn. Reson. Chem.*, **26**, 867 (1988).
69. R. Timkovich and L.L. Bondoc, *Magn. Reson. Chem.*, **27**, 1048 (1989).
70. L. Lerner and A. Bax, *Carbohydr. Res.*, **166**, 35 (1987).
71. R.A. Byrd, W. Egan, M.F. Summers, and A. Bax, *Carbohydr. Res.*, **166**, 47 (1987).
72. P. Kovac, V. Sklenar, and C.P.J. Glaudemans, *Carbohydr. Res.*, **175**, 201 (1988).
73. P. Kovac and L. Lerner, *Carbohydr. Res.*, **184**, 87 (1988).
74. W. Bermel, C. Griesinger, H. Kessler, and K. Wagner, *Magn. Reson. Chem.*, **25**, 325 (1987).
75. M. Hofmann, M. Gehrke, W. Bermel, and H. Kessler, *Magn. Reson. Chem.*, **27**, 877 (1989).
76. E.T. Olejniczak, R.T. Gampe Jr., T.W. Rockway, and S.W. Fesik, *Biochemistry*, **27**, 7124 (1988).
77. I.P. Gerothanassis, M. Bourdonneau, T. Karayannis, M. Sakarellos-Daitsiotis, and C. Sakarellos, *J. Magn. Reson.*, **80**, 309 (1988).
78. A. Demarco, L. Zetta, and C. Anklin, *Gazz. Chim. Ital.*, **118**, 295 (1988).
79. H. Kessler, A.G. Klein, R. Obermeier, and M. Will, *Liebigs Ann. Chem.*, 269 (1989).
80. M. Goodman and D.F. Mierke, *J. Am. Chem. Soc.*, **111**, 3489 (1989).
81. V. Sklenar, H. Miyashiro, G. Zon, H.T. Miles, and A. Bax, *FEBS Lett.*, **208**, 94 (1986).
82. W. Leupin, G. Wagner, W.A. Denny, and K. Wüthrich, *Nucleic Acids Res.*, **15**, 267 (1987).
83. S.R. LaPlante, J. Ashcroft, D. Cowburn, G.C. Levy, and P.N. Borer, *J. Biomol. Struct. Dyn.*, **5**, 1089 (1988).
84. S.R. LaPlante, E.A. Boudreau, N. Zanatta, G.C. Levy, P.N. Borer, and D. Cowburn, *Biochemistry*, **27**, 7902 (1988).
85. V. Sklenar and A. Bax, *J. Am. Chem. Soc.*, **109**, 2221 (1987).
86. J. Ashcroft, S.R. LaPlante, P.N. Borer, and D. Cowburn, *J. Am. Chem. Soc.*, **111**, 363 (1989).
87. L. Legendre, J. Mahuteau, and M. Miocque, *Magn. Reson. Chem.*, **26**, 624 (1988).
88. S. Berger and B.W.K. Diehl, *Magn. Reson. Chem.*, **27**, 201 (1989).
89. J.-K. Luo, R.N. Castle, R.C. Crouch, and G.E. Martin, *J. Heterocycl. Chem.*, **28**, in press (1991).
90. R. Benn, H. Brenneke, J. Heck, and A. Rufinska, *Inorg. Chem.*, **26**, 2826 (1987).
91. R. Benn and A. Rufinska, *Magn. Reson. Chem.*, **26**, 895 (1988).
92. R. Benn, H. Brenneke, A. Frings, H. Lehmkuhl, G. Mehler, A. Rufinska, and T. Wildt, *J. Am. Chem. Soc.*, **110**, 5661 (1988).
93. M. Bown, J. Plesek, K. Base, B. Stibr, X.L.R. Fontaine, N.N. Greenwood, and J.D. Kennedy, *Magn. Reson. Chem.*, **27**, 947 (1989).
94. W.P. Niemczura, G.L. Helms, A.S. Chesnick, R.E. Moore, and V. Bornemann, *J. Magn. Reson.*, **81**, 635 (1989).
95. L.D. Sims, L.R. Soltero, and G.E. Martin, *Magn. Reson. Chem.*, **27**, 599 (1989).
96. D.E. Barnekow, J.H. Cardellina II, A.S. Zektzer, and G.E. Martin, *J. Am. Chem. Soc.*, **111**, 3511 (1989).
97. G. Eich, G. Bodenhausen, and R.R. Ernst, *J. Am. Chem. Soc.*, **104**, 3731 (1982).
98. H. Kessler, M. Bern, H. Kogler, O.W. Sørensen, G. Bodenhausen, and R.R. Ernst, *J. Am. Chem. Soc.*, **105**, 6944 (1983).
99. P. Bigler, W. Ammann, and R. Richarz, *Org. Magn. Reson.*, **22**, 109 (1984).
100. G.E. Martin, R. Sanduja, and M. Alam, *J. Nat. Prod.*, **49**, 405 (1986).
101. S.R. Johns, J.A. Lamberton, H. Suares, and R.I. Willing, *Aust. J. Chem.*, **38**, 1091 (1985).
102. C.J. Turner, *Magn. Reson. Chem.*, **22**, 531 (1984).
103. A. San Feliciano, A.F. Barrero, M. Medarde, J.M. Miguel del Corral, A. Aramburu, A. Perales, and J. Faykos, *Tetrahedron Lett.*, 2369 (1985).
104. G.S. Linz, M.J. Musmar, A.J. Weinheimer, G.E. Martin, and J.A. Matson, *Spectrosc. Lett.*, **19**, 545 (1986).
105. J.R. Everett and J.W. Typler, *J. Chem. Soc., Perkin Trans. 1*, 2599 (1985).
106. D.A. Torchia, S.W. Sparks, and A. Bax, *Biochemistry*, **27**, 5135 (1988).

107. D.A. Torchia, S.W. Sparks, and A. Bax, *Biochemistry*, **28**, 5509 (1989).
108. A.M. Gronenborn, A. Bax, P.T. Wingfield, and G.M. Clore, *FEBS Lett.*, **243**, 93 (1989).
109. H. Kessler, S. Mronga, M. Will, and U. Schmidt, *Helv. Chim. Acta*, **73**, 25 (1990).
110. T.C. McKee, C.M. Ireland, N. Lindquist, and K.W. Fenical, *Tetrahedron Lett.*, 3053 (1989).
111. H. Kessler, M. Will, J. Antel, H. Beck, and G.M. Sheldrick, *Helv. Chim. Acta*, **72**, 530 (1988).
112. R.C. Crouch, R.B. McFayden, S.M. Daluge, and G.E. Martin, *Magn. Reson. Chem.*, **28**, 792 (1990).
113. R.C. Crouch, G.E. Martin, J.-K. Luo, and R.N. Castle, *J. Heterocyl. Chem.*, submitted (1990).
114. M.J. Musmar, G.E. Martin, M.L. Tedjamulia, H. Kudo, R.N. Castle, and M.L. Lee, *J. Heterocycl. Chem.*, **21**, 929 (1984).
115. M.J. Musmar, G.E. Martin, R.T. Gampe Jr., M.L. Lee, R.E. Hurd, M.L. Tedjamulia, H. Kudo, and R.N. Castle, *J. Heterocycl. Chem.*, **22**, 219 (1985).
116. M.J. Musmar, G.E. Martin, R.T. Gampe Jr., V.M. Lynch, S.H. Simonsen, M.L. Lee, M.L. Tedjamulia, and R.N. Castle, *J. Heterocycl. Chem.*, **22**, 545 (1985).
117. J.G. Stewart, M.J. Quast, G.E. Martin, V.M. Lynch, S.H. Simonsen, M.L. Lee, R.N. Castle, J.L. Dallas, B.K. John, and L.F. Johnson, *J. Heterocycl. Chem.*, **23**, 1215 (1986).
118. A.S. Zektzer, J.G. Stuart, G.E. Martin, and R.N. Castle, *J. Heterocycl. Chem.*, **23**, 1587 (1986).
119. M.J. Musmar, A.S. Zekzter, R.T. Gampe Jr., M.L. Lee, M.L. Tedjamulia, R.N. Castle, and R.E. Hurd, *Magn. Reson. Chem.*, **24**, 1039 (1986).
120. S. Berger, *J. Magn. Reson.*, **81**, 561 (1988).
121. C.S. Narayanan, K.S. Kulkarni, A.S. Vaidya, S. Kanthamani, G. Lakshmi Kumari, B.V. Bapat, S.K. Paknikar, S.N. Kulkarni, G.R. Kelkar, and S.C. Bhattacharyya, *Tetrahedron*, **20**, 963 (1964).
122. C. Bauer, S. Wimperis, and R. Freeman, *J. Magn. Reson.*, **58**, 526 (1984).
123. M.J. Quast, A.S. Zektzer, G.E. Martin, and R.N. Castle, *J. Magn. Reson.*, **71**, 554 (1987).
124. A.S. Zektzer, B.K. John, R.N. Castle, and G.E. Martin, *J. Magn. Reson.*, **72**, 556 (1987).
125. M. Salazar, A.S. Zektzer, and G.E. Martin, *Magn. Reson. Chem.*, **26**, 24 (1988).
126. M. Salazar, A.S. Zektzer, and G.E. Martin, *Magn. Reson. Chem.*, **26**, 28 (1988).
127. W.F. Reynolds, D.W. Hughes, M. Perpick-Dumont, and R.G. Enriquez, *J. Magn. Reson.*, **63**, 415 (1985).
128. M. Perpick-Dumont, R.G. Enriquez, S. McLean, F.V. Puzzuoli, and W.F. Reynolds, *J. Magn. Reson.*, **75**, 416 (1987).
129. V.V. Krishnamurthy and J.E. Casida, *Magn. Reson. Chem.*, **25**, 837 (1987).
130. H. Kogler, O.W. Sørensen, G. Bodenhausen, and R.R. Ernst, *J. Magn. Reson.*, **55**, 157 (1983).
131. A. Bax and D. Marion, *J. Magn. Reson.*, **78**, 186 (1988).
132. D.S. Williamson, R.A. Smith, D.L. Nagel, and S.M. Cohen, *J. Magn. Reson.*, **82**, 605 (1989).
133. H. Seto, *Pure Appl. Chem.*, **61**, 365 (1989).
134. S. Abuzar and H. Kohn, *J. Am. Chem. Soc.*, **111**, 4895 (1989).
135. S. Abuzar, H. Kohn, J.D. Korp, A.S. Zektzer, and G.E. Martin, *J. Heterocycl. Chem.*, **25**, 1511 (1988).
136. J. Rohr, A. Zeeck, and H.G. Floss, *J. Antibiot.*, **41**, 126 (1988).
137. H. Seto, N. Otake, S. Sato, H. Yamaguchi, K. Takada, M. Itoh, H.S.M. Lu, and J. Clardy, *Tetrahedron Lett.*, 2343 (1988).
138. H. Seto, K. Furihata, and M. Ohuchi, *J. Antibiot.*, **41**, 1158 (1988).
139. S. Gomi, M. Sezaki, S. Kondo, T. Hara, H. Naganawa, and TG. Takeuchi, *J. Antibiot.*, **41**, 1019 (1988).
140. R. Grote, A. Zeeck, and J.M. Beale Jr., *J. Antibiot.*, **41**, 1186 (1988).
141. J.E. Hochlowski, M.H. Buytendorp, D.N. Whittern, A.M. Buko, R.H. Chen, and J.B. McAlpine, *J. Antibiot.*, **41**, 1300 (1988).
142. S. Fushimi, K. Furihata, and H. Seto, *J. Antibiot.*, **42**, 1026 (1989).
143. S. Imai, K. Furihata, Y. Hayakawa, T. Noguchi, and H. Seto, *J. Antibiot.*, **42**, 1197 (1989).
144. K. Shindo, A. Takenaka, T. Noguchi, Y. Hayakawa, and H. Seto, *J. Antibiot.*, **42**, 1526 (1989).
145. H. Seto, T. Fuioka, K. Furihata, I. Kaneko, and S. Takahashi, *Tetrahedron Lett.*, 4987 (1989).
146. S. Berger, *J. Magn. Reson.*, **81**, 561 (1988).
147. J. Kobayashi, J.-f. Cheng, M.R. Wälchli, H. Nakamura, Y. Hirata, T. Sasaki, and Y. Ohizumi, *J. Org. Chem.*, **53**, 1800 (1988).
148. J.-f. Cheng, Y. Ohizumi, M.R. Wälchli, H. Nakamura, Y. Hirata, T. Sasaki, and J. Kobayashi, *J. Org. Chem.*, **53**, 4621 (1988).
149. J. Kobayashi, J.-f. Cheng, M. Ishibashi, H. Nakamura, Y. Ohizumi, Y. Hirata, T. Sasaki, H. Lu, and J. Clardy, *Tetrahedron Lett.*, 4939 (1987).
150. B.R. Copp, J.W. Blunt, M.H.G. Munro, and L.K. Pannell, *Tetrahedron Lett.*, 3703 (1989).

151. G.P. Gunawardana, S. Kohmoto, and N.S. Burres, *Tetrahedron Lett.*, 4359 (1989).
152. A.R. Carroll, N.M. Cooray, A. Poiner, and P.J. Scheuer, *J. Org. Chem.*, **54**, 4231 (1989).
153. J. Kobayashi, T. Murayama, Y. Ohizumi, T. Sasaki, T. Ohta, and S. Nozoe, *Tetrahedron Lett.*, 4833 (1989).
154. N. Fusetani, K. Yasumuro, S. Matsunaga, and H. Hirota, *Tetrahedron Lett.*, 6891 (1989).
155. Y. Kashman, S. Hirsh, O.J. McConnell, I. Ohtani, T. Kusumi, and H. Kakisawa, *J. Am. Chem. Soc.*, **111**, 8925 (1989).
156. A. Cherif, G.E. Martin, L.R. Soltero, and G. Massiot, *J. Nat. Prod.*, **53**, 793 (1990).
157. J. Bosly, *J. Pharm. Belg.*, **6**, 150 (1951).
158. N.G. Bisset, J. Bosly, B.C. Das, and G. Spiteller, *Phytochemistry*, **14**, 1411 (1975).
159. G. Pant, M.S. Panwar, D.S. Negi, M.S.M. Rawat, G.A. Morris, and R.I.G. Thompson, *Magn. Reson. Chem.*, **26**, 911 (1988).
160. P. Sharma and M. Alam, *J. Chem. Soc., Perkin Trans 1*, 2537 (1988).
161. M. Alam, P. Sharma, A.S. Zektzer, G.E. Martin, X. Ji, and D. van der Helm, *J. Org. Chem.*, **54**, 1896 (1989).
162. H. Seto, K. Furihata, X. Guangyi, C. Xiong, and P. Deji, *Agric. Biol. Chem.*, **52**, 1797 (1988).
163. T. Nishitoba, S. Goto, H. Sato, and S. Sakamura, *Phytochemistry*, **28**, 193 (1989).
164. S. Zhang, X. Yao, Y. Chem. C. Cui, Y. Tezuka, and T. Kikuchi, *Chem. Pharm. Bull.*, **37**, 1966 (1989).
165. N. Fusetani, H. Nagata, H. Hirota, and T. Tsuyuki, *Tetrahedron Lett.*, 7079 (1989).
166. A.A. Basaran, I. Calus, C. Anklin, S. Nishibe, and O. Sticher, *Helv. Chim. Acta*, **71**, 1483 (1988).
167. D.G. Davis, *J. Magn. Reson.*, **83**, 212 (1989).
168. H. Kessler, G. Gemmecker, A. Haupt, M. Klein, K. Wagner, and M. Will, *Tetrahedron*, **44**, 745 (1988).
169. H. Kessler, M. Will, G.M. Sheldrick, and J. Antel, *Magn. Reson. Chem.*, **26**, 501 (1988).
170. H. Kessler, S. Mronga, M. Will, and U. Schmidt, *Helv. Chim. Acta*, **73**, 25 (1990).
171. T. Kusumi, T. Ooi, M.M. Watanabe, H. Takahashi, and H. Kakisawa, *Tetrahedron Lett.*, 4695 (1987).
172. G.R. Pettit, Y. Kamano, H. Kizu, C. Dufresne, C.L. Herald, R.J. Bontems, J.M. Schmidt, F.E. Boettner, and R.A. Nieman, *Heterocycles*, **28**, 553 (1989).
173. D.E. Williams, R.E. Moore, and V.J. Paul, *J. Nat. Prod.*, **52**, 732 (1989).
174. C. Ireland and P.J. Scheuer, *J. Am. Chem. Soc.*, **102**, 5688 (1980).
175. D.F. Sesin, S.J. Gaskell, and C.M. Ireland, *Bull. Soc. Chim. Belg.*, **95**, 853 (1986).
176. M. Gunasekera and S.P. Gunasekera, *J. Nat. Prod.*, **52**, 753 (1989).
177. F.J. Schmitz, M.B. Ksebati, J.S. Chang, G.L. Wang, M.B. Hossain, D. van der Helm, M.H. Engel, A. Serban, and J.A. Silfer, *J. Org. Chem.*, **54**, 3463 (1989).
178. G.R. Pettit, Y. Kamano, C.L. Herald, C. Dufresne, R.L. Cerny, D.L. Herald, J.M. Schmidt, and H. Kizu, *J. Am. Chem. Soc.*, **111**, 5015 (1989).
179. G.R. Pettit, Y. Kamano, C. Dufresne, R.L. Cerny, C.L. Herald, and J.M. Schmidt, *J. Org. Chem.*, **54**, 6005 (1989).
180. A. Bax, S.W. Sparks, and D.A. Torchia, *J. Am. Chem. Soc.*, **110**, 7926 (1988).
181. G.M. Clore, A. Bax, P. Wingfield, and A.M. Gronenborn, *FEBS Lett.*, **238**, 17 (1988).
182. D.G. Davis, *J. Am. Chem. Soc.*, **111**, 5466 (1989).
183. A.M. Gronenborn, P.T. Wingfield, and G.M. Clore, *Biochemistry*, **28**, 5081 (1989).
184. J. Wang, A.P. Hinck, S.N. Loh, and J.L. Markley, *Biochemistry*, **29**, 102 (1990).
185. J.D. Forman-Kay, A.M. Gronenborn, L.E. Kay, P.T. Wingfield, and G.M. Clore, *Biochemistry*, **29**, 1566 (1990).
186. J.W. Blunt, J.D. McCombs, M.H.G. Munro, and F.N. Thomas, *Magn. Reson. Chem.*, **27**, 792 (1989).
187. A.S. Zektzer, L.D. Sims, R.N. Castle, and G.E. Martin, *Magn. Reson. Chem.*, **26**, 287 (1988).
188. R.E. Fischer, J. Dabrowski, A. Ejchart, and H.A. Staab, *Magn. Reson. Chem.*, **26**, 834 (1988).
189. M.D. Johnston Jr., M. Salazar, L.D. Sims, A.S. Zektzer, R.N. Castle, and G.E. Martin, *Magn. Reson. Chem.*, **27**, 318 (1989).
190. Y. Tezuka, K. Nagashim, H. Hirano, and T. Kikuchi, *Chem. Pharm. Bull.*, **37**, 1667 (1989).
191. J. Kobayashi, M. Ishibashi, M.R. Wälchli, H. Nakamura, Y. Hirata, T. Sasaki, and Y. Ohizumi, *J. Am. Chem. Soc.*, **110**, 490 (1988).
192. D.G. Corley, R.E. Moore, and V.J. Paul, *J. Am. Chem. Soc.*, **110**, 7920 (1988).
193. J. Kobayashi, J.-f. Cheng, T. Ohta, H. Nakamura, S. Nozoe, Y. Hirata, Y. Ohizumi, and T. Sasaki, *J. Org. Chem.*, **53**, 6147 (1988).

194. J. Kobayashi, M. Ishibashi, H. Nakamura, Y. Ohizumi, T. Yamasu, Y. Hirata, T. Sasaki, T. Ohta, and S. Nozoe, *J. Nat. Prod.*, **52**, 1036 (1989).
195. W. Eisenreich, B. Schwarzkopf, Q.L. Van, P.J. Keller, and A. Bacher, *J. Chem. Soc., Chem. Commun.*, 1294 (1988).
196. K. Ichinose, Y. Ebizuka, and U. Sankawa, *Chem. Pharm. Bull.*, **37**, 2873 (1989).
197. R.H. Griffey and A.G. Redfield, *Q. Rev. Biophys.*, **19**, 51 (1987).
198. R.C. Crouch, G.E. Martin, J.-K. Luo, and R.N. Castle, *Magn. Reson. Chem.*, **28**, 774 (1990).
199. D. Marion, P.C. Driscoll, L.E. Kay, P.T. Wingfield, A. Bax, A.M. Gronenborn, and G.M. Clore, *Biochemistry*, **28**, 6150 (1989).
200. P.R. Gooley, M.S. Caffrey, M.A. Cusanovich, and N.E. Mackenzie, *Biochemistry*, **29**, 2278 (1990).
201. R.C. Crouch, J.P. Shockcor, and G.E. Martin, *Tetrahedron Lett.*, 5273 (1990).
202. R.C. Crouch and G.E. Martin, *J. Magn. Reson.*, in press (1991).
203. S. Fushimi, S. Nishikawa, N. Mito, M. Ikemoto, M. Sasaki, and H. Seto, *J. Antibiot.*, **42**, 1370 (1989).

Received 23 July 1990